

**INSULATOR POLLUTION
MONITORING DEVICE:
Development, Calibration and Field
Evaluation**



UNIVERSITEIT • STELLENBOSCH • UNIVERSITY
jou kennisvennoot • your knowledge partner

Wilhelm H Schwardt

**Thesis submitted for the degree of Master of Science in Engineering at the
University of Stellenbosch**

Promoters:

Prof. H. J. Vermeulen, Dr. J. P. Holtzhausen

APRIL 2005

DECLARATION

I, the undersigned, hereby declare that the contents contained in this thesis are my own original work and has not in its entirety, or in part, been submitted at any university for a degree.

Wilhelm H Schwardt

SYNOPSIS

The calibration and field evaluation of an Insulator Pollution Monitoring Relay (IPMR) were the main aims of this research programme. A repeatable artificial wetting test method was developed after several modifications were made to the steam system, test chamber and the test routine.

The IPMR was successfully calibrated with insulators that were artificially polluted according to the solid layer method. Linear and polynomial relationships were determined after curve-fitting techniques were performed on the results. The calibration showed that the IPMR is capable as a device relating the maximum conductivity during artificial wetting to the ESDD, a severity classification parameter. The IPMR was successfully used in a salt fog chamber to determine if the device is capable to evaluate the severity of an instantaneous pollution event.

The IPMR was successfully installed at a natural pollution test site along the Cape west coast. The conductivity measurements with natural wetting showed good correlation to flashovers experienced. A rule of thumb, developed to indicate a possible risk of flashover, was based on observations made on the relationship between humidity and surface conductivity. The measured IPMR data was successfully applied to quantify the site severity according to the conductivity measurement with natural wetting. This calculated severity value could be used in the assessment of flashover probability of high voltage insulators.

OPSOMMING

Die hoofdoel van die tesis was die kalibrasie en veldtoetse van 'n isolator-besoedelingsmonitor (IPMR). 'n Herhaalbare nagebootste benatting-toetsmetode is ontwikkel na veranderinge aan die stoomstelsel, toetsruimte en die toetsproses.

Die IPMR is suksesvol gekalibreer met isolators wat besoedel was met 'n nagebootste besoedeling volgens die "solid layer method". Liniêre sowel as kwadratiese verwantskappe is ontwikkel na krommepassings op die resultate uitgevoer was. Die kalibrasie het gewys dat die IPMR in staat is om die maksimum geleidingsvermoë wat d.m.v. nagebootste benatting verkry is, met die ESDD, 'n besoedelingsklassifikasie, kan vergelyk. Die apparaat is ook suksesvol gebruik tydens soutmistoetse om te bepaal of dit in staat is om 'n skielike besoedelingsgebeurtenis te kan meet.

Na die afhandeling van laboratorium werk is die apparaat by 'n natuurlike isolator besoedeling-toetsstasie langs die Kaapse westkus geïnstalleer. Die geleidingsvermoë metings met natuurlike benatting het goeie korrelasie getoon met isolator oorvonkings. 'n Skattingsmetode wat ontwikkel is om maandelike oorvonkings te voorspel, is gebaseer op waarnemings wat gemaak is van die humiditeit sowel as die oppervlakte geleidingsvermoë. Die IPMR se geleidingsvermoë metings met natuurlike benatting is aangewend om die besoedelingsgraad van die gebied te bepaal. Die bepaalde besoedelingsgraad kan verder gebruik word om die waarskynlikheid van die oorvonking van isolators vas te stel.

ACKNOWLEDGEMENTS

I would like to thank the following people:

- My supervisor, Dr. J. P. Holtzhausen, for his guidance, encouragement and patience.
- Dr. Wallace Vosloo
- Prof. H. J. Vermeulen
- Petrus Pieterse, for help whenever I needed it.
- Johan Strauss, for his technical support towards the IPMR.
- The workshop staff at the University of Stellenbosch.
- Rob Watson and Thamsanqa Mvayo, for helping me at KIPTS.
- Ludwig Schwardt, for supplying insightful approaches to MATLAB[®] related problems.
- My family, especially my parents, Detlef and Marita, who always showed support during this project.

TABLE OF CONTENTS

1	INTRODUCTION	1
1.1	Overview	1
1.2	Insulator Pollution Monitoring	1
1.2.1	The Pollution Flashover Process	2
1.2.2	Methods Used In The Assessment of Site Severity.....	3
1.3	Literature Review	4
1.3.1	Research Based on Salt Fog Tests	4
1.3.2	Research Based on Insulator Pollution Severity and Leakage Current ...	5
1.3.3	Commissioning of Various Natural Pollution Test Stations.....	8
1.3.4	The First Insulator Surface Conductivity Monitor Project.....	9
1.3.5	The Second Insulator Surface Conductivity Monitor Project.....	10
1.3.6	The Third Insulator Surface Conductivity Monitor Project	12
1.3.7	Research in the Performance of Different Insulating Materials at a Severe Coastal Site.....	13
1.4	Project Objectives	14
1.5	Structure of this Thesis	14
2	REVIEW OF METHODS TO DETERMINE POLLUTION SEVERITY	16
2.1	Introduction	16
2.2	Environmental Monitoring	16
2.2.1	Geographical Location	16
2.2.2	Directional Deposit Gauge.....	18
2.2.3	Meteorological Monitoring	21
2.3	Non-Electrical Insulator Tests	22
2.3.1	The Equivalent Salt Deposit Density	22

2.3.2	Non Soluble Deposit Density.....	25
2.4	Electrical Insulator Tests.....	27
2.4.1	Surface Conductivity Measurement.....	27
2.4.2	Leakage Current Measurement.....	29
2.5	Summary.....	30
3	THE INSULATOR POLLUTION MONITORING RELAY (IPMR)	32
3.1	Introduction	32
3.2	The Principle of the IPMR	32
3.3	The Hardware Components of the IPMR	33
3.3.1	The IPMR Enclosure	33
3.3.2	The Steam Generator.....	34
3.3.3	The Hot Air Dryer	35
3.3.4	The Test Transformer.....	35
3.3.5	The Moving Platform	35
3.3.6	The Test Insulator	37
3.3.7	The Steam Supply Pipes.....	38
3.4	IPMR Measuring and Control Units.....	39
3.4.1	IPMR Measurements.....	39
3.4.2	IPMR Measurement and Control Systems	43
3.4.3	IPMR Software	45
3.5	Summary.....	48
4	IPMR MEASUREMENTS DURING ARTIFICIALLY POLLUTED CONDITIONS	49
4.1	Introduction	49
4.2	Developmental Work performed on the IPMR.....	49
4.2.1	Thermal Tests	49
4.2.2	Verification of the measuring system using a fixed resistor.....	52

4.3	Calibration Tests	54
4.3.1	Description of the Solid Layer Method.....	54
4.3.2	Determination of the IPMR calibration curve	54
4.3.3	Repeatability Tests.....	56
4.4	Salt fog tests performed on the IPMR	57
4.4.1	Salt Fog Chamber	58
4.4.2	Description of the OLCA leakage current monitor	58
4.4.3	Test Insulators Used During Salt Fog Tests.....	59
4.4.4	Comparison of Measured Conductivities and Leakage Currents.....	60
4.4.5	Critical Flashover Voltage Derived from the measured IPMR Surface Conductivity	61
4.4.6	Critical leakage current (I_{max}).....	63
4.4.7	Results obtained from Salt Fog Tests	64
4.5	Summary.....	65
5	IPMR MEASUREMENTS DURING NATURALLY POLLUTED CONDITIONS	66
5.1	Introduction	66
5.2	Koeberg Insulator Pollution Test Station (KIPTS)	66
5.3	Operational Performance of the IPMR at KIPTS.....	68
5.4	Calculation of Site Severity Using IPMR Measurements Over a 30-Week Period.....	71
5.5	Discussion of Flashover Events experienced at KIPTS During Week 15	78
5.6	Summary.....	82
6	RESULTS AND RECOMMENDATIONS.....	83
	REFERENCES	86

LIST OF FIGURES

Figure 1-1: Relationship between Peak Leakage Current (mA) and Salinity (g/l).....	5
Figure 1-2: Relationship between Surface Conductance (μS) and Salinity (kg/m^3).....	6
Figure 1-3: Relationship between Peak Leakage Current (A) and Salinity (kg/m^3).....	6
Figure 1-4: Relationship between Peak Leakage Current (A), Applied Stress (peak V/mm) and Salinity (kg/m^3).....	7
Figure 1-5: Image of the second IPMA installed at a coastal site.....	10
Figure 2-1: DDG collection tube and container.....	19
Figure 3-1: The IPMR shown with top and side panels removed.....	34
Figure 3-2: View of the IPMR test chamber, showing the various components.....	36
Figure 3-3: The IPMR insulator.....	37
Figure 3-4: Top view of the IPMR test chamber.....	39
Figure 3-5: Flow chart of the surface conductivity test with artificial wetting.....	41
Figure 3-6: Flow chart during an artificial wetting cycle.....	41
Figure 3-7: Graphical view of typical measured IPMR data.....	45
Figure 3-8: Artificial wetting test setup menu.....	47
Figure 4-1: Brass adaptor before and after machining.....	50
Figure 4-2: Thermal measurements during an artificial wetting test.....	52
Figure 4-3: IPMR measurements with the standard resistor installed.....	53
Figure 4-4: Calibration curve derived for the IPMR.....	55
Figure 4-5: IPMR Surface Conductivity (μS) vs. Salinity (kg/m^3).....	60
Figure 4-6: Critical Flashover Voltage (kV_{peak}) vs. Salinity (kg/m^3).....	62
Figure 4-7: Peak Leakage Current (A) vs. Salinity (kg/m^3).....	63
Figure 5-1: Koeberg Insulator Pollution Test Station (KIPTS).....	67
Figure 5-2: Operational performance for the naturally wetted conductivity tests.....	70
Figure 5-3: Stress-strength concept.....	71

Figure 5-4: IPMR surface conductivity histogram used for KIPTS site severity calculation.....	72
Figure 5-5: ESDD histogram used for KIPTS site severity calculation.....	74
Figure 5-6: Normal probability plot for IPMR measurements.....	75
Figure 5-7: Lognormal probability plot for IPMR measurements.....	77
Figure 5-8: Normal probability plot for ESDD measurements.....	77
Figure 5-9: Week 15 IPMR conductivity and weather parameters.....	79
Figure 5-10: Week 15 IPMR conductivity and calculated critical flashover voltage.....	80
Figure 5-11: Week 15 IPMR conductivity, leakage currents and flashover risk.....	81

LIST OF TABLES

Table 2-1: Classification of pollution levels according to the environment.....	17
Table 2-2: Specific Creepage Distance required for each pollution level.	17
Table 2-3: DDG Pollution Index Classification.....	21
Table 2-4: ESDD Pollution Index Classification.....	25
Table 2-5: NSDD Pollution Classification.	27
Table 3-1: IPMR test insulator dimensions and parameters.....	37
Table 4-1: Statistics of the tests performed at each severity range.....	55
Table 4-2: Curve fitting coefficients and statistical measures of model adequacy.....	56
Table 4-3: Salinity withstand values and recommended specific creepage lengths.....	61
Table 5-1: Summary of pollution sources around KIPTS.....	67
Table 5-2: Surface conductivity test instability matrix.	69
Table 5-3: Operational problems experienced with IPMR.	69
Table 5-4: Surface conductivity percentiles and associated severity classification.	73
Table 5-5: ESDD percentiles and associated severity classification.	74
Table 5-6: Information on insulators which flashed during Week 15.	79
Table 5-7: Statistics of measured conductivity and weather values.	80

LIST OF ABBREVIATIONS

BIPTS	Brandbaai Insulator Pollution Test Station
CESI	Centro Elettrotecnico Sperimentale Italiano (Italian Electrotechnical Testing Authority)
CIGRÉ	Conseil International des Grands Réseaux Electriques (International Council on Large Electric Systems)
CLIMAT	Classify Industrial and Marine Atmosphere
DDG	Directional Deposit Gauge
EPDM	Ethylene Propylene Diene Monomer
ESDD	Equivalent Salt Deposit Density
HFO	Heavy Fuel Oil
IEC	International Electrotechnical Commission
IPMA	Insulator Pollution Monitoring Apparatus
IPMR	Insulator Pollution Monitoring Relay
IPSAM	Insulator Pollution Severity Application Map
KIPTS	Koeberg Insulator Pollution Test Station
NEC	National Energy Council
NSDD	Non Soluble Deposit Density
OLCA	Online Leakage Current Analyser
PME	Pollution Monitoring Equipment
RH	Relative humidity
RMS	Root Mean Square
SCD	Specific Creepage Distance
TESP	Tertiary Education Support Program
TSI	Technology Services International
UV	Ultra-violet

1 INTRODUCTION

1.1 OVERVIEW

The project was initiated after the development of a pollution monitoring device in conjunction with ESKOM. This device was the third pollution monitor to be developed as part of the insulator pollution monitoring programme at the University of Stellenbosch. The development of the device was in response to a need to have a device that could assist in site pollution severity measurements and also be able to give an alarm when dangerous levels of pollution accumulated on the insulator surface.

1.2 INSULATOR POLLUTION MONITORING

Insulator pollution monitoring is used to relate the expected insulation performance to the reliability of existing and planned high voltage overhead lines. The information obtained by measurements should be useful when designing new lines, when determining the correct maintenance intervals and procedures or when defining effective countermeasures to pollution related problems. There are thus three main uses to the measured insulator pollution parameters:

- **Pollution severity measurement:** The main aim of this method is to determine the pollution severity in the area. This information can then be used to map the particular pollution or to study the mechanisms of pollution deposition and the subsequent wetting of this pollution layer. The measured pollution severity can also be used during the design of a new overhead line or substation to determine the correct insulation to be used in the area.

CHAPTER 1

- **Maintenance:** The pollution monitoring can be applied to measure the build-up of pollution over time. The use of meteorological information and the previous pollution experience at the site can be used with the pollution measurement to determine the correct maintenance interval and to evaluate the correct procedure e.g. hand cleaning, high pressure washing with an outage, live line insulator washing or re-greasing.
- **Insulator characterisation:** Pollution monitoring can also be applied to compare the behaviour of various insulation materials and insulator dimensions to the exposed conditions. This method can also be used to determine the most suitable insulation for the particular area. This comparative study can also include sample insulators incorporating insulation remedies, e.g. the application of booster sheds or shed extenders, semi-conducting glazes, greases or spray-coatings.

1.2.1 The Pollution Flashover Process

The Electra No. 64 document [1] describes the pollution flashover process for ceramic insulation as follows:

“The following sequence of events can usually be recognised in cases of pollution flashover.

- (a) The insulator becomes coated with a layer of pollution containing soluble salts or dilute acids or alkalis. If the pollution is deposited as a layer of liquid electrolyte, e.g. salt spray, stages (c) to (f) may proceed immediately. If the pollution is non-conducting when dry some wetting process (stage (b)) is necessary.*
- (b) The surface of the polluted insulator is wetted either completely or partially by fog, mist, light rain, sleet or melting snow or ice and the pollution layer becomes conducting. Heavy rain is a complicating factor: it may wash away the electrolytic components of part or all of the pollution layer without initiating*

CHAPTER 1

other stages in the breakdown process, or it may, by bridging the gaps between sheds, promote flashover.

- (c) Once an energised insulator is covered with a conducting pollution layer, surface leakage currents flow and their heating effect starts to dry out parts of the pollution layer.*
- (d) The drying of the pollution layer is always non-uniform, and in places the conducting pollution layer becomes broken by dry bands which interrupt the flow of leakage current.*
- (e) The line-to-earth voltage applied across dry bands which may be only a few centimetres wide causes air breakdown and the dry bands are bridged by arcs which are electrically in series with the resistance of the undried portion of the pollution layer. This causes a surge of leakage current each time the dry bands on an insulator spark over.*
- (f) If the resistance of the undried part of the pollution layer is low enough, the arcs bridging the dry bands are able to burn continuously and to extend along the insulator, bridging more and more of its surface. This in turn decreases the resistance in series with the arcs, increasing the current and permitting them to bridge still more of the insulator surface. Ultimately it is completely bridged and a line-to-earth fault is established."*

1.2.2 Methods Used In The Assessment of Site Severity

The ideal site severity measurement is an assessment method that is able to relate all the information needed to determine the flashover probability for any insulator installed at the test site operating at a specified system voltage. This ideal method should therefore include all the factors influencing the insulator flashover process at the site. Various pollution assessment methods are applied to determine site severity or relate insulator performance. The tests include environmental monitoring, non-electrical insulator tests, electrical insulator tests and air pollution measurements. The important tests used in the field of pollution monitoring and site severity measurements are discussed thoroughly in Chapter 2.

CHAPTER 1

1.3 LITERATURE REVIEW

The University of Stellenbosch started research in the field of insulator pollution research in the 1980 s. The content is discussed in the chronological order that the research was performed in. A bibliography is presented at the end of this thesis, containing all the publications dealing with insulator pollution monitoring. It will be pointed out that various models of insulator surface conductivity monitoring devices were developed. These developments culminated in the device that is the subject of the present research.

1.3.1 Research Based on Salt Fog Tests

The first insulator pollution research work at the University of Stellenbosch was done by L. P. du Toit in conjunction with ESKOM. L. P. Du Toit designed and built the first salt fog testing facility at the University of Stellenbosch. This work stretched over several years. (See section 1.3.2) C. K. Du Toit [2] performed related work during this period by investigating the relationship between highest leakage current (I_{highest}), applied stress (V/cm), and pollution severity (g/l) on a single insulator during a salt fog test. A PC-based measurement system was designed and built to measure peak leakage currents (I_{highest}) on up to 8 insulators simultaneously.

Using the results from extensive artificial pollution tests, performance could be predicted for each applied stress at varying severities. C. K. Du Toit only used one porcelain long rod test insulator that was shorted at different insulation lengths to change the applied stress (V/cm). An example of such a relationship is shown in Figure 1-1. The work done played a large role in future work at the university.

CHAPTER 1

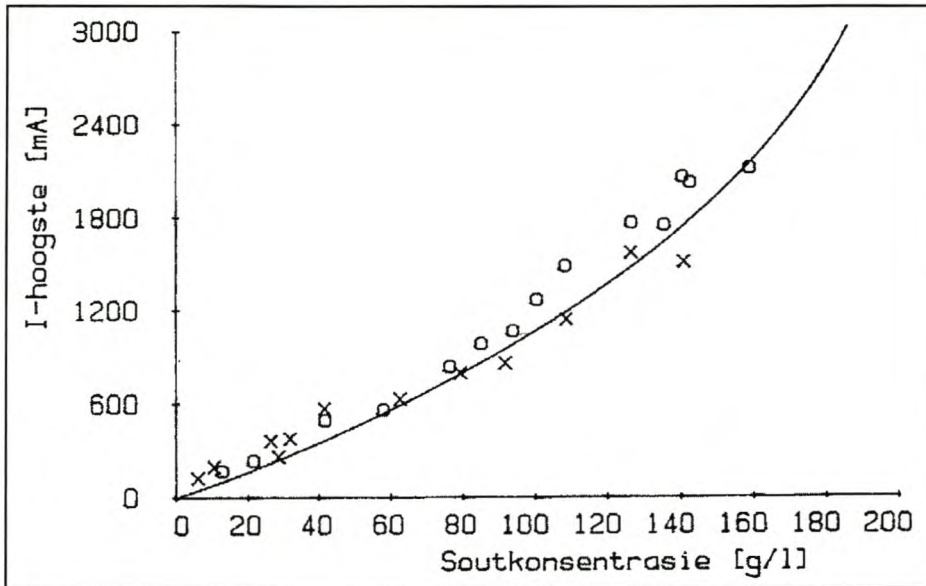


Figure 1-1: Relationship between Peak Leakage Current (mA) and Salinity (g/l). ($E = 260 \text{ V/cm}$, $SCD = 38.46 \text{ mm/kV}$) [2].

1.3.2 Research Based on Insulator Pollution Severity and Leakage Current

L. P. Du Toit [3] investigated different flashover mechanisms and tried to compare two different severity assessment methods, viz. surface conductivity and peak leakage current (I_{highest}). The two methods were compared with each other to determine if there was any correlation between their predicted severities. The three test insulators that were used included profiles for a standard glass disc, a longrod insulator and an anti-fog insulator. Artificial pollution tests were performed and the relationship between the different profiles was determined. The relationships between the test salinities and assessment parameters are shown below in Figure 1-2 and Figure 1-3. The test set-up was then moved to a marine location for the natural pollution tests. The test site was an existing test site at the Koeberg Nuclear Power Plant used by ESKOM's research department. The insulators were exposed to natural conditions for a long time to include the effect of weather on the insulators.

CHAPTER 1

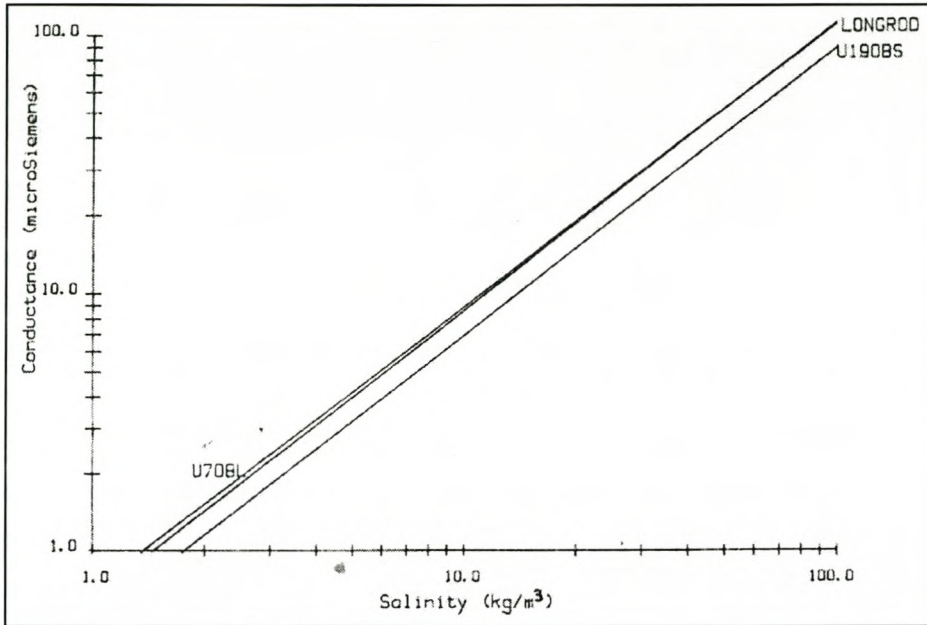


Figure 1-2: Relationship between Surface Conductance (μS) and Salinity (kg/m^3) [3].

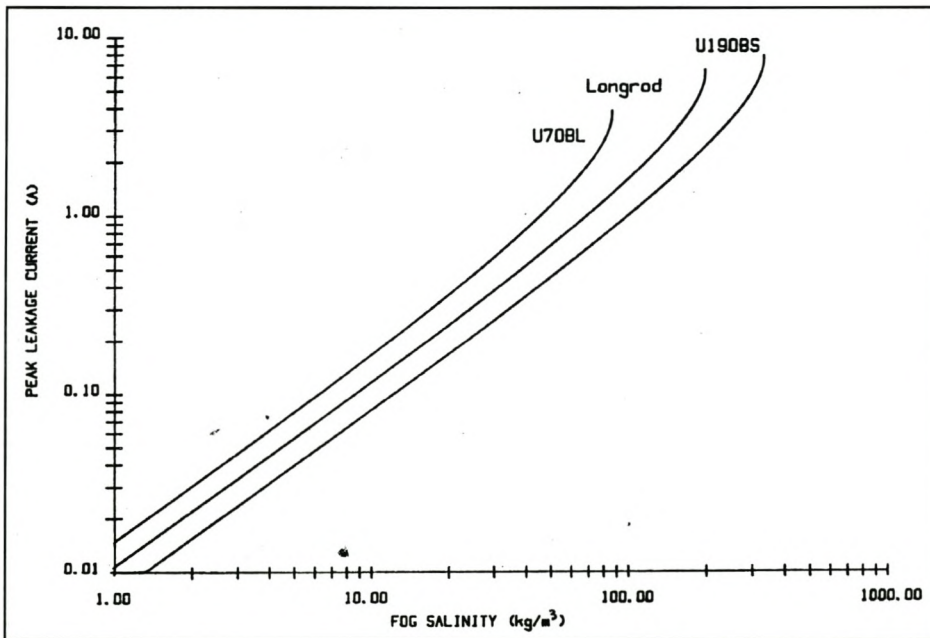


Figure 1-3: Relationship between Peak Leakage Current (A) and Salinity (kg/m^3) [3].

CHAPTER 1

The continued collection of data at the natural pollution site proved unsuccessful due to failures of the test equipment attributed to the harsh environmental conditions. After a year the testing was stopped and it was decided to redesign the testing equipment. A new test site was also proposed closer to Stellenbosch.

A very useful relationship was found to exist between insulator parameters and measured results [4]. This relationship is shown below in Figure 1-4, based on curves fitted to data obtained by C. K. du Toit during salt fog tests. From this figure it was determined that for a constant severity, insulators with a high stress (V/mm) or, low specific creepage distance (mm/kV), will experience a “run-away” condition as a certain critical current, I_{max} , as defined by Verma (see section 2.4.2), is approached.

This showed that I_{max} by itself is problematic in the assessment in pollution performance. The leakage current of the insulator must also remain clear from the steep vertical curve nearing 100% I_{max} . This theory led to the introduction of [4]:

$$I_{\text{permissible}} < 0.25 * I_{\text{max}} \quad (\text{Eq. 1.1})$$

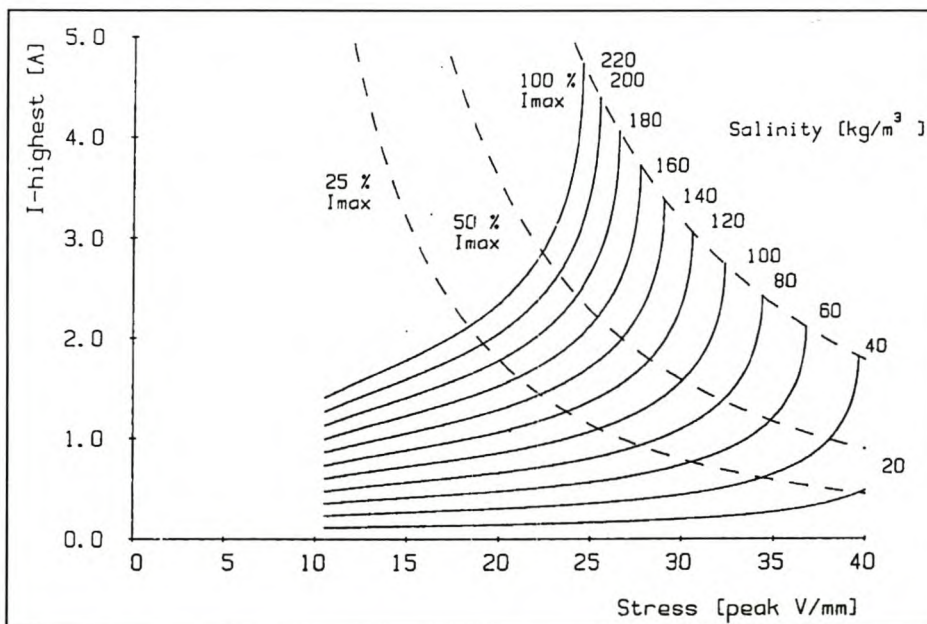


Figure 1-4: Relationship between Peak Leakage Current (A), Applied Stress (peak V/mm) and Salinity (kg/m^3) [4].

CHAPTER 1

This $I_{\text{permissible}}$ approach has been used more regularly in insulator condition monitoring than I_{max} since it allows enough time to remedy a problem without the insulator flashing over.

1.3.3 Commissioning of Various Natural Pollution Test Stations

After the unsuccessful tests performed at Koeberg, Holtzhausen et al. [5] constructed two new insulator pollution tests sites in Kuils River and Elands Bay. Both sites were chosen due to the severe pollution conditions experienced. This research was supported by the National Energy Council (NEC).

The Kuils River site was located approximately 20 km east from Cape Town and approximately 15 km from the sea. The site was located in an ESKOM substation (Cisco) in the vicinity of a steel smelting plant. It was reported that the substation insulation had to be washed fortnightly during that period due to the industrial pollution deposits.

The Elands Bay site was located along the West Coast of South Africa approximately 180 km north of Cape Town and approximately 50 meters from the sea. The site was next to the 50 kV Sishen – Saldanha railway traction line. This railway line is only used for the transport of iron ore to Saldanha. The contaminants at this test site were marine (salt spray) and industrial (iron ore blowing up from the passing trains).

Both test sites were equipped with various insulators of different materials and specific creepage distances (mm/kV). During the first test period at Elands Bay ceramic and some non-ceramic insulators were tested. Some ceramic insulators were greased or had their creepage distances extended after flashovers. During follow-up test periods mainly non-ceramic insulators were tested.

The Kuils River site results showed no flashovers or excessive leakage currents. The pollution appeared to be in the very light range, presumably due to the low wettability of the pollution from the steel smelting plant. Testing was stopped at Kuils River after

CHAPTER 1

a year and the test setup was moved back to the original Koeberg test site to accommodate new tests being made at the site.

The Elands Bay pollution measurements were more successful. After two years of measurements, the following recommendations regarding insulator materials and dimensions could be made [6]:

- Insulators in such severe areas must have specific creepage distances at a minimum of 30 mm/kV.
- Cyclo-aliphatic insulators were found as unsuitable for use in these areas as irreversible surface degradation was experienced.
- Silicone Rubber and EPDM insulators having specific creepage distances of 25 mm/kV and higher are recommended after acceptable performance was experienced.

1.3.4 The First Insulator Surface Conductivity Monitor Project

Another project, supported by the National Energy Council (NEC), involved the development of the first Insulator Pollution Monitoring Apparatus (IPMA) by Potgieter [7]. The IPMA was inspired directly by the Pollution Monitoring Equipment (PME) built by CESI [8] as it also measures layer conductivity on two test insulators that was naturally polluted and artificially wetted during the measurement cycle.

Both devices also had a chamber that was able to move upwards to cover the test insulators in a chamber to perform artificial wetting tests. The IPMA shell was lifted over the insulators when the steam was ready and the steam flowed into the chamber. This testing method directly simulated the clean fog method used in laboratories as the chamber is filled with steam.

Potgieter's project objectives were to design and build a pollution monitor and to commission this device at a test site. A further objective was to establish if a correlation existed between measured leakage currents and surface conductivities at this test site.

CHAPTER 1

Test insulators that were used included glass discs and porcelain long rods of different specific creepage distances. A poor correlation was found and this can be possibly attributed to the difference in the relative humidity between the two types of tests (an expected 100% humidity for the IPMA measurements compared to the ambient humidity for the leakage current measurements).

1.3.5 The Second Insulator Surface Conductivity Monitor Project

Davel's project [9] involved the second Insulator Pollution Monitoring Apparatus (IPMA). This project was supported by ESKOM's Tertiary Education Support Program (TESP). This IPMA was substantially redesigned from the previous version, in the physical construction as well as the control algorithm. Another result from the new design was an attempt to have a much smaller device than the previous device. The first IPMA measured 1.5 m × 1.0 m × 3.16 m (4.74 m³) compared to the new dimensions of 1.2m × 0.6m × 1.6m (1.15 m³). An image of the second IPMA is shown in Figure 1-5.

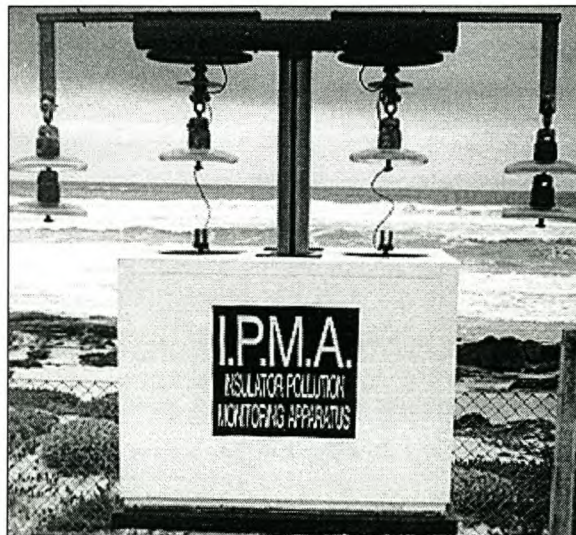


Figure 1-5: Image of the second IPMA installed at a coastal site [10].

CHAPTER 1

The project only comprised of the laboratory calibration of the device as various different techniques were tried to determine if the artificial wetting tests worked correctly. The calibration curve was to relate the measured surface conductivity to a well-known pollution severity classification, the Equivalent Salt Deposit Density (ESDD). Problems that were experienced during the tests were the selection of the correct testing voltage and whether the pollution layer was sufficiently wetted during tests.

The redesigned artificial wetting system had a pressurised steam generator compared to the open steam generator used in the first IPMA that resulted in washing when the humidity was too high. The new steam generator was used to inject bursts of steam into the test chamber compared to the previous steam generator that allowed the natural flow of steam into the test chamber.

It was determined through the humidity measurement on the insulator surface that the relative humidity during artificial wetting tests was not at an expected value of humidity. This resulted that measurements were made during conditions when the pollution layer was not completely dissolved into a conductive solution. This condition was also responsible at times to wash away the pollution layer, which was unwanted as the IPMA testing technique was designed to be a non-destructive testing technique.

Davel developed a method to relate the artificial wetting added to the test chamber to an amount of condensation deposited on the insulator surface. The use of this method was limited as the conditions for which the formula was valid were not compatible with IPMA conditions.

The IPMA was nevertheless found to be suitable device to determine pollution severity based on the artificial wetting process.

1.3.6 The Third Insulator Surface Conductivity Monitor Project

Van Wyk's project [10] was the third IPMA project at the University of Stellenbosch. The project objectives were the calibration and installation of the device described in the previous section at the Koeberg Insulator Pollution Test Station (KIPTS) and the implementation of a Round Robin test protocol at KIPTS and the Brandbaai Insulator Pollution Test Station (BIPTS). The IPMA and Round Robin field results were compared to determine if correlation existed between the two pollution assessment methods. This project was also supported by ESKOM (TESP).

The IPMA was calibrated in the laboratory using the solid layer method prescribed in the IEC 60507 [11]. The calibration curve was to relate the measured surface conductivity to the pollution severity classification, the Equivalent Salt Deposit Density (ESDD). The calibration curve showed a strong linear relationship between the measured conductivity and the ESDD value of the disc after the test. The IPMA was installed at KIPTS after the calibration process and used a single standard glass disc as a test insulator. The test disc was chosen to be the identical as the Round Robin test disc.

The IPMA was configured to perform two daily ESDD tests, one at midday and one at midnight. These measurements were used to determine the daily fluctuations in the test insulator's pollution severity.

The results obtained in this project reflected that the IPMA is a useful tool to determine insulator pollution severity. The Round Robin pollution test protocol showed definite trends for the different seasons and that the environmental factors such as wind speed, wind direction and rain plays an important role in the collection of pollution on insulation. The project, however, showed a poor correlation between measured IPMA values and measured Round Robin values. This was attributed to the fact that the Round Robin measurements were determined on a monthly basis compared to the accumulated daily ESDD values.

CHAPTER 1

Van Wyk also showed that the IPMA could be used to measure the surface conductivity of non-ceramic insulators providing an indication of the ageing of the insulator surface [12].

1.3.7 Research in the Performance of Different Insulating Materials at a Severe Coastal Site

Vosloo [13] conducted a research programme in which different insulating materials and coatings used in South Africa were compared during natural exposure at KIPTS. The insulators used during this programme were specially manufactured so that they all exhibited identical creepage distances, connecting lengths, inter-shed spacings, profiles, etc.

The insulators were installed as new and monitored over a period of one year. One insulator of each type was energised and one insulator of each type was exposed to the same environment, non-energised. A third insulator of each type was kept in storage and was used as a reference insulator when surface observations and material analysis were performed on the exposed insulators.

Leakage currents, electrical discharge (corona) activity, climatic and environmental data were collected over the test period. The peak leakage current, peak leakage current waveform surface conductivity, accumulated electrical charge and calculated critical flashover voltage of each insulator was statistically applied to investigate the correlation between measured electrical performance and environmental influences.

The statistical results showed very good correlation between the measured electrical and environmental values. The results were applied to rank the various materials and coatings according to performance.

During this project the IPMA, as used by Van Wyk (see section 1.3.5), was in operation at KIPTS and was used to assist in obtaining the surface conductivity of the insulators used in the research. The apparatus was thus used to perform regular

CHAPTER 1

tests on the different insulating materials, including non-ceramic insulation, under investigation. Vosloo also derived the surface conductivity of insulators from measured peak leakage currents and voltages.

1.4 PROJECT OBJECTIVES

The project objectives of this research are divided into two main groups. Firstly, the device was tested in a laboratory and thereafter installed at a natural pollution test site.

The laboratory tests initially consisted of the commissioning and calibration of the device. During this process the apparatus had to be “fine tuned” and certain design modifications of the software and the steam supply circuit in particular had to be done. The IPMR was thereafter used during artificial pollution tests to determine whether the device was capable of relating critical insulator performance based on the measured results.

The IPMR was installed at a natural pollution test site along the Cape west coast after the laboratory tests were completed. The IPMR measurements obtained were firstly analysed to determine whether the device was capable of predicting critical insulator performance and thereafter used to determine the site severity classification.

1.5 STRUCTURE OF THIS THESIS

Chapter 1: A general introduction to the applications of pollution monitoring measurements, a literature study focussing on more than 20 years of pollution monitoring work performed by the University of Stellenbosch and the objectives of this project are stated.

Chapter 2: A review of the main methods employed to measure pollution severity.

CHAPTER 1

Chapter 3: The Insulator Pollution Monitoring Relay (IPMR) is introduced including a discussion of the design principles, hardware components and the measuring and control units.

Chapter 4: Various modifications to the device and tests performed at the University of Stellenbosch are discussed. These tests include the calibration of the device as well as surface conductivity measurements during salt fog tests.

Chapter 5: This chapter discusses the installation of the device at a severe coastal site. The instantaneous severity measurements obtained by IPMR are related to flashover events that occurred. The IPMR measurements are also used to develop the pollution severity profile for the particular insulator test site.

Chapter 6: The conclusions and recommendations of this project are given in this chapter.

Appendix A: The appendix includes all the measured IPMR data for the test period.

2 REVIEW OF METHODS TO DETERMINE POLLUTION SEVERITY

2.1 INTRODUCTION

This chapter introduces the most important measurement techniques that are employed to determine the pollution severity and performance on high voltage insulators. The techniques include environmental monitoring, non-electrical insulator tests and electrical insulator tests. The different measurement procedures and the equations used to determine the severity or performance are discussed.

2.2 ENVIRONMENTAL MONITORING

An important aspect for the determination of the pollution severity of a specific area is to study the effect that the environmental conditions have on the occurrence of pollution to the site. Vosloo [13] concluded that the performance of insulators under polluted conditions could largely be attributed to the insulation materials used and the environmental factors experienced. Pietersen [14] investigated the possibility to develop an Insulator Pollution Severity Application Map (IPSAM) based on environmental measurements (DDG), corrosion measurements (CLIMAT) and non-electrical insulator tests (ESDD) made at various distances from the coast.

2.2.1 Geographical Location

The performance of insulation can directly be related to the geographical location where the line or substation is planned or situated. The IEC document 60815, "Guide for the Selection of Insulators in Respect of Polluted Conditions" [15], classifies the location under investigation into four groups of pollution levels according to the type

CHAPTER 2

of environment and the industrial or agricultural activities performed in the vicinity of this location. This pollution classification can be seen in Table 2-1.

Table 2-1: Classification of pollution levels according to the environment [15]

Pollution Level	Examples of Typical Environments
I – Light	Areas without industries and with low density of houses equipped with heating plants Areas with low density of industries or houses but subjected to frequent winds and/or rainfall Agricultural areas ¹⁾ Mountainous areas All these areas shall be situated at least 10 km to 20 km from the sea and shall not be exposed to winds directly from the sea ²⁾
II – Medium	Areas with industries not producing particularly polluting smoke and/or with average density of houses equipped with heating plants Areas with high density of houses and/or industries but subjected to frequent winds and/or rainfall Areas exposed to wind from the sea but not too close to the coast (at least several kilometres distant) ²⁾
III – Heavy	Areas with high density of industries and suburbs of large cities with high density of heating plants producing pollution Areas close to the sea in any case exposed to relatively strong winds from the sea ²⁾
IV – Very Heavy	Areas generally of moderate extent, subjected to conductive dusts and to industrial smoke producing particularly thick conductive deposits Areas generally of moderate extent, very close to the coast and exposed to sea-spray or to very strong and polluting winds from the sea Desert areas, characterised by no rain for long periods, exposed to strong winds carrying sand and salt, and subjected to regular condensation

1) Use of fertilizers by spraying, or the burning of crop residues, can lead to a higher pollution level due to dispersal by wind.

2) Distances from seacoast depend on the topography of the coastal area and on extreme wind conditions.

The pollution classification found from Table 2-1 is then used to select the minimum specific creepage distance (mm/kV) from Table 2-2 as required for the insulation to be used in the proposed area. The method to determine expected severity from Table 2-1 is only applied as a guideline.

Table 2-2: Specific Creepage Distance required for each pollution level [15]

Pollution Classification	Minimum Nominal Specific Creepage Distance (mm/kV)
Light	16
Medium	20
Heavy	25
Very Heavy	31

CHAPTER 2

2.2.2 Directional Deposit Gauge

2.2.2.1 Description

The Directional Deposit Gauge (DDG) was designed as a method to collect wind-deposited particles through a vertical slot facing each of the four main wind directions. Each gauge can relate the amount of contamination collected and a rough account of the main direction of the contributors of contamination to the specific location.

The test set-up is a very simple and inexpensive method to determine the pollution severity of a site. The set-up is ideal for use in the planning stages of an overhead line or substation.

The DDG is constructed by the following components [16]:

- Four vertical collection tubes having a $\pm 370\text{mm} \times 40\text{mm}$ slot milled into each. The tubes are aligned so that each slot faces one of the main wind directions (north, east, south and west). The top of the pipe must be sealed to ensure that the slot is the only opening collecting the particles.
- Four removable containers for the collection of the particles. The containers are mounted underneath the pipe to collect the particles. The container's volume must be of such a size that rainwater is also collected.
- A pole structure to attach the gauges to the height of 3 metres.

One DDG collection tube and container assembly is shown in Figure 2-1.

Macey [17] prescribed a different amount of distilled water that must be applied to the containers to dissolve the low soluble salts in the container. He determined that 500 ml distilled water must be added to the container to sufficiently dissolve all the particles. When rainwater was collected in the test period, distilled water should be added until the total volume was 500 ml. No distilled water should be added to the container if more than 500 ml rainwater was collected in the container.

CHAPTER 2

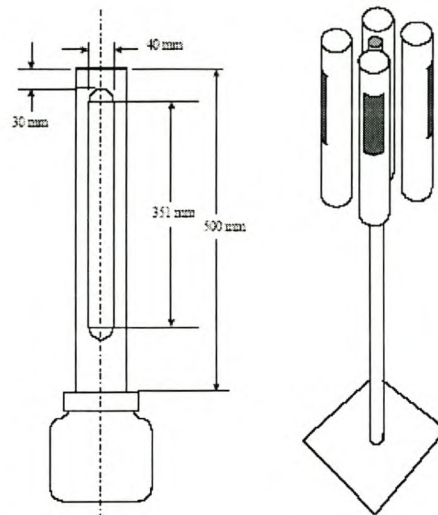


Figure 2-1: DDG collection tube and container [16]

2.2.2.2 Measurement Procedure

- Spray distilled water in the collection tube before the container is removed to ensure that particles that remained on the wall of the tube are collected in the container.
- Remove the container clearly marking the wind direction and location where it was removed and replace it with the container for the next testing period.
- Remove any insects, leaves or twigs that were collected in the container, as it would affect the measurement.
- Add 500ml distilled water to the container to dissolve the particles. If the container already contains collected rainwater, the remaining volume can be filled up to 500ml by adding distilled water. No distilled water is added when more than 500ml of rainwater was collected in the container.
- Note the volume of collected rainwater and distilled water added.
- Note the number of days the gauges was exposed. This value must be between 20 and 40 days.
- Measure the volume conductivity of the solution with a conductivity meter.

CHAPTER 2

2.2.2.3 Calculation of the DDG Pollution Index

The measured volume conductivity must be normalised to a volume of 500 ml and 30 days. The following equation is used to calculate the normalised conductivity:

$$\sigma_n = C \cdot (V/500) \cdot (30/N) \quad (\text{Eq. 2.1})$$

Where:

σ_n = normalised conductivity ($\mu\text{S}/\text{cm}$)

C = measured volume conductivity ($\mu\text{S}/\text{cm}$)

V = volume (ml)

N = number of days

The mean conductivity is obtained by averaging the four normalised conductivities measured for each of the wind directions. The pollution index is therefore defined as the mean value of the conductivities. The following equation is used to calculate the normalised conductivity:

$$\text{Average } \sigma = \frac{(\sigma_N + \sigma_S + \sigma_E + \sigma_W)}{4} \quad (\text{Eq. 2.2})$$

Where:

σ_N , σ_S , σ_E and σ_W are the normalised measured conductivities for the four main wind directions.

2.2.2.4 Classification of the DDG Pollution Index

After the DDG value has been established, the severity can be established by using Table 2-3.

CHAPTER 2

Table 2-3: DDG Pollution Index Classification.

Pollution Classification	DDG Pollution Index ($\mu\text{S}/\text{cm}$) [18]
Light	0 75
Medium	76 200
Heavy	201 350
Very Heavy	> 350

The disadvantage of the use of the DDG to determine site severity is that no insulators are used in test. This method cannot assess the self-cleaning properties of an insulator and the effect of the insulator profile in the area. The DDG can thus predict a high Pollution Index, although insulation in heavily polluted conditions, which are cleaned regularly, can operate correctly for long periods. Another example of inconsistencies that can be measured with the DDG is in areas with low rainfall but with a high occurrence of fog. These areas will actually have a higher pollution severity than that indicated by the DDG Pollution Index.

2.2.3 Meteorological Monitoring

Conductive and inert materials are transported due to air movement onto the surface of an insulator. It is therefore important to investigate the effect that wind speed and direction has on the area under investigation. It is also of great importance to determine the position of possible pollution sources in the vicinity of the location and to study the amount of pollution that these sources contribute to the location.

An example of the effect of temperature that can be seen on the performance of insulation is when the electrical activity increases due to moisture formation when the temperature drops below the dew point temperature. Fog or light rain can wet the surface of an insulator to such an extent that leakage currents increase. Heavier rainfall, on the other hand, can contribute to the natural washing of the insulator, cleaning it of pollutants. The effect of solar radiation can be seen on the degradation of the surface condition of non-ceramic insulators.

CHAPTER 2

A small, portable weather station can thus be employed to monitor the following meteorological variables:

- Temperature (°C)
- Relative Humidity (%RH)
- Wind Speed & Direction (m/s & deg.)
- Rainfall (mm)
- UV Radiation ($\mu\text{W}/\text{cm}^2$)
- Dew Point Temperature (°C)

2.3 NON-ELECTRICAL INSULATOR TESTS

2.3.1 The Equivalent Salt Deposit Density

2.3.1.1 Description

The equivalent salt deposit density (ESDD) can be defined as the equivalent deposit of NaCl on the insulator surface that will have the same electrical conductivity as that of the actual deposit dissolved in the same amount of water. The ESDD is performed by carefully removing the pollutant from the insulator surface by using various types of tools e.g. tissues, sponges, scrapers, spatulas or brushes. The removed contaminant is then dissolved in a known quantity of distilled water. The conductivity of the solution is measured and the results normalised to a temperature of 20°C.

2.3.1.2 Measurement Procedure

- Avoid touching the areas of the insulator when handling to prevent loss of pollution.
- Use a large washbowl and place the insulator in the bowl.

CHAPTER 2

- Measure 1ℓ distilled water, measure the conductivity of the water and pour it into the bowl.
- Wear surgical gloves or make sure that hands are washed thoroughly to avoid contamination.
- Carefully wash the insulator area with even strokes assuring that the pollution are removed.
- Avoid touching other areas that is not part of the area that is being sampled during the washing process, as it will give an inaccurate representation of the deposit. Care should be taken not to wipe the metallic end parts of the insulator.
- Ensure that no water is spilt during the washing process, as it will give an inaccurate representation of the deposit.
- Carefully stir the solution until all deposits are properly dissolved in the distilled water.
- Make sure to include all utensils used to remove the pollution from the insulator surface in the conductivity measurement.
- Measure and note the conductivity and temperature of the solution.

2.3.1.3 Calculation of the ESDD Pollution Index

The ESDD is calculated by measuring the volume conductivity, temperature of the solution, volume of the solution and the area of the insulator that was cleaned. The volume conductivities must be corrected to 20 °C [16].

The following equation is used to relate the conductivity:

$$\sigma_{20} = \sigma_{\theta} [1 - 0.02277 \cdot (\theta - 20) e^{0.01956 \cdot (\theta - 20)}] \quad (\text{Eq. 2.3})$$

Where:

σ_{θ} = measured volume conductivity at θ °C (S/m)

σ_{20} = volume conductivity corrected to 20 °C (S/m)

CHAPTER 2

Brushes, sponges, scrapers and spatulas can be used for the removal of stubborn dirt but the tools must also be included in the conductivity test. This is to ensure that no contaminants stay behind on the instruments when the conductivity measurement is taken.

The salinity of the solution is determined by the use of the following formula:

$$S_a = (5.7 \cdot \sigma_{20})^{1.03} \quad (\text{Eq. 2.4})$$

Where:

S_a = salinity (kg/m³)

σ_{20} = normalized conductivity (S/m)

The ESDD in mg/cm² can then be calculated by the using the following formula:

$$\text{ESDD} = \frac{S_a \cdot V}{A} \quad (\text{Eq. 2.5.})$$

Where:

V = volume of the solution (cm³)

A = area of the cleaned surface (cm²)

These equations are valid when the temperature range is between 5 – 30°C and σ_{20} is in the range 0.004 – 0.4 S/m.

2.3.1.4 Classification of the ESDD Pollution Index

After the ESDD value has been established, the severity can be determined by using Table 2-4 below. Two similar ESDD classifications [18], [19] are shown below in Table 2-4. The advantage of the CIGRÉ classification [19] is that a finer classification can be obtained.

CHAPTER 2

Table 2-4: ESDD Pollution Index Classification.

Pollution Classification	ESDD (mg/cm ²) [18]	ESDD (mg/cm ²) [19]
None		0.0075 0.015
Very Light		0.015 0.03
Light	< 0.06	0.03 0.06
Medium	0.06 0.12	0.06 0.12
Heavy	0.12 0.24	0.12 0.24
Very Heavy	> 0.24	0.24 0.48
Exceptional		> 0.48

ESDD is a useful test that can be applied to naturally and artificially polluted insulators. The performance of an insulator profile can be determined when ESDD tests are performed on regular intervals on a set of insulators. The process of the determination of pollution severity via ESDD measurement is however time-consuming. Another disadvantage of the ESDD measurement is that the pollution layer is destroyed during the test which creates a problem when a study is to be done over a long period of time. Another problem encountered with this testing method is that the measurement only quantifies the severity of the pollution layer at a specific point in time.

2.3.2 Non Soluble Deposit Density

2.3.2.1 Description

The Non Soluble Deposit Density (NSDD) is used to indicate the amount of non-soluble inert material that was deposited on the surface of an insulator. The inert materials have little or no electrical properties but act as a bonding material for electrical significant deposits e.g. ionic salts. Non-soluble deposits largely occur in areas where mining, agricultural and industrial activities occur and include cement, lime, dust and clay.

CHAPTER 2

The measurement of the amount of NSDD on an insulator surface is done by the filtration of the washed solution obtained from the insulator surface. The NSDD test is usually performed after the ESDD of the solution was determined. This also allows for a better understanding of the amount of conductive and non-soluble material deposited on the insulator surface. Riquel [20] showed by experimental results that a minimum of non-soluble material is needed to form a conductive channel between the electrodes of an artificially polluted insulator.

2.3.2.2 Measurement Procedure

- Measure the weight of the filter paper before the filtration process starts.
- Filter the solution through a funnel fitted with wet-strengthened filter paper. Repeat the process at least three times to ensure that all the particles are collected.
- Allow for the filter paper to dry. An oven can be used to speed up the process. Remove the filter paper and leave the paper at room temperature for a day to allow for the dried paper to settle at room temperature.
- Measure the weight of the dried filter paper.

2.3.2.3 Calculation of the NSDD Pollution Index

The NSDD is calculated by dividing the difference in weights of the filter paper before and after the filtration process by the area it was removed from.

The NSDD in mg/cm² can then be calculated by the using the following formula:

$$\text{NSDD} = \frac{\text{Mass2} - \text{Mass1}}{\text{Area}} \quad (\text{Eq. 2.6})$$

CHAPTER 2

Where:

Mass1 = weight of the dry clean filter paper (mg).

Mass2 = weight of the dry used filter paper (mg).

Area = area of the cleaned surface (cm²)

2.3.2.4 Classification of the NSDD Pollution Index

Riquel [20] suggested a rough classification guide of NSDD values but these values are not classification guidelines laid down by the IEC. This classification can be seen in Table 2-5.

Table 2-5: NSDD Pollution Classification.

Pollution Classification	NSDD (mg/cm²) [20]
Light	0.15
Medium	0.45
Heavy	0.90
Very Heavy	1.95

2.4 ELECTRICAL INSULATOR TESTS

2.4.1 Surface Conductivity Measurement

The degree of pollution on an insulator surface can be determined by the surface conductivity measurement. This useful information can be used to acquire useful knowledge in the behaviour of insulation in polluted areas. The surface conductivity method can be used to relate site severity to electrical performance.

CHAPTER 2

2.4.1.1 Surface Conductivity Measurement With Natural Wetting

The use of a device to determine site severity by the surface conductivity measurement with natural wetting was reported during the late 1960 s in the Federal Republic of Germany [21], [22].

Sforzini et al. [23] developed an approach for the selection of insulators to be used in polluted areas based on natural surface conductance measurements. The test insulators were energized every 15 minutes with two cycles of the 50 Hz wave of the 10 kV_{rms} test voltage to determine the surface conductance. The short application of the test voltage is to avoid the formation of dry bands that can distort the leakage current measurements. The voltage must also be high enough to avoid wrong measurements due to discontinuities in the pollution surface. The application of a test voltage and the logging of the resulting leakage current accomplish this measurement.

Various insulators were tested in artificial pollution tests using both salt fog and solid layer methods. The artificial pollution test parameter (Salt Fog: ESDD (mg/cm²), Solid Layer: Salinity (kg/m³)) and the surface conductance were measured for each insulator during the artificial pollution tests. The equivalent laboratory severity of the test location could then be determined by comparing the naturally measured surface conductance with the relevant artificial pollution test surface conductance measurement.

The main disadvantage of this type of surface conductivity measurement combined with natural wetting is that after a long dry period the pollution could build up to high pollution levels. Surface conductivity measurements would indicate low presence of pollution due to the high resistance of the dry pollution layer.

CHAPTER 2

2.4.1.2 Surface Conductivity Measurement With Artificial Wetting

The use of artificial wetting in the determination of surface conductivity on polluted insulators is the solution to the shortcoming explained in the previous measurement. The surface conductivity measurement technique including artificial wetting was included in pollution monitors described by Bertazzi [8], Potgieter [7], Davel [9] and Van Wyk [10].

The monitors described above each required a movable enclosure to allow for the insulator to be enclosed before being wetted artificially. The conductivity measurement is performed similarly although the pollution layer's conductivity value is the maximum value that would occur if critical wetting were applied. The method of surface conductivity measurement with artificial wetting can give the true representation of the pollution layer and can therefore be used to determine pollution severity more accurately. The pollution monitoring device described in this thesis uses both surface conductivity measurement techniques to assess site severity.

2.4.2 Leakage Current Measurement

Leakage currents can provide important information on the performance of insulation under polluted conditions. The application of specialised equipment for the measurement and recording of these leakage currents can give valuable insights to the electrical performance of insulation. The benefit of the application of leakage current monitoring is that it is a non-destructive monitoring method.

Petrusch et al. [24] performed leakage current monitoring over a few years to determine the actual insulation strengths in a number of substations. The results obtained from these tests gave better information to the site severity, the necessity and the frequency of greasing and cleaning of insulation. As an example, a test site that was re-greased yearly was extended to a cleaning period of 4 years. This example demonstrates the reduction of maintenance costs and maintenance time.

CHAPTER 2

Verma [25] derived the well-known I_{\max} theory after a large number of experiments were performed on artificially polluted insulators. The I_{\max} was defined as the minimum amount of peak leakage current needed to cause a flashover. The I_{\max} theory was found to be independent of the insulator profile, type of pollutant applied or test procedure followed. This proved valuable since it could be applied to insulators tested under natural or artificial conditions. I_{\max} was expressed by the following equation:

$$I_{\max} = \left[\frac{SCD}{15.32} \right]^2 \quad (\text{Eq. 2.7})$$

Where:

SCD = specific creepage distance of the insulator (mm / kV).

I_{\max} represents the critical current required for a flashover to occur. It is therefore a value that corresponds to the critical arc length required for flashover. I_{\max} is calculated as a function of the insulator creepage distance for the specific operating voltage.

The leakage current method can only produce accurate severity measurement results when relative humidity is higher than 90%. The use of leakage current monitoring can only effectively be used during conditions with a high likelihood of flashover occurrence. The measurement of leakage current, however, can serve a very important function as an experimental tool in the study of the behaviour of insulation under polluted conditions.

2.5 SUMMARY

This chapter was used to discuss various methods that can be employed to assess site severity. Methods ranged from site severity classification linked to geographical location to electrical tests performed on a specific insulator. The description of the

CHAPTER 2

various test methods available was made to underline the test methods employed by the IPMR to determine site severity and relative insulator performance.

3 THE INSULATOR POLLUTION MONITORING RELAY (IPMR)

3.1 INTRODUCTION

The Insulator Pollution Monitoring Relay (IPMR) is introduced in this chapter showing the hardware components, different IPMR measurements, control system and IPMR software.

3.2 THE PRINCIPLE OF THE IPMR

The need arose to develop a new pollution monitor after extensive experience that was gained from the two previous insulator pollution monitors [7], [9], [10]. New functions were developed as certain shortcomings were evident in the previous devices designs. The experience gained from the previous models was used to improve the mechanical reliability of the device.

The IPMR concept was conceived by W. L. Vosloo (ESKOM, TSI), who was also involved with the two previous IPMA projects. HellKorr cc manufactured the IPMR and delivered it to the University of Stellenbosch for final commissioning and calibration, including the introduction of the steam injection tubing.

The main aims were to design a device that can:

- Measure the amount of pollution build-up experienced on a test insulator as a surface conductivity value with natural wetting. The site severity can then be expressed as a surface conductivity value.
- Measure the amount of pollution build-up experienced on a test insulator as a surface conductivity value with artificial wetting. The site severity can then be

CHAPTER 4

expressed as an ESDD value after a relationship between the measured surface conductivity value and the site severity parameter (ESDD) was determined.

- The device must be able to measure the I_{highest} currents on energized insulators in the surrounding area.
- The device must be able to give out alarms when the measured pollution levels exceed maximum permissible values.

The IPMR was designed so that the insulator was mounted on a movable platform that raised or lowered the insulator into the test chamber that was situated below the insulator. The idea was based on the movement of the insulator into the test chamber rather than moving the test chamber over the insulator. This design made the size of the IPMR to 1.3 m × 0.6 m × 0.6 m (0.47 m³). The IPMR's weight makes it possible for two men to carry it.

3.3 THE HARDWARE COMPONENTS OF THE IPMR

3.3.1 The IPMR Enclosure

The IPMR enclosure is constructed from a basic frame consisting of square stainless steel tubing. Stainless steel cladding is attached to the frame to form the IPMR enclosure. Access to the various components is easily obtained by the removal of the top lid or any one of three side panels. The enclosure is divided in three parts to create an instrumentation chamber, steam generator chamber and a test chamber. The IPMR enclosure is shown without panels in Figure 3-1.

The instrumentation chamber contains the control circuitry, high voltage transformer and the hot air blower. The steam generator chamber contains the steam generator. The test chamber contains the movable platform, the test insulator and the steam pipes. Thermal insulation panels line the test chamber to reduce temperature fluctuations in the test chamber.

CHAPTER 4

3.3.2 The Steam Generator

The IPMR steam generator is used to inject the steam into the test chamber during artificial wetting tests. The steam generator is a self-contained unit having both its control and protection units operating separately from the IPMR controller. The generator is equipped with a liquid level sensor to aid the filling process and a pressure switch to switch off the boiler element when the desired pressure (1,5 bar) is reached. Another liquid level sensor is used to switch off the boiler element when the water level is too low due to a possible loss of water supply. The steam generator is also equipped with a 3 bar mechanical steam relief valve to protect the steam generator in case of the failure of the pressure switch.

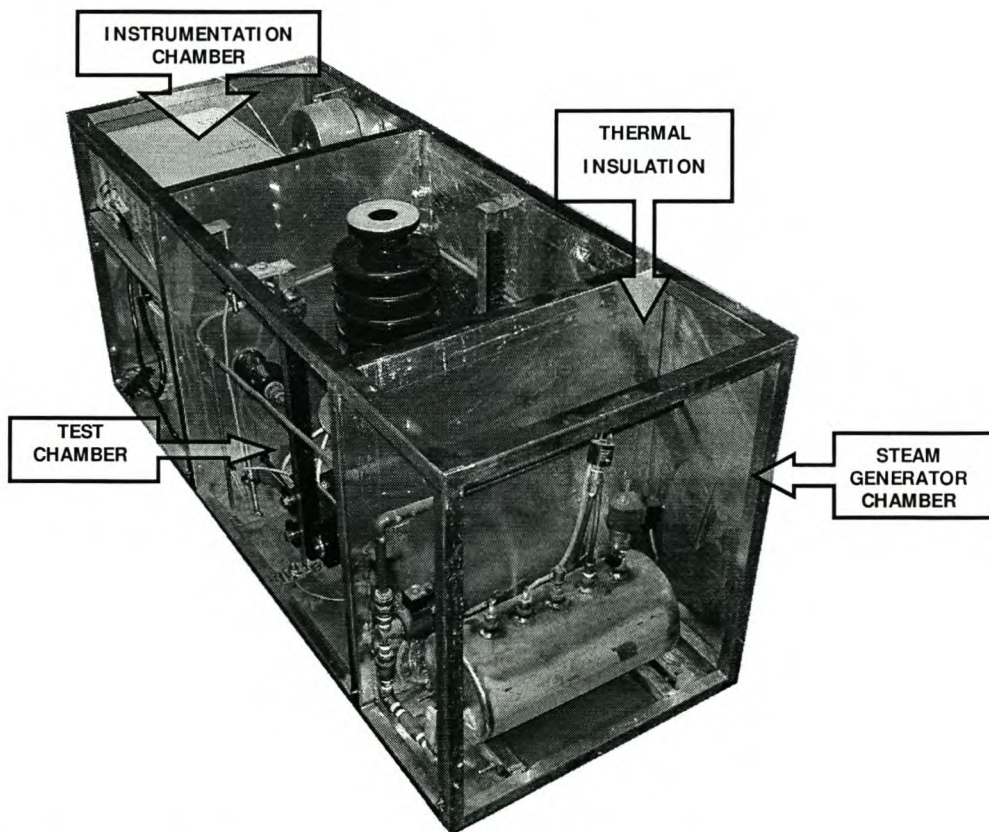


Figure 3-1: The IPMR shown with top and side panels removed.

CHAPTER 4

3.3.3 The Hot Air Dryer

The hot air dryer was constructed by placing a heating element in the outlet of a blower fan. The dryer is used to inject warm air into the test chamber. The insulator is dried at the start of each test to ensure that the insulator surface is dry before the wetting cycle is started. The insulator is dried at the end of each test to ensure that the insulator surface is dry when the insulator is returned to the environmental conditions. The dryer is switched by a triac that is controlled by the software.

3.3.4 The Test Transformer

A 3 kV, 4 kVA transformer was chosen as the test transformer. The transformer is capable of supplying 1.3 A at the secondary terminals which is more than enough than the maximum currents expected to flow during highly polluted conditions. The low voltage terminals are connected triac that is used to switch the transformer. The insulator is energised for five cycles of the 50 Hz wave. This was again done to avoid the formation of dry bands and the distortion of the measured values. The high voltage is applied across the insulator surface when the transformer is switched. Both neutrals of the transformer's terminals are joined to avoid unacceptable floating voltages. The high voltage is taken through the wall separating the test chamber from the instrumentation enclosure by means of two high voltage bushings. Connections were made between the transformer terminals and the bushings by using high voltage cable.

3.3.5 The Moving Platform

The test insulator is exposed to the surrounding environmental conditions under normal operation. At the start of the artificial wetting test the insulator is lowered into the test chamber. The test chamber acts as a controlled environment that shields the insulator from the surrounding environmental conditions during the tests. A geared

CHAPTER 4

motor is used to move the platform vertically by means of two sets of rack-and-pinion support columns. The test chamber is shown in Figure 3-2.

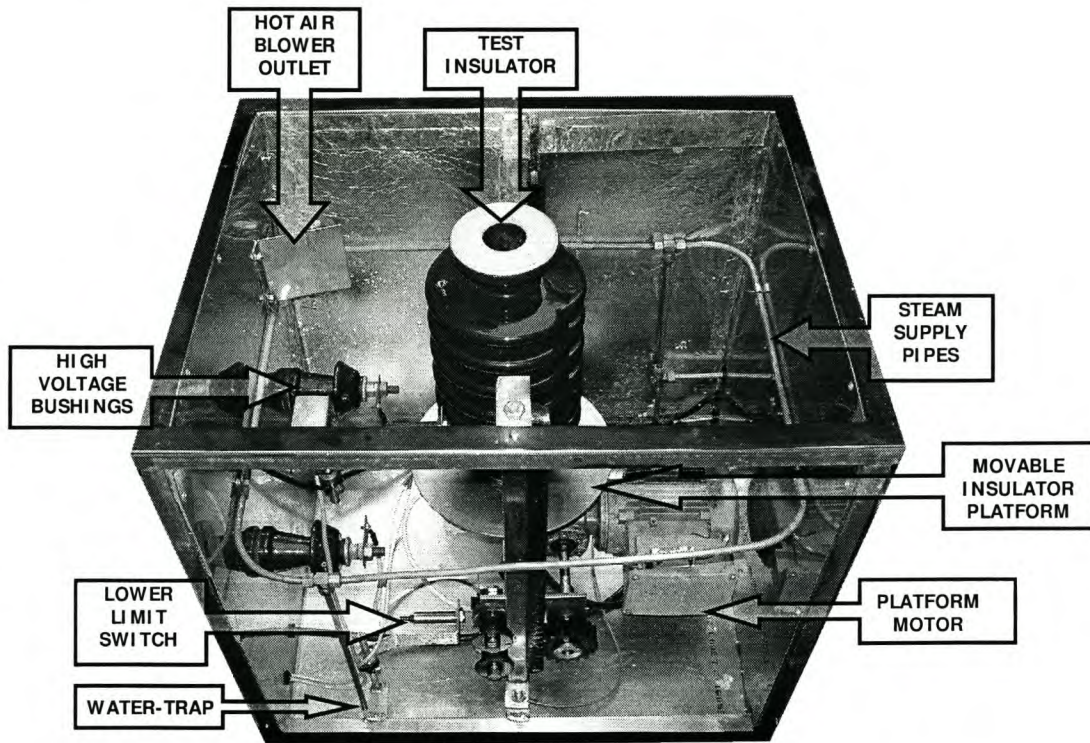


Figure 3-2: View of the IPMR test chamber, showing the various components.

The insulator is mounted on the platform, which in turn raises or lowers the insulator. Stainless steel discs fitted to the top and bottom of the insulator allows the test chamber to be sealed in both the raised or lowered positions. Magnetic reed switches positioned at the top and bottom of the chamber are used to stop the platform when it has reached the raised or lowered positions. The platform motor is also equipped with overcurrent protection. The time to raise (and lower) time-outs in the control software will also stop the platform in the case of a limit switch failing.

3.3.6 The Test Insulator

The IPMR test insulator used is a modified porcelain bushing. Figure 3-3 shows a cut-away view of the construction of the IPMR test insulator. Two copper straps (2&3) are used as the measurement points on the insulating surface (1). These straps are connected with high voltage cables (4) through the hollow core of the insulator to the high voltage supply. The important insulator dimensions and parameters of the test insulator are displayed below in Table 3-1.

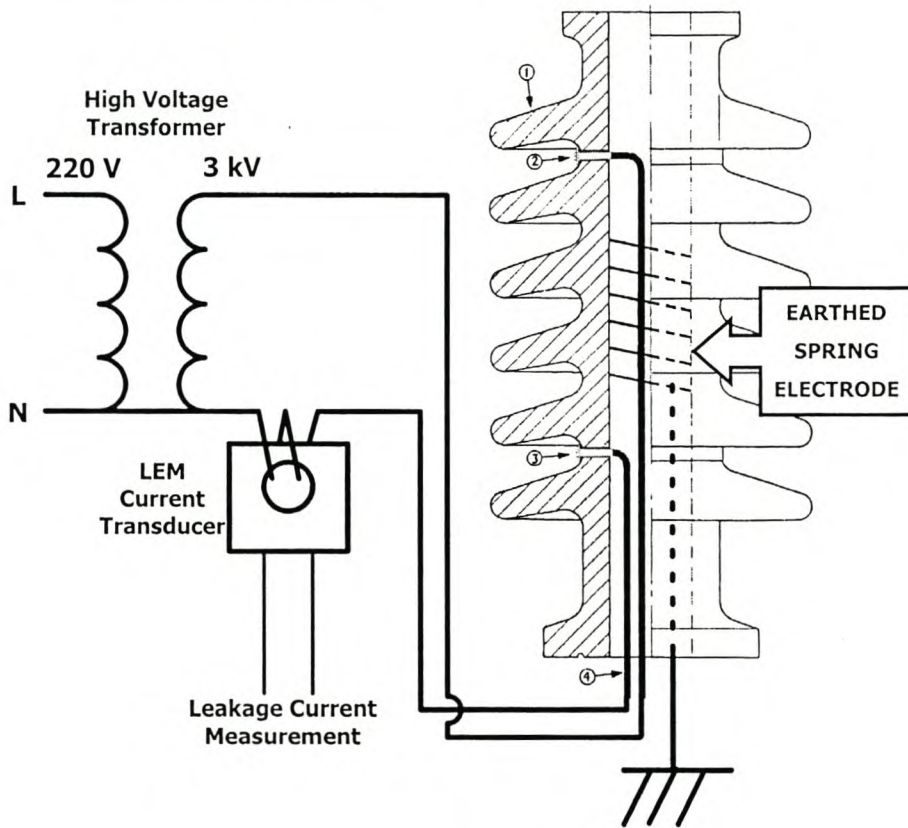


Figure 3-3: The IPMR insulator

Table 3-1: IPMR test insulator dimensions and parameters.

Creepage Distance	468.11 mm
Vertical height between straps	146.48 mm
Average Diameter	118.67 mm
Area	1780.761 cm ²
Form Factor	1.338

CHAPTER 4

During artificial pollution tests it was realised that there was a shorter internal leakage path through the hollow core of the insulator. This posed the problem that the measured leakage current actually consisted of two parallel leakage currents, one flowing on the outside of the insulator surface and one flowing internally through the hollow core. The bottom of the insulator core was open to allow the feeding of the high voltage cables through the platform base. This opening also exposed the hollow core to the steam during tests and moisture could enter into up the hollow core thus increasing leakage currents in the core.

A watertight connection box was mounted at the base of the platform to seal the opening, allowing the high voltage leads to pass through two compression glands. An earthed stainless steel spiral was also inserted in the hollow core of the insulator between the two high voltage terminals. This earthed spiral acts as a guard electrode shunting the unwanted leakage current directly to earth. The earthed electrode solved the problem encountered with the unwanted parallel leakage paths leading to wrong measurements.

3.3.7 The Steam Supply Pipes

The steam supply system that injects steam into the test chamber consist of 5/16" (7.93 mm) copper pipes. The steam pipes were constructed such that it terminates in a ring around the IPMR test insulator in the lowered position. Eight 1mm holes were drilled into the sides of the pipes allowing the steam to be injected from all sides along the test insulator. A top view of the test chamber in Figure 3-4 shows the direction of steam from the eight holes in the steam pipes indicated by arrows.

It was found that water sometimes splattered onto the insulator surface, leading to undesirable insulator washing. Two "water-traps" were thus included in the design to allow condensate to drain from the steam pipes. Condensate is formed when the steam, (at $\pm 110^{\circ}\text{C}$), comes into contact with the colder pipes, which are at ambient temperature at the start of the test. The amount of condensate formed becomes less over time as the pipes heat up to the steam temperature. The ring was slanted for the condensate to run down into the "water-traps".

CHAPTER 4

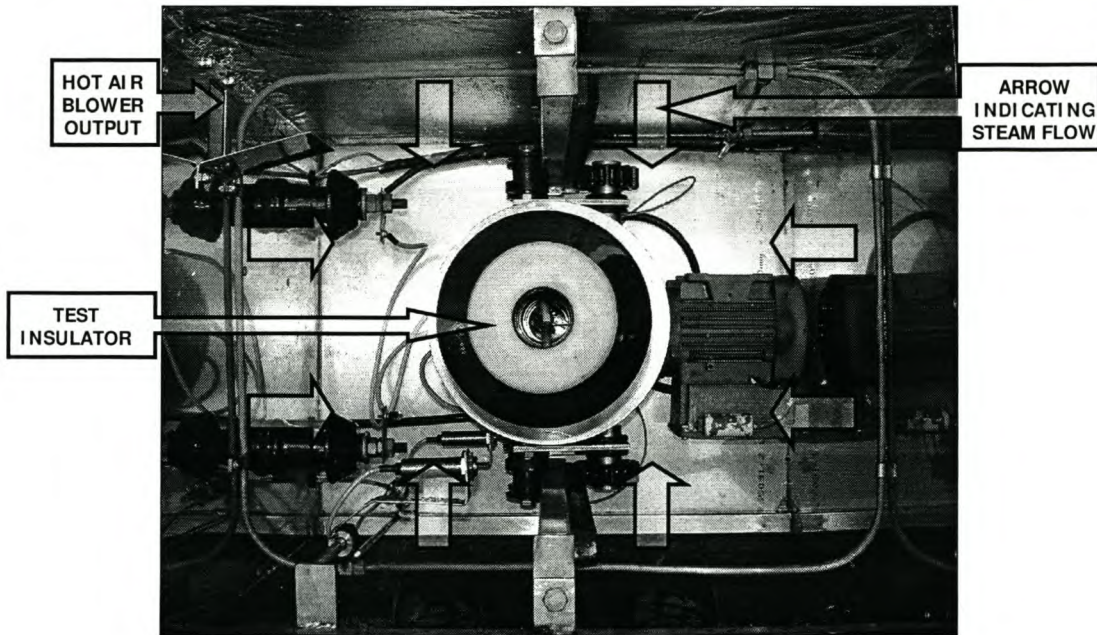


Figure 3-4: Top view of the IPMR test chamber.

3.4 IPMR MEASURING AND CONTROL UNITS

3.4.1 IPMR Measurements

The IPMR is utilised to monitor the pre-deposited pollution as well as the instances when instantaneous pollution deposits can occur. Pre-deposited pollution occurs at a natural rate and the surface conductivity is dependent on the degree of wetting on the insulator surface.

Instantaneous pollution deposits occur when highly conductive fog moves into the area causing flashovers but leaves a very low resultant pollution level on the insulator. This phenomenon is a serious threat to insulation since this condition typically occurs within less than an hour.

CHAPTER 4

The IPMR was thus designed to monitor:

- Surface conductivity on pre-deposited pollution with natural wetting.
- Surface conductivity on pre-deposited pollution with artificial wetting.
- Leakage currents on pre-deposited pollution with natural wetting as well as monitoring for the onset of instantaneous pollution deposits.

3.4.1.1 Surface Conductivity with Natural Wetting

In this mode the test insulator is energised at set intervals for five cycles to assess the surface conductivity under natural, pre-deposited pollution and natural wetting conditions.

3.4.1.2 Surface Conductivity with Artificial Wetting

In this mode the test insulator, having a naturally polluted surface, is enclosed in the test chamber while the surface conductivity is assessed under artificial wetting conditions. (Assuming that critical wetting occurs on the pre-deposited pollution.)

The IPMR measures the surface conductivity on the test insulator. At the beginning of the artificial wetting test, the insulator is lowered into the test chamber by the movable platform. The air dryer heats the air inside the chamber drying the pollution layer on the insulator. The reference conductivity is logged after applying five cycles of the 3 kV wave. The flow chart of the test is illustrated below in Figure 3-5.

During the measurement cycle the humidifier raises the humidity levels by repeatedly opening the steam valve for a short time to allow moisture absorption by the pollution layer. The humidifying process is repeated after a set time delay. A voltage of 3 kV is applied for five cycles to the insulator after every steam application and the resultant leakage currents are logged.

CHAPTER 4

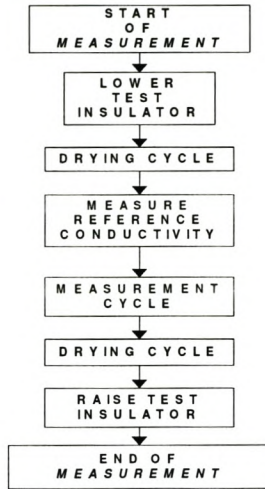


Figure 3-5: Flow chart of the surface conductivity test with artificial wetting.

The flow chart of a single measurement cycle with artificial wetting is shown below in Figure 3-6.

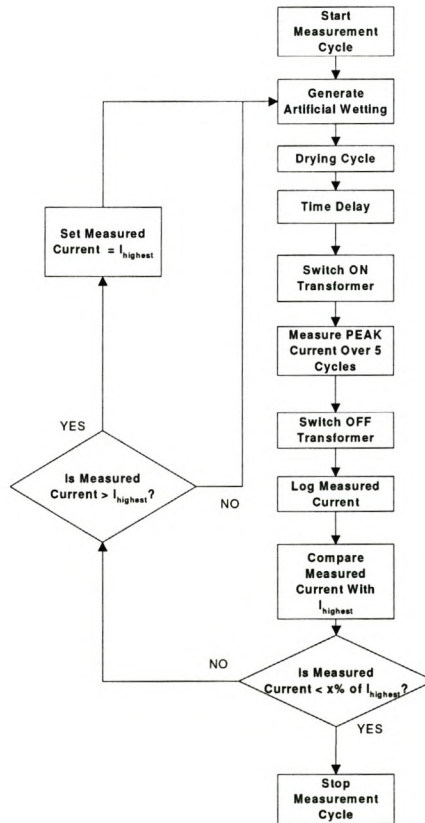


Figure 3-6: Flow chart during an artificial wetting cycle

CHAPTER 4

The test is repeated while the leakage currents stay within a set tolerance ($x\%$) of I_{highest} , the highest measured leakage current. If the measured leakage current is higher than I_{highest} , it will be stored as the new I_{highest} value. When the measured current is smaller than $x\%$ of I_{highest} , the test is stopped and the dryer dries the insulator. The test insulator will be raised to return the insulator to the natural environment.

The conductivity of an insulator is a function of leakage current through the contamination layer due to the applied voltage and depends on the specific insulator profile. It is therefore difficult to compare different insulators based on their conductance values. To overcome this effect, the surface conductivity value can be used to compare different insulators since it is independent of the insulator's geometry.

The measured surface conductance (G_s) is multiplied by the form factor (F) of the test insulator to determine the layer conductivity (σ_s) of the pollution layer.

$$\sigma_s = F \cdot G_s \quad (\text{Eq. 3.1})$$

The form factor identifies each insulator's shape in terms of the insulator radius (r) as a function of creepage length (dL_s) [11].

$$F = \int_0^{L_s} \frac{dL_s}{2 \cdot \pi \cdot r} \quad (\text{Eq. 3.2})$$

The surface conductivity measurement with artificial wetting values were related to ESDD values, as it existed as a standard defining the characteristics of the pollution layer. The ESDD can be defined as the equivalent deposit of NaCl on the insulator surface that will have the same electrical conductivity as that of the actual deposit dissolved in the same amount of water.

 CHAPTER 4

3.4.1.3 Leakage Current Measurement

Verma [25] published the well-known I_{max} theory in the late 1970 s. I_{max} was defined as the minimum amount of leakage current that was necessary to cause flashover. I_{max} was independent of the insulator shape, pollutant or test procedure. The only governing factor was the specific creepage distance (SCD, in mm/kV) of the insulator.

$$I_{max} = \left[\frac{SCD}{15.32} \right]^2 \quad (\text{Eq. 3.3})$$

I_{max} values can thus be used to predict the actual risk of flashover on a real-time basis. The $I_{permissible}$ is used as a criterion since the calculated I_{max} value was too close to the actual flashover. (Refer to the discussion in Section 1.3.2.)

$$I_{permissible} = I_{hfactor} \cdot \left[\frac{SCD}{15,32} \right]^2 \quad (\text{Eq. 3.4})$$

The $I_{permissible}$ value gives an indication of excessive leakage current rise that can lead to flashover, but can allow a large enough time margin to perhaps correct the poor insulation performance.

3.4.2 IPMR Measurement and Control Systems

3.4.2.1 IPMR Controller: (*IPMonitor*)

The control and measurement components are housed in the control box mounted inside the IPMR instrumentation chamber. The box is also used to supply the alarm and trip signals via relays. Three relays are allocated to give alarm signals when high levels of pollution are measured, viz. Conductivity Alarm, ESDD Alarm and Leakage

CHAPTER 4

Current Alarm. A fourth relay was allocated to give a signal (Diagnostic Alarm) when an error occurred in the IPMR control/measurement processes.

A microprocessor is used to control the different hardware components (described in section 3.3) during artificial and natural wetting tests and to log the measured values. The microprocessor is also used to handle communications, being either by RS485 or by remote communications via cellular modem. The measured values are stored on non-volatile RAM.

The memory has the following sizes available:

- ESDD: 400 loggings
- Micro Siemens: 2500 loggings
- Leakage Current: 2500 loggings
- Alarms: 200 loggings

The IPMR current measurement is obtained by allowing the leakage current to flow through a current sensor. The current sensor used is a LEM LA 55-P current transducer capable of measuring up to $\pm 400\text{mA}$. The applied voltage is measured at the low voltage side of the transformer. The voltage transducer used is a LEM LV 25-P, capable of measuring nominal voltages up to 500 V. Both current and voltage transducers have an insulation level of 2.5 kV.

3.4.2.2 Leakage Current Monitor: (*LCMonitor*)

The IPMR leakage current monitor was designed as a self-contained measurement device, only requiring an external supply voltage and communications connection. The leakage current monitor consists of two parts: the measurement enclosure (housing the current sensor) and the data logging enclosure (housing the microprocessor). A communications cable with a maximum length of $\pm 10\text{m}$ connects the two enclosures. Since the leakage current monitor was designed as a self-contained unit, it is capable of logging leakage current values without being connected to an IPMR.

CHAPTER 4

Multiple leakage current monitors can be connected forming a network using the RS485 LocalBus communications protocol used by the IPMR. The IPMR then acts as a RS485 LocalBus Controller. The IPMR is set up to monitor whether any of the leakage current monitors connected measured excessive leakage currents. The IPMR will trip the Leakage Current Alarm as soon as the IPMR senses that a leakage current monitor measured values exceeding a pre-set limit. This method simplifies the communications, as the user would only have to connect onto the IPMR as the IPMR facilitates the communication to the various leakage current sensors.

3.4.3 IPMR Software

HellKorr cc developed the software used to connect the IPMR with a PC. Figure 3-7 shows an image of the IPMR Software, graphically displaying measured field data. The software is used to communicate with the IPMR controller via a RS 232 / RS 485 converter.

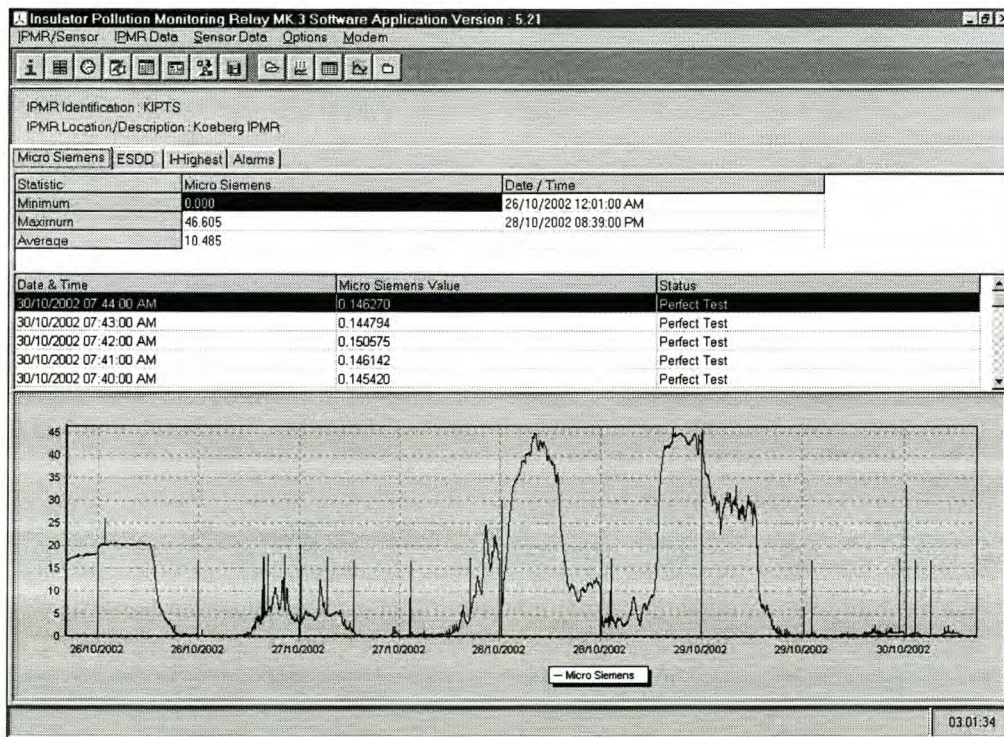


Figure 3-7: Graphical view of typical measured IPMR data.

CHAPTER 4

The IPMR software can be used to:

- Upload saved data from the IPMR.
- Upload saved data from the leakage current monitor(s).
- Modify time constants used in the measurement processes.
- Modify constants used to determine pollution values (form factor and specific creepage distance).
- Set up times of the surface conductivity with artificial wetting tests.
- Graphically view or export the measured values to a spreadsheet or printer.

The following IPMR test routine is used during the surface conductivity test using artificial wetting and the relevant user selectable times and constants are also shown in Figure 3-8. The rationale of the test cycle and its development is discussed in Chapter 4.

1. **Steam Preparation (s):** Opens the steam valve to clear and heat the steam pipes.
2. **Dryer 1 (s):** Switch on first drying cycle to disperse the remaining steam.
3. The insulator is lowered into the test chamber.
4. Apply test voltage and measure leakage current for the conductivity on the naturally wetted insulator surface. This measurement reflects at which state the insulator was before the start of the test.
5. **Dryer 2 (s):** Switch on second drying cycle to dry the insulator surface.
6. Apply test voltage and measure leakage current for the reference conductivity on the dry insulator surface.
7. **First Sample Humidify Time (s):** First steam injected into the chamber.
8. **Dryer 3 (s):** Switch on third drying cycle to swirl injected steam around chamber.
9. **After Humidify Time (s):** Time to wait for steam to settle between steam application and conductivity measurement.
10. Apply test voltage and measure leakage current.
11. **Wait Between Time (s):** Time to wait between conductivity measurement and next process.
12. **Humidify Time (s):** Steam injected into the chamber

CHAPTER 4

13. **Dryer 3 (s):** Switch on third drying cycle to swirl injected steam around chamber.
14. **After Humidify Time (s):** Time to wait for steam to settle between steam application and conductivity measurement.
15. Apply test voltage and measure leakage current.
16. **Dryer 4 (s):** Switch on fourth drying cycle to dry the insulator surface.
17. Raise insulator.
18. Calculate ESDD by using stored measured values and stored constants.

Steps 11-15 are repeated and the measured values logged until one of the following occurs (also explained in section 3.4.1.2):

- The measured leakage current drops below the **Decline Percentage (%)** of the maximum measured leakage current.
- A number of cycles/iterations indicate a decline in measured leakage currents (**Maximum Decline (value)**).
- A set amount (**Maximum Cycles (value)**) of iterations was performed.

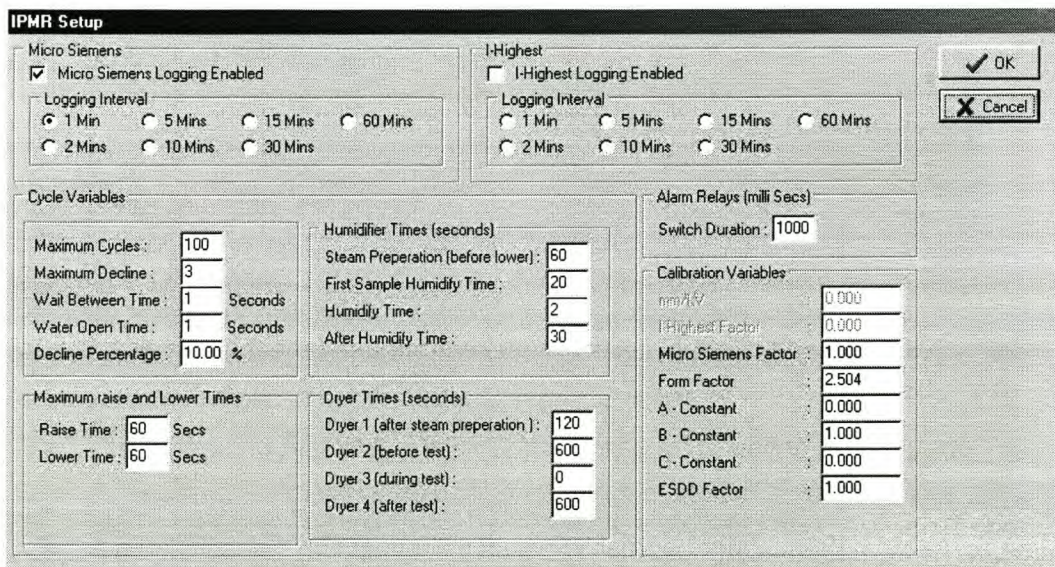


Figure 3-8: Artificial wetting test setup menu.

CHAPTER 4

3.5 SUMMARY

An Insulator Pollution Monitoring Relay (IPMR) prototype was designed and built before the start of the project. It was shown that the IPMR was based on a design improvement of two previous pollution monitoring devices developed and built at the University of Stellenbosch. The various hardware components of the IPMR were introduced and discussed. Unique hardware problems encountered and the solutions to these problems were discussed. The three types of IPMR measurements were introduced as well as the dedicated software developed to retrieve data and to change control and measurement constants.

4 IPMR MEASUREMENTS DURING ARTIFICIALLY POLLUTED CONDITIONS

4.1 INTRODUCTION

Various laboratory tests were conducted prior to field installation to determine whether the IPMR performs correctly. The tests included thermal tests, conductivity measurements with a standard resistor, calibration tests and repeatability tests. The IPMR was placed in a salt fog chamber after the successful completion of the above-mentioned tests to investigate the relationship between measured leakage current and surface conductivity during salt fog tests.

4.2 DEVELOPMENTAL WORK PERFORMED ON THE IPMR

4.2.1 Thermal Tests

This section outlines the tests that were done during the development of the control cycle of the device. The performance and repeatability of the artificial wetting tests were found to be very variable since the conditions pertaining to sequential tests in the test chamber differed substantially due to various factors. These factors include variation in the ambient levels in the test chamber and in the amount of steam injected into the chamber.

An early observation showed that the ambient temperature inside the test chamber rose to ± 65 °C during summer afternoons. This was directly attributed to the heat transferred from the stainless steel top and side covers into the test chamber. The

CHAPTER 4

test chamber walls and top were therefore insulated by the installation of thermal insulation panels. The installation of these panels resulted in a more constant temperature inside the chamber.

The only IPMR controller output linked to the steam generator is that to open and close the output steam valve. The IPMR controller outputs are only timed in second intervals and a problem was thus also encountered when smaller amounts of steam were required during iterations. The output steam valve was equipped with a needle valve that could be set to allow various amounts of steam to be injected into the test chamber. The correct steam output rate was thus obtained by adjusting the needle valve until acceptable wetting of the artificially polluted insulator was obtained. This process involved a time consuming series of tests and had to be repeated for every new IPMR. It also proved difficult to determine whether a repeatable needle valve setting could be made from one device to another.

It was therefore decided to experiment with various sizes of orifices in a restrictor. After some testing a restrictor with a 1.2 mm opening was found suitable. A restrictor was built by press-fitting a brass rod into a brass adaptor. A hole having a 1.2 mm diameter was then drilled into the adaptor. The restrictor was connected directly onto the output steam valve and the needle valve was turned to the fully open position. The construction of the restrictor is shown in Figure 4-1.



Figure 4-1: Brass adaptor before and after machining

CHAPTER 4

During initial testing it was found that the steam condensed in the cold steam piping, forming undesirable water droplets. To prevent this, a technique was implemented to inject steam into the test chamber before the test commences. (See sections 3.3.7 and 3.4.3.)

The insulator is only lowered after a blower cycle (Dryer 1) to remove steam remaining from the Steam Preparation cycle, from the chamber. The lowered insulator is then dried (Dryer 2) for typically 10 minutes. During this time the air in the chamber becomes very dry and requires a large amount of steam on the first steam injection cycle of the test to raise the ambient humidity. The First Sample Humidify cycle was therefore introduced. The First Sample Humidify time constant is however too large to be used during the test to introduce small increments of steam. The second steam injection cycle and onwards, called Humidify Time , is used to introduce small increments of steam. The selection of a correct First Sample Humidify cycle value is important since a too large a value over-saturates the pollution layer causing washing and a too small value will cause insufficient raising of the ambient humidity resulting into a failed test.

Various tests were performed where the Steam Preparation time was fixed at 1 minute, the Dryer 1 time 2 minutes and the insulator drying time (Dryer 2) at 10 minutes. The First Sample Humidify injection of steam was varied from test to test to determine a suitable setting. After repeated tests a value was found that resulted in successful tests. Figure 4-2 shows the measured Temperature ($^{\circ}\text{C}$), Humidity (%RH) and Dew Point Temperature ($^{\circ}\text{C}$) during such a test.

From Figure 4-2 the steep rise in humidity in the first 3 minutes is due to the first steam injection (Steam Preparation). The temperature rises between minutes 4 and 13 are due to the 10-minute heater Dryer 2 cycle and the humidity falls below 30% during the same period. The use of the First Sample Humidify cycle is clearly visible after the dryer cycle as the humidity rises above 80% relative humidity between minutes 13 and 15. The smaller steam increments of the Humidify Time cycle only inject enough steam to keep the humidity levels between 94% and 97%. At the end of the test (between minutes 61 and 69) the dryer is switched on again to dry the insulator surface (Dryer 4), raising the temperature and lowering the humidity.

CHAPTER 4

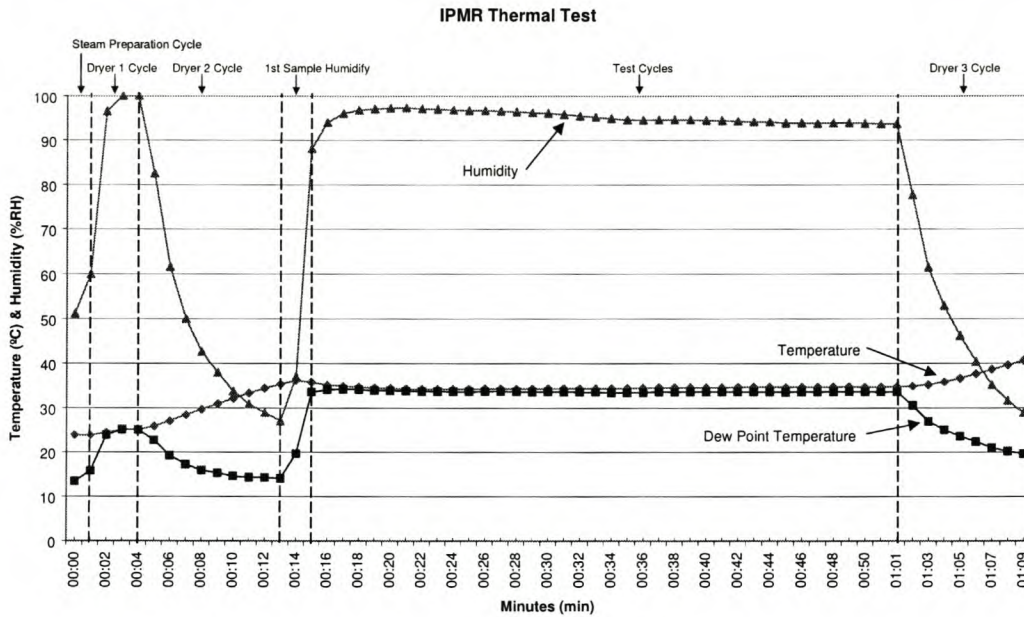


Figure 4-2: Thermal measurements during an artificial wetting test.

4.2.2 Verification of the measuring system using a fixed resistor

In order to verify the accuracy of the measuring system, a standard resistor was constructed using six high voltage resistors previously used in a high voltage resistive divider. Each resistor used had a rating of 6 M Ω ($\pm 5\%$), 25kV. The six resistors were connected in parallel so that the total resistance would be ± 1 M Ω , 25 kV. The standard resistor would then give a 1 μ S conductance measurement when installed in the IPMR. This conductance value was kept small enough not to damage the standard resistor with large currents flowing through the components. The 1 μ S value was also large enough to be inside the measurement range of the IPMR.

The total resistance was measured with a Megger at 3kV for 20 seconds and found to be 0.915 M Ω (1.093 μ S). The standard resistor was connected to the IPMR for 1 hour and the results logged. The average logged conductance value of 1.049 μ S was within 4.019% of the measured value.

CHAPTER 4

Three resistors were removed during a following test to double the resistance to 2 M Ω . The total resistance was measured with a Megger at 3 kV for 20 seconds and found to be 1.889 M Ω (0.529 μ S). The standard resistor was connected to the IPMR for 1 hour and the results logged. The average logged conductance value of 0.527 μ S was within 0.517% of the measured value. The standard resistor measurements performed are shown below in Figure 4-3.

The standard resistor can thus be used to verify the measurements of a newly built IPMR as well as a tool to ascertain whether the measurements of a field-installed IPMR are still correct. It is recommended that this test be performed from time to time to verify the measuring system.

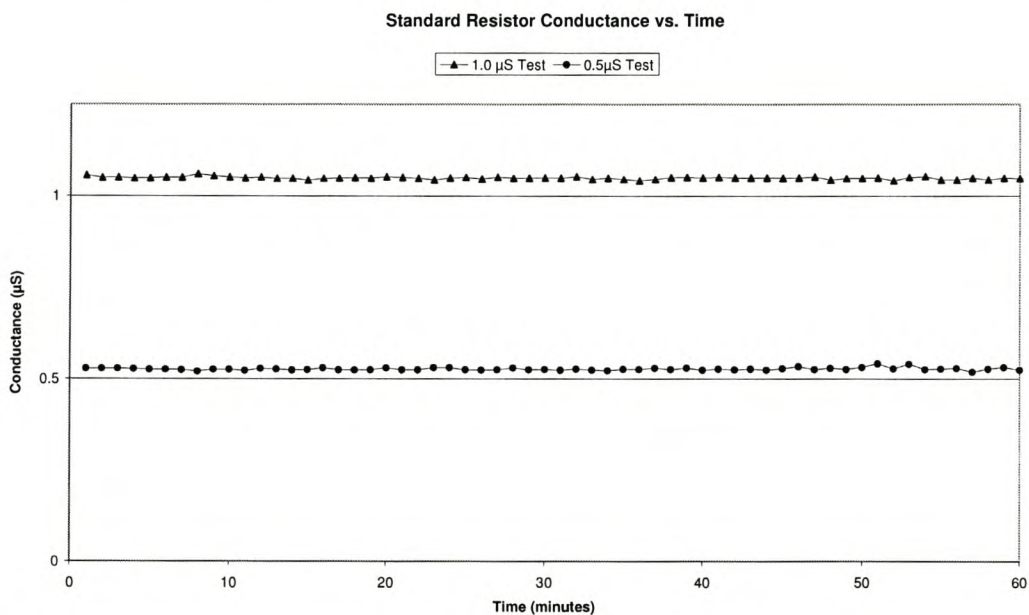


Figure 4-3: IPMR measurements with the standard resistor installed.

4.3 CALIBRATION TESTS

4.3.1 Description of the Solid Layer Method

The artificial pollution process was done according to the solid layer method prescribed in the IEC 60507 document [11]. The solution consisted of 40 grams of kaolin per litre water. By adding different amounts of NaCl to the solution, the different pollution levels can be simulated. The kaolin in the solution is a non-dissolving inert material, used as a bonding agent for the NaCl to the insulator surface. The kaolin simulates inert materials, e.g. cement, lime, dust, clay, etc., that performs the same bonding function when insulators are exposed under natural conditions. The test insulator is dipped in the solution, ensuring that a uniform pollution layer is applied to the surface. The insulator is then allowed to dry before it is placed in the IPMR.

4.3.2 Determination of the IPMR calibration curve

The test insulator, a porcelain post type insulator, is polluted using the solid layer method as described above and is left to dry. Thereafter it is placed in the IPMR and a test is performed. After the test the insulator is removed and washed to determine the ESDD of the deposit on the insulator surface. By using the surface conductivity and ESDD values of each test, a calibration curve surface conductivity (μS) vs. ESDD (mg/cm^2) was drawn [26].

The calibration curve was determined by performing regression analysis on the measured data points. Figure 4-4 below shows the derived IPMR calibration curve. The CIGRÉ pollution ranges [19] as defined in Table 2-4 are also included in the calibration curve below.

CHAPTER 4

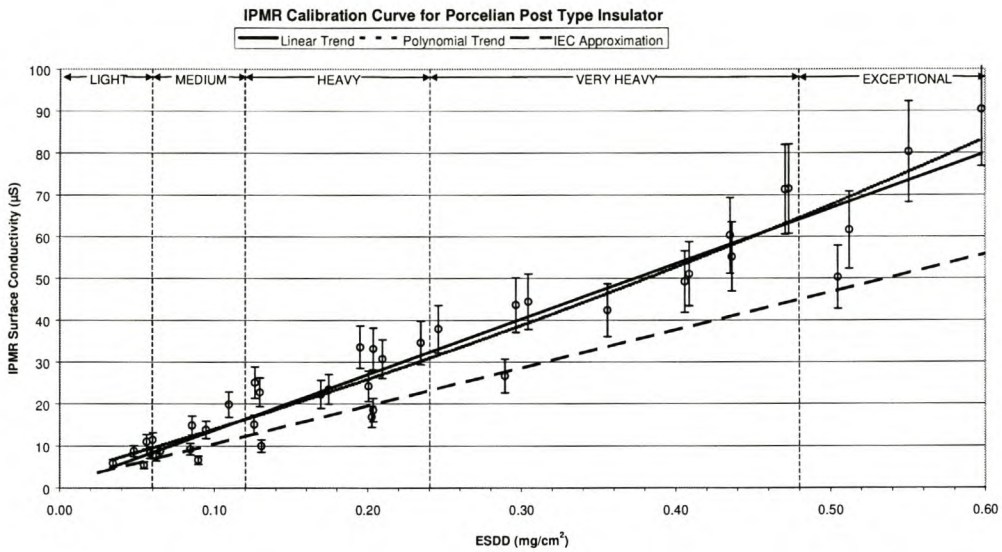


Figure 4-4: Calibration curve derived for the IPMR.

The actual test data and the 15% vertical error bars are displayed on the calibration curve. The linear and polynomial trends are displayed by a solid black line and dotted black line respectively. The dashed black line is an approximate guide based on data given in the IEC 60507 document [11] for standard cap and pin insulators tested vertically using the kaolin as the inert material. By viewing Table 4-1 below, it was determined that 54.76% of all the performed tests fell within 15% of the developed linear trend.

Table 4-1: Statistics of the tests performed at each severity range.

Severity Range	Number of Tests	% Tests within certain Tolerance	
		±10%	±15%
Light	13	23.07%	30.76%
Medium	8	25.00%	37.50%
Heavy	21	47.61%	76.19%
TOTAL	42	35.71%	54.76%

The following equations were developed using curve fitting techniques for the linear and polynomial relationships respectively.

CHAPTER 4

$$\text{Conductivity } (\mu\text{S}) = B*(\text{ESDD}) + C \quad (\text{Eq. 4.1})$$

$$\text{Conductivity } (\mu\text{S}) = A*(\text{ESDD})^2 + B*(\text{ESDD}) + C \quad (\text{Eq. 4.2})$$

Table 4-2 below contains the coefficients required for equation 4.1 and equation 4.2 to determine the expected conductivity. The measures of adequacy for the linear and polynomial models, R^2 and the correlation coefficients, are also supplied.

Table 4-2: Curve fitting coefficients and statistical measures of model adequacy.

Coefficient	Linear	Polynomial
A	0	51.259
B	132.5	103.1
C	0.5146	3.222
R^2	0.928	0.931
Correlation Coefficient	0.963	0.965

It can be seen that both equations can be used to determine the expected conductivity since both models used fitted the measured data adequately. The calibration curve shows that the IPMR is capable as a device to introduce artificial wetting to a polluted insulator surface and relating the result to the ESDD, a severity classification parameter.

4.3.3 Repeatability Tests

After the successful completion of the calibration tests, the IPMR was set up to perform repeated tests on an artificially polluted insulator. The results were compared to determine whether successive tests measured the same conductivity showing that the pollution layer was not washed away. The tests were set up to run at twelve-hourly intervals. The results show that the measured conductivities vary over the 10 tests points, or, 5 days. It must be borne in mind that if the insulator was exposed to the natural environment during the same duration of the test, an increase or decrease in surface conductivity can be expected. The variation in the measurements is due to

CHAPTER 4

ambient environmental conditions and how each test was concluded. During the first 2 days of testing (4 tests) the values differed by only 7.41% of each other, showing that the artificial wetting test can be successfully applied without the loss of pollution.

4.4 SALT FOG TESTS PERFORMED ON THE IPMR

In section 4.3 tests were performed by pre-depositing a solid layer on the IPMR test insulator. The calibration curve that was obtained is useful to evaluate site severity where solid pollutants and subsequent wetting by fog is a problem. Insulators installed close to the coast are however often exposed to a spray mist, so-called instantaneous pollution. Artificial salt fog tests are useful to represent this type of condition. It was therefore decided to evaluate the performance of the IPMR in a salt fog test.

This section reports on tests where the IPMR was used to measure surface conductivity on a test insulator while a salt fog test was being performed on typical power line insulators. The leakage currents were measured on the test insulators and the data was captured together with the surface conductivity values. The purpose of the investigation was to determine whether the IPMR is capable of the early detection of an instantaneous pollution event. The obtained results are also utilised to determine the relationship between measured surface conductivity and leakage current values, thus being able to predict flashover.

For this experiment, the IPMR is placed inside the salt fog chamber near the test insulators. The test insulators were energised from a separate high voltage source and the leakage currents were monitored for the duration of the salt fog test. The leakage current monitoring system used was an OLCA leakage current monitor as no IPMR Leakage Current Monitor (LCMonitor) unit was available at the time. The test insulator was exposed to the salt fog for the full duration of the experiment and the artificial wetting feature was not used.

CHAPTER 4

4.4.1 Salt Fog Chamber

The salt fog chamber was built according to the specifications supplied in the IEC 60507 [11]. The chamber measures 6m (w) x 6m (w) x 3m (h). A number of different salt fog tests were done with different salinities, representing different pollution levels. The salt water for the fog test was prepared by mixing the required amount of NaCl with water in the storage tanks. Care was taken to ensure thorough mixing and complete solution. The salt fog chamber is equipped with filters in both the solution and air supply lines to remove unwanted impurities.

4.4.2 Description of the OLCA leakage current monitor

The OLCA was developed by CT Lab (PTY) Ltd. to measure leakage currents on nine different channels while operating at normal voltages. The Main Data Acquisition System can accommodate [27], [28]:

- Nine current sensor inputs
- Three voltage sensor inputs
- AC or DC power supply inputs

Communications to the Main Data Acquisition System can be via:

- A high speed RS323 communications port
- An external modem via a dedicated RS323 serial port

The leakage current sensors are high accuracy Hall effect current transducers. The sensors can ensure galvanic isolation of up to 6 kV between the current input and instrument while maintaining a high level of accuracy.

The leakage current sensors must be installed at ground potential. A stand-off insulator must be inserted with the insulator under test. One terminal of the current sensor is then connected to the section between the two insulators and the other to

CHAPTER 4

the grounded structure. Any leakage current that will flow across the insulator will then be automatically shunted through the current sensor.

The OLCA is thus utilised to monitor the following electrical and weather parameters:

- Positive and negative peak value of the leakage current
- Positive and negative average value of the leakage current
- Positive and negative charge of the leakage current
- The RMS value of the leakage current and the applied voltage
- The power loss over each insulator

The OLCA samples each channel continuously at 2 kHz. The sampled values are stored in flash memory located in the Main Data Acquisition System.

4.4.3 Test Insulators Used During Salt Fog Tests

The test insulators used during the IPMR surface conductivity tests were the porcelain IPMR test insulator and one standard glass cap and pin insulator. A test at a specific value of severity was done twice, once with the porcelain IPMR test insulator and thereafter with the standard glass cap and pin insulator. The energised test insulator used during the salt fog tests consisted of two standard glass cap and pin discs. Each disc had a 146mm connecting length and 280mm creepage distance.

All the test insulators were cleaned before each test to simulate the onset of an instantaneous pollution event on clean insulation. The test voltage was raised to a value such that the specific creepage distance on the test insulator was 25mm/kV. The tests were started as soon as the salt-water solution and air was applied to the nozzles. The IPMR and leakage current monitor were both set up to measure surface conductivity and leakage currents at 1-minute intervals. Each test insulator was connected to the high voltage supply via an explosive Mace fuse, which was designed to isolate a test insulator when leakage currents exceed 750 mA_{peak}.

CHAPTER 4

4.4.4 Comparison of Measured Conductivities and Leakage Currents

The measured IPMR surface conductivities (μS) are plotted against the corresponding test salinities (kg/m^3) in Figure 4-5. The standard glass disc conductivities are plotted as triangles and the IPMR insulator conductivities as dots. A reasonable linear relationship can be seen to exist for both test insulators during these tests. The pollution classification [19] for the corresponding conductivities is also shown in the right-hand column on the graph.

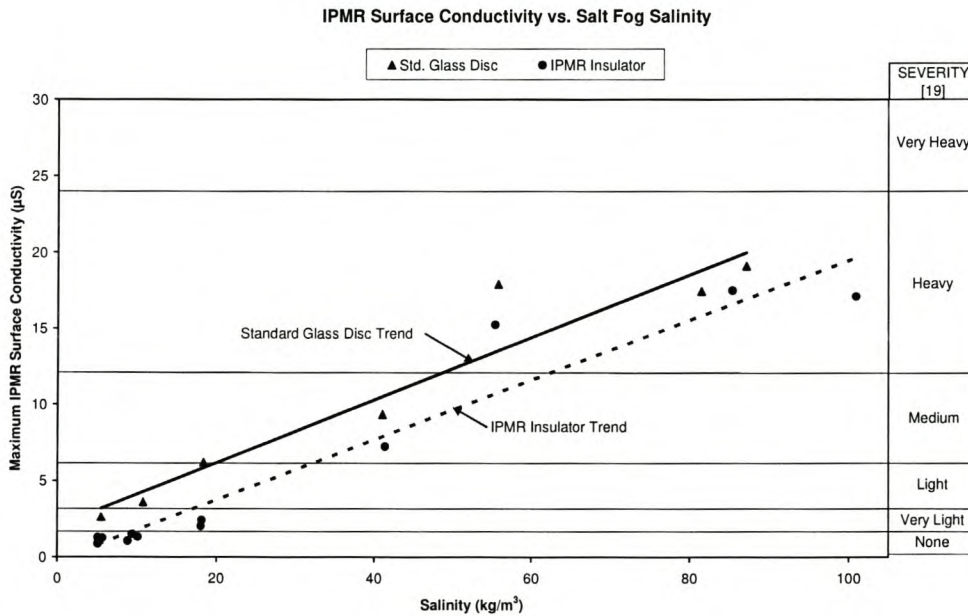


Figure 4-5: IPMR Surface Conductivity (μS) vs. Salinity (kg/m^3).

The salinity withstand levels for salt fog tests are given below in Table 4-3. The test insulator, energised at 25 mm/kV, experienced fuse operations during tests when the salinity exceeded $80 \text{ kg}/\text{m}^3$. Referring to Table 4-3, it can be seen that an energised insulator having a specific creepage distance of 25mm/kV is expected to withstand salinities up to $40 \text{ kg}/\text{m}^3$ [19].

CHAPTER 4

Table 4-3: Salinity withstand values and recommended specific creepage lengths.

Degree of Pollution	CIGRÉ Salinity Withstand (kg/m ³) [19]	Recommended specific creepage length* (mm/kV) [18]
None	1.25 – 2.5	
Very Light	2.5 – 5	
Light	5 – 10	16
Medium	10 – 20	20
Heavy	20 – 40	25
Very Heavy	40 – 80	31
Exceptional	> 80	

4.4.5 Critical Flashover Voltage Derived from the measured IPMR Surface Conductivity

Theoretical models to predict insulator flashover have been developed and applied by Rizk [29], Holtzhausen [30] and Vosloo [13]. According to these models the critical flashover voltage of an insulator depends on the surface conductivity of the pollution layer and the shape (form factor) of the insulator.

This critical flashover voltage is given by the following semi-empirical formula [29, 30]:

$$V_c = k_1 \cdot 10^{-3} \cdot \left[\frac{F \cdot 10^6}{\sigma_s \cdot L} \right]^{k_2} \cdot L \quad (\text{Eq. 4.2})$$

where:

V_c : critical insulator flashover voltage (kV_{peak})

F: form factor of the insulator

σ_s : surface conductivity (μS)

L: creepage length of the insulator (mm)

$k_1 = 7.6$

$k_2 = 0.35$

CHAPTER 4

As the relationship between the surface conductivity and salt fog salinity is known from Figure 4-5, the critical voltage (V_c) was calculated and plotted against the test salinity in Figure 4-6. The dashed black horizontal line represents the applied voltage (19.76 kV_{peak}) and the trendlines the calculated critical voltages for each test insulator. The standard glass disc critical voltages are plotted as triangles and the IPMR insulator critical voltages as dots. The standard glass disc parameters, form factor and creepage distance, were used in both sets of critical voltage calculations. It can clearly be seen that flashover probability is increased when the critical flashover voltage approaches the applied voltage. This increased flashover probability coincides with a salinity larger than 80 kg/m³. Fuse operations were experienced when the test salinities were larger than 80 kg/m³.

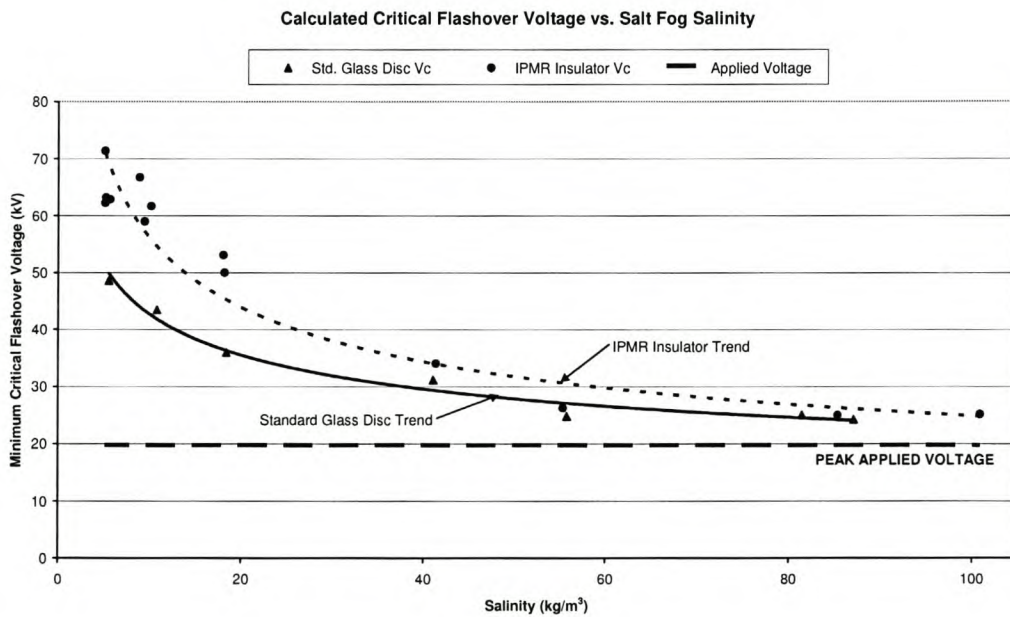


Figure 4-6: Critical Flashover Voltage (kV_{peak}) vs. Salinity (kg/m³).

Insulators having a specific creepage length of 25 mm /kV are suitable for polluted areas classified as Heavy . It is interesting to note that these insulators only experienced fuse operations during conditions having a Exceptional severity range (larger than 80 kg/m³).

CHAPTER 4

It must be borne in mind that the IPMR surface conductivity values were measured on a cold (non-energised) insulator surface whereas the peak leakage currents were measured on a hot (full-time energised) insulator surface. Lambeth [31] showed that the pollution layer exhibited a negative resistance-temperature coefficient. It was found that the resistance of the pollution layer would become smaller as leakage currents heat the pollution layer. The actual surface conductivity of the insulator was thus appreciably higher it could be as high as double the value [30].

4.4.6 Critical leakage current (I_{max})

Theoretical and empirical investigations indicate that there exists a critical value of leakage current that presents a threshold above which the flashover probability increases sharply. [4], [30], and [32]. The peak leakage current, measured in each test, was plotted against the test severity in Figure 4-7.

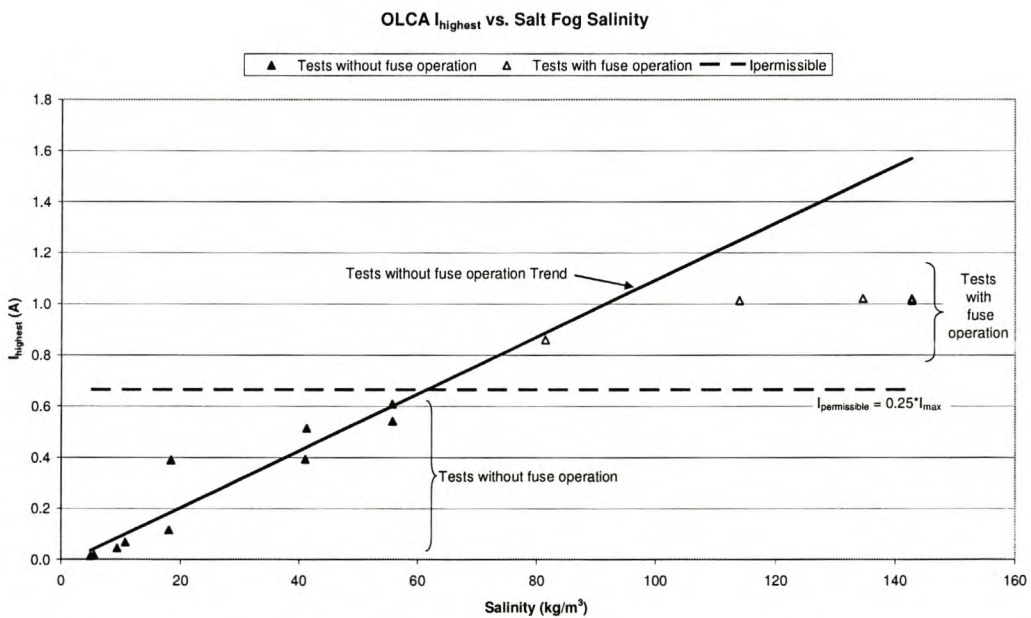


Figure 4-7: Peak Leakage Current (A) vs. Salinity (kg/m³).

CHAPTER 4

The standard glass disc tests that did not result in fuse operations are plotted as solid triangles and the standard glass disc tests that did result in flashover are plotted as hollow triangles. The solid line represents the linear relationship of the values of the tests without fuse operations. The permissible leakage current ($I_{\text{permissible}}$) (described in section 1.3.2) was plotted as a dashed horizontal line.

Similarly to Figure 4-5, fuse operations, or flashovers, can be experienced when the peak leakage currents exceed the maximum permissible peak leakage current. It will be noted that fuse operations coincided with salinities larger than 80 kg/m^3 and peak leakage currents larger than $I_{\text{permissible}}$. These tests were done at a fixed specific creepage length for the specific test insulators.

4.4.7 Results obtained from Salt Fog Tests*

It appears that IPMR can be used to evaluate the severity of an instantaneous pollution event as simulated by the salt fog tests. The results obtained show that the occurrence of pollution related fuse operations were observed in all cases when the measured values and calculated parameters approached the critical insulator performance limits (surface conductivity, critical flashover voltage and $I_{\text{permissible}}$ ($0,25 \cdot I_{\text{max}}$)).

An important point to note is that the data points represent a single salt fog test and not that of a withstand salinity test. (A withstand salinity is only determined after no flashovers were experienced after a number of one hour tests performed at the same salinity. A preconditioning process, performed before the salt fog tests, determines the test voltage to be used.) Further work is suggested to investigate the effect of variation in specific creepage distance and the effect of different insulator shapes.

**The use of Mace fuses to isolate the test insulator from excessive leakage currents was found to be a limiting factor in leakage current measurements larger than $I_{\text{permissible}}$. It was observed that the peak leakage currents during tests that resulted in fuse operations never neared 100% of I_{max} . The maximum peak leakage current plotted in Figure 4-7 was thus the highest peak leakage current prior to the fuse*

CHAPTER 4

operating. The term “fuse operation” was chosen since it was difficult to determine whether a flashover, having a peak leakage current approaching I_{max} , really occurred. Mace fuses are also used at the Koeberg Insulator Pollution Test Station (KIPTS) where a fuse operation is used as an indication of critical insulator performance.

4.5 SUMMARY

It was shown in this chapter how laboratory tests were performed on the IPMR to determine if the IPMR measurements and tests performed correctly. Thermal tests, conductivity measurement verification tests and repeatability tests were performed. The IPMR was also calibrated to relate measured conductivity with artificial wetting to ESDD, a pollution classification parameter. Artificial pollution tests, in the form of salt fog tests, were performed to investigate if the IPMR is capable of determining critical insulator performance linked to the surrounding severity. The salt fog test results showed that the IPMR measurements were capable to relate critical insulator performance.

5 IPMR MEASUREMENTS DURING NATURALLY POLLUTED CONDITIONS

5.1 INTRODUCTION

The IPMR was installed at Koeberg Insulator Pollution Test Station (KIPTS) after the successful calibration of the device at the University of Stellenbosch. The device was set up to perform surface conductivity tests with natural and artificial wetting. The measured conductivities were compared with insulator leakage current data measured by the test site's leakage current logging system. Critical insulator performance parameters were calculated and compared with flashover events experience at the test station. The site pollution severity was also determined by the application of a statistical approach to the measured conductivities.

5.2 KOEBERG INSULATOR POLLUTION TEST STATION (KIPTS)

The Koeberg Insulator Pollution Test Station (KIPTS) is situated along the Cape west coast, about 50 meters from the sea in the vicinity of the Koeberg Nuclear Power Station (KNPS). The test site is located where Macey [17] conducted tests on energised insulators during the late 1970 s. The test site was also used as the location to the tests performed by L. P. du Toit [3] and Potgieter [7]. The test site was rebuilt during the early 1990 s [33], [34] being equipped with testing voltages of 22kV and 66kV. During this time the second IPMA was tested at KIPTS [10]. The test station was upgraded in 2001 to include 11, 22, 33, 66 and 132kV testing bays [35]. The instrumentation is housed in the control room. The KIPTS test station is shown in Figure 5-1.

CHAPTER 5

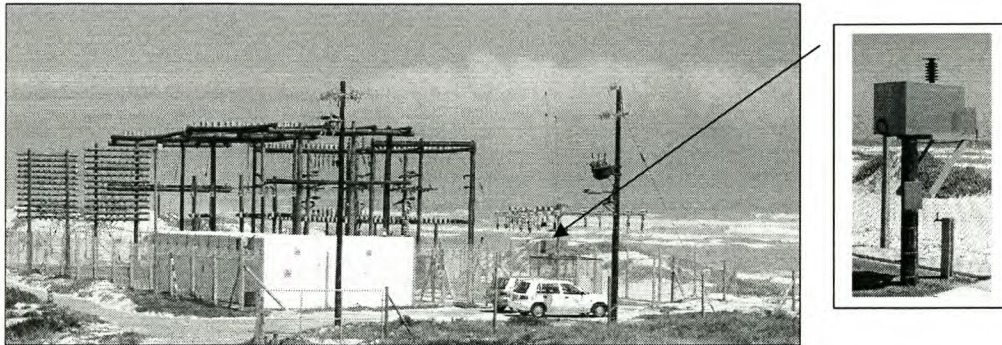


Figure 5-1: Koeberg Insulator Pollution Test Station (KIPTS).

(The inserted picture displays the location of the IPMR installation at KIPTS).

The climate at KIPTS is characterised by dry summers, winter rainfall, high winds, mist banks, and heavy marine and industrial pollution. Vosloo [13] reported various pollution sources in a 20km radius around KIPTS. The main pollution sources around KIPTS were found to be marine, industrial and agricultural sources. Table 5-1 gives a brief summary to the different sources of pollution observed around the test station. The pollution index at KIPTS is in the order of 2000 mS/cm, which is extremely high and would be classified as 'very heavy'. It was reported that the insulator material ageing measured at KIPTS was correlated to the IEC Publication 601109 [36], an accelerated composite insulator test procedure, and a factor of 2:1 was found. The location of the test station is therefore ideally suited due to the very severe pollution experienced in this area.

Table 5-1: Summary of pollution sources around KIPTS.

Pollution Source	Type of Pollution
Marine	Wave action, sea breezes or winds produce mist banks or salt spray.
Agricultural	Occasional veld fires, ploughing, harvesting and crop spraying.
Industrial	Industries burning diesel, coal and heavy fuel oil (HFO). Quarries including lime, concrete and other aggregates. Heavy industries within 20 km such as oil refineries and fertiliser plants emit severe emissions including SO _x and NO _x ,

CHAPTER 5

The various pollution monitoring parameters measured at KIPTS include environmental monitoring using an on-site weather station, non-electrical insulator tests described in the Round Robin Pollution Monitor Study [16] and leakage current measurements performed on energised insulators. Visual observations are made at KIPTS at regular intervals, with emphasis on the hydrophobicity, material degradation, erosion, tracking and puncturing. Ultra-violet (UV) video recordings are also performed at KIPTS during the visual observations using a Corocam image intensified camera. The UV recordings are used to pinpoint and document the occurrence of corona activity, dry band arcing and surface discharges.

5.3 OPERATIONAL PERFORMANCE OF THE IPMR AT KIPTS

The IPMR was installed at KIPTS to perform surface conductivity measurements with natural and artificial wetting. The IPMR was set up to perform two artificial wetting tests per day, one at midday and one at midnight. The success of the various tests is dependent on the correct functioning of the IPMR components or requirements. In Table 5-2 below, an X in the matrix indicates the components or requirements that affect the different conductivity tests. Problems were experienced with some of the components during the year of testing that was performed. The problems and remedies applied are displayed in Table 5-3.

The operational performance of the IPMR during surface conductivity tests with artificial wetting was severely hampered due to the failure of various components. The main problem encountered with the steam generator was that the pressure switch would intermittently operate at lower pressures. The generated steam at KIPTS was thus less than the steam generated during the testing period at the University of Stellenbosch. The main challenge experienced with this problem was that it was difficult to determine which tests were performed correctly. It was therefore decided not to include the artificially wetted conductivity measurement values in this analysis, as the steam function did not perform acceptably.

CHAPTER 5

Table 5-2: Surface conductivity test instability matrix.

IPMR Component / Requirement	Surface Conductivity Test	
	Natural Wetting	Artificial Wetting
IPMR Controller	X	X
IPMR Test Insulator	X	X
Test Transformer	X	X
Moveable Platform	(X)	X
Hot Air Dryer		X
Steam Supply Piping		X
Steam Generator		X
Water Supply		X
Electricity Supply	X	X
PC Communications	X	X

(X): As soon as the platform fails to complete the lowering or raising operation, the associated timeout will stop all controller processes (including naturally wetted μS measurements) until user intervention occurs.

Table 5-3: Operational problems experienced with IPMR.

IPMR Component / Requirement	Problems experienced	Remedy performed
IPMR Controller	The controller lost all the calibration settings by the inadvertent resetting of all the constants to a value of 5 .	None
IPMR Test Insulator	Tracking inside the test insulator caused the breaking of a high voltage cable, tripping the supply.	A watertight connection box was added at the platform base as well as an earthed spring in the hollow core to act as a guard electrode.
Moveable Platform	The moveable platform stopped intermittently as the insulator was lowered or raised. As a timeout was reached, test data was lost.	Magnetic reed switches replaced the inductive proximity sensors. Timing components exchanged in the IPMR controller.
Steam Generator	<ol style="list-style-type: none"> 1. The generator would not create pressure. 2. The generator would not reach 1.5 bar pressure. 3. The level probes corroded severely causing the overflowing of the steam generator. 	<ol style="list-style-type: none"> 1. Replaced burnt-out element. 2. Adjusted pressure switch until pressure was reached. 3. Refurbish steam generator with new corrosion resistant probes.
Water Supply	Supply lost at test station as well as pipes connected to the IPMR leaking.	Leaking pipes replaced or fixed.
Electricity Supply	Supply lost at test station due to extreme flashovers in the test bay.	None
PC Communications	Connection to device not possible due to software related problems.	Requested the attention from manufacturer.

CHAPTER 5

The conductivity measurements with natural wetting proved more successful at KIPTS. Working through all measured data, periods were seen where no measurements were possible coinciding with the dates when problems were experienced. The periods that the IPMR operated sufficiently to perform the conductivity test with natural wetting added up to 71% (37 weeks) of the total operational time (52 weeks), having a maximum uptime of 11 weeks. The IPMR experienced 8 weeks of downtime from Week 35 to Week 42, during which time the IPMR was removed from the site to repair problems associated with the moving platform and the steam generator. During this period most of the insulators being tested at KIPTS were removed as their one-year testing period came at an end. The 132kV test transformer as well as the leakage current measuring system at the test site also experienced problems during these last weeks of the IPMR tests.

The IPMR operated successfully for seven weeks tests after re-installation, until the steam generator element failed during Week 49. The IPMR was removed after one year and refurbished at the University of Stellenbosch. Special attention was given to these components, especially the steam generator that was severely corroded. The steam supply piping was also replaced by the standard arrangement (described in section 3.3.7) during this refurbishment period.

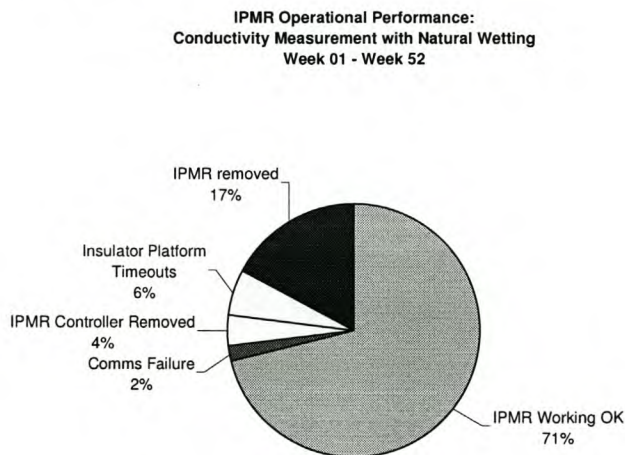


Figure 5-2: Operational performance for the naturally wetted conductivity tests.

CHAPTER 5

5.4 CALCULATION OF SITE SEVERITY USING IPMR MEASUREMENTS OVER A 30-WEEK PERIOD

The IPMR was designed as a device that can be used to determine the site severity of a particular location in terms of a pollution classification parameter. This severity information can be applied during the design of a new overhead line to determine the most suitable insulation to be used, or, to determine suitable insulator maintenance intervals.

The statistical approach of site severity assessment has been discussed by various authors [23], [37], [38], [39]. The correct insulator dimensioning is obtained after the determination of two parameters: the variation of pollution severity and the flashover performance of the insulator according to pollution severity. The variation of pollution severity is usually referred to as the stress of the location describing the variability of the polluted insulator surface. The flashover performance of the insulator is expressed as the strength, mainly derived from the flashover probability during artificial pollution tests. Both the stress and strength functions are used to determine the risk of flashover of the particular insulator at the particular site. The IPMR measurements can therefore be applied to determine the stress of the specific location. The stress-strength concept is shown below in Figure 5-3.

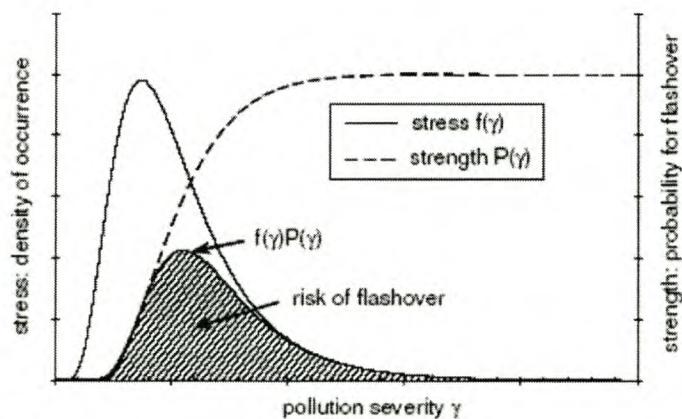


Figure 5-3: Stress-strength concept [39].

CHAPTER 5

The first method used to quantify the pollution severity at KIPTS was to sort all the measured IPMR surface conductivities in ascending order in groups of 0.75 μS increments. The relative frequency of measurements were determined for each grouping and plotted against the conductivity. The conductivity values less than 0.75 μS were omitted, as it fell below the “No Significant” Cigré pollution classification range [19].

The site severity classification is deemed to be the conductivity value at which only 2% of all the measurements exceeded this value. By determining the 98th percentile value, a pollution severity of 21 μS was calculated for KIPTS. This value coincides with a pollution classification of “Heavy” (12 – 24 μS). The maximum surface conductivity measured during this period was 33.183 μS , a value that falls within the “Very Heavy” classification. The histogram of conductivity measurements and the Cigré pollution classification ranges are plotted in Figure 5-4.

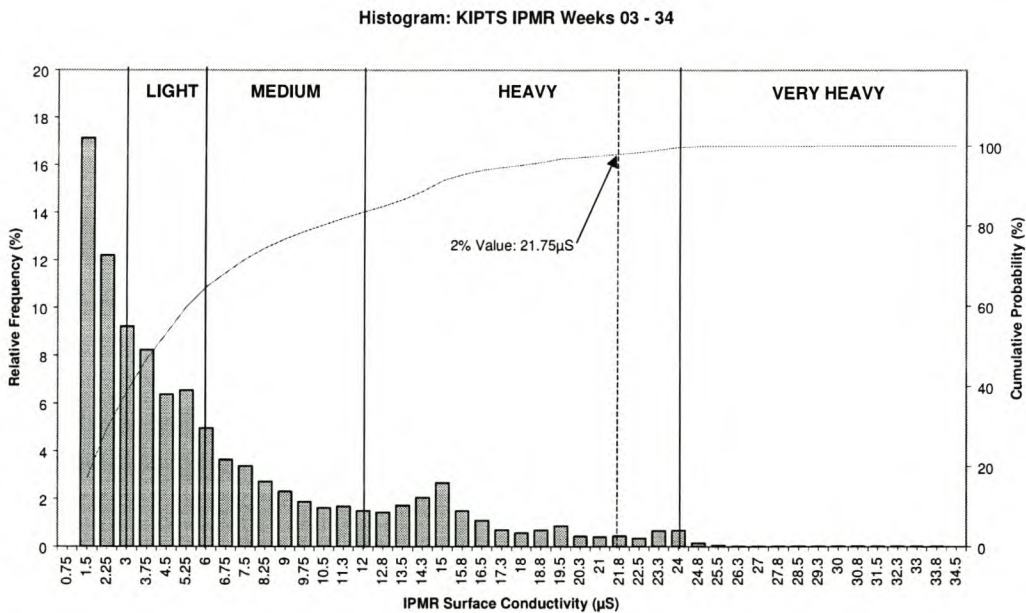


Figure 5-4: IPMR surface conductivity histogram used for KIPTS site severity calculation.

By referring to the Figure 5-4, it becomes apparent that the data points are not distributed normally. The histogram is successful in displaying the number of

CHAPTER 5

occurrences of surface conductivities during the 30-week period. It is evident that the insulator surface condition is either mostly dry, or, that a pollution layer with a light surface conductivity is present. Table 5-4 is given below to display the percentile values and the associated severity classification for the surface conductivity histogram.

Table 5-4: Surface conductivity percentiles and associated severity classification.

Percentile	Layer Conductivity Value (μS)	Layer Conductivity Severity Classification [19]
2nd	0.807	No significant
10th	1.072	No significant
25th	1.775	Very Light
50th	3.614	Light
75th	7.536	Medium
90th	14.147	Heavy
98th	21.132	Heavy

A similar approach was used to determine the KIPTS site severity by using all the one- and three-monthly Round Robin data collected between 1996 and 2004. The measured ESDD values were sorted in groups of $0.025\text{mg}/\text{cm}^2$.

The site severity classification is deemed to be the ESDD (in mg/cm^2) value at which only 2% of all the measurements exceeded this value. In this case, the 98th percentile value indicates a pollution severity of $0.800\text{mg}/\text{cm}^2$ for KIPTS. This value coincides with a pollution classification of "Exceptional" ($\geq 0.48\text{mg}/\text{cm}^2$)[19]. The maximum ESDD measured during this period was $1.002\text{mg}/\text{cm}^2$, a value that falls within the "Exceptional" classification. The histogram of ESDD measurements and the Cigré pollution classification ranges [19] are plotted in Figure 5-5.

By referring to the Figure 5-5, it becomes apparent that the data points are not distributed normally. The histogram is successful in displaying the number of occurrences of ESDD during the 8-year period. The distribution of the ESDD data is less skewed than the surface conductivity data.

CHAPTER 5

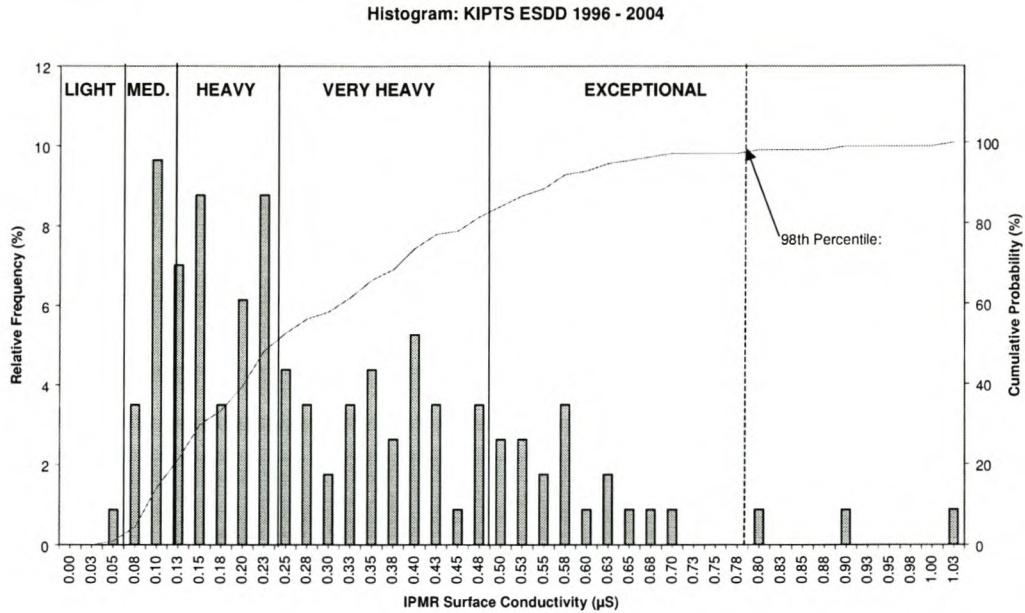


Figure 5-5: ESDD histogram used for KIPTS site severity calculation.

Table 5-5 is given below to display the percentile values and the associated severity classification for the ESDD histogram.

Table 5-5: ESDD percentiles and associated severity classification.

Percentile	ESDD Value (mg/cm ²)	ESDD Severity Classification [19]
2nd	0.060	Light
10th	0.085	Medium
25th	0.139	Heavy
50th	0.237	Heavy
75th	0.411	Very Heavy
90th	0.557	Exceptional
98th	0.769	Exceptional

The variation between the two KIPTS severity values can be attributed to the different measurement types and intervals used. The Round Robin tests are non-electrical pollution tests only quantifying the residual pollution after each month, neglecting to

CHAPTER 5

display the daily accumulation and washing (or seeping) of pollutants. The ESDD measurement is also a once-monthly measurement of the pollution layer severity. The 10-minute IPMR measurements clearly relate the daily changes in the pollution layer as well as the degree of natural wetting of this layer. The IPMR measurements should therefore present a better understanding to the effects of the surrounding area on high voltage insulation than the Round Robin tests.

The second method used to quantify the pollution severity at KIPTS was to determine the normal probability distribution of the measured conductivity data. The normal probability distribution plot displayed in Figure 5-7 was plotted using MATLAB®.

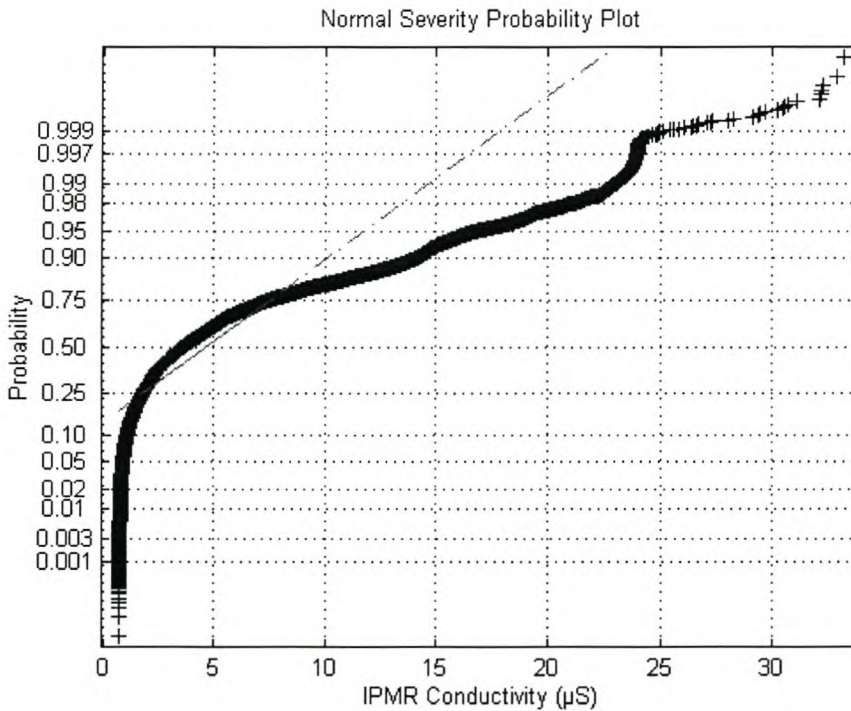


Figure 5-6: Normal probability plot for IPMR measurements.

Figure 5-7 displays the distribution of conductivity values if a model assumption was made that the conductivity values were distributed with a normal distribution. The dashed red line indicates a normal probability distribution. The plotted probability values in blue never follow the dashed red line, indicating that the data are not normally distributed. If a model assumption was made that the conductivity values

CHAPTER 5

was distributed with a normal distribution, the resultant site severity would have been calculated as $\pm 15 \mu\text{S}$. This calculated pollution severity value would have underestimated the actual pollution.

The third method used to quantify the pollution severity at KIPTS was to determine the lognormal probability distribution of the measured data. The lognormal conductivity probability distribution plot displayed in Figure 5-7 was plotted using MATLAB[®]. The dashed red line indicates a lognormal probability distribution. The plotted probability values in blue deviate from the dashed red line at the lower and higher conductivity values, indicating that those data points are not lognormally distributed.

The pollution classification of KIPTS was determined as the 98th percentile of the surface conductivity distribution. This value was determined as $21 \mu\text{S}$ (classified as “Heavy” [19]) and can be seen in Figure 5-7 as the intersection of the 98% probability line to the plotted lognormal probability values. If a lognormal distribution is fitted to the data, the 98th percentile of this estimated distribution gives a pollution severity of $\pm 37 \mu\text{S}$ (classified as “Very Heavy”), which is larger than $33.183 \mu\text{S}$, the maximum value measured during the testing period. This points out that the assumption that all the data has a lognormal distribution in the range is false. This can especially be seen in the tails of the distribution, which are important for severity analysis. From Figure 5-4 it is also evident that the relative frequency of data is high for the lower measurement values and the relative frequency is low for the higher conductivity measurement values.

The lognormal ESDD probability distribution plot displayed in Figure 5-8 was plotted using MATLAB[®]. The dashed red line indicates a lognormal probability distribution. The plotted probability values in blue deviate from the dashed red line at the lower and higher conductivity values, indicating that those data points are not lognormally distributed. By comparing Figure 5-7 and Figure 5-8 it can be seen that the probability distribution of the ESDD values are distributed more lognormally than the conductivity probability distribution.

CHAPTER 5

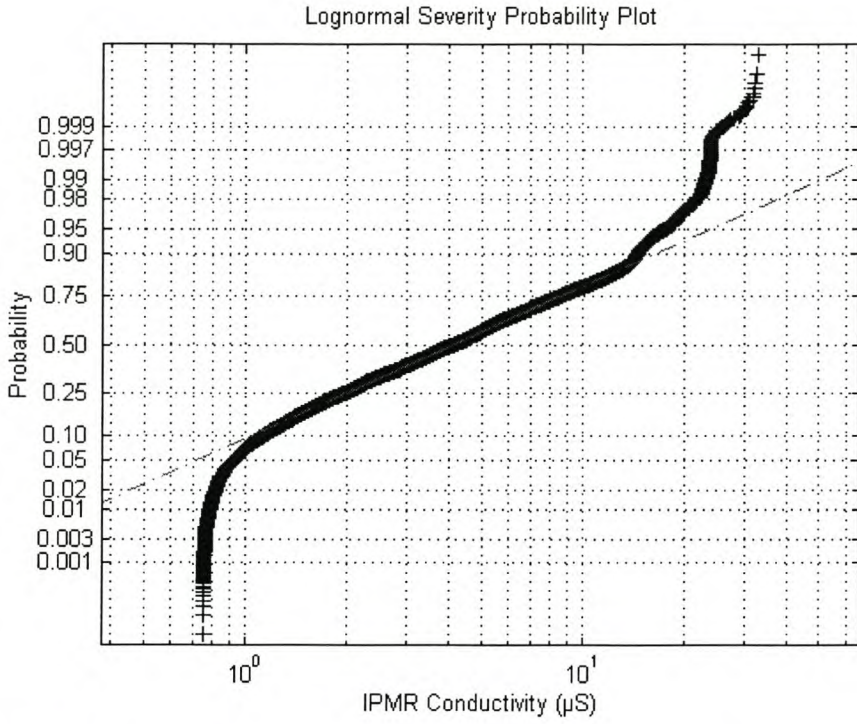


Figure 5-7: Lognormal probability plot for IPMR measurements.

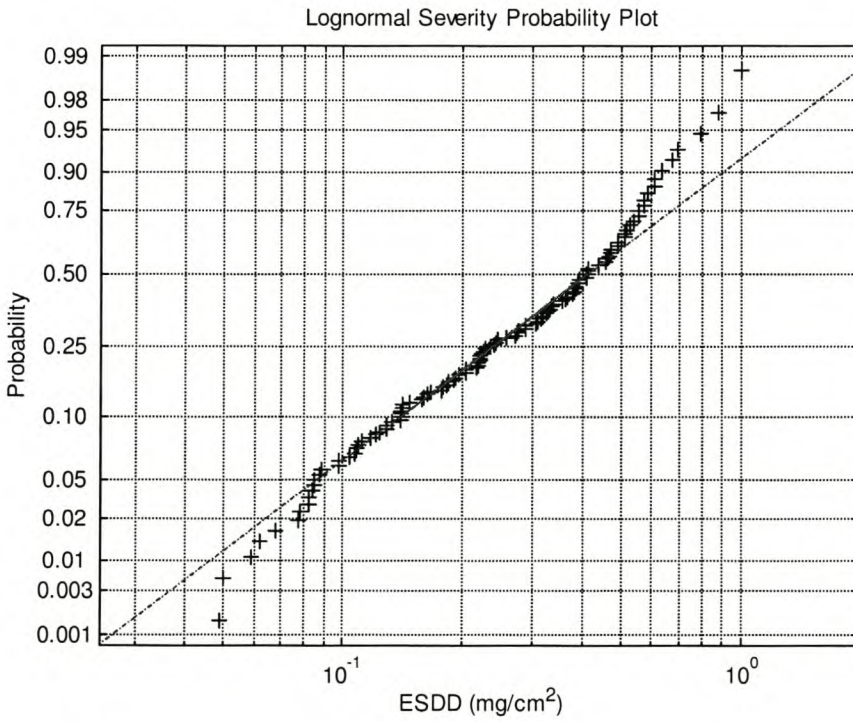


Figure 5-8: Normal probability plot for ESDD measurements

CHAPTER 5

Two of the statistical methods used, the histogram and lognormal distribution, proved to be robust in determining the site severity value. The normal probability distribution assumption proved wrong. The site severity value quantified by both approaches resulted in the same value, but the histogram-derived value can become erroneous if a too large bin increment is chosen.

The severity value based on IPMR measurements can be used as the stress in the stress-strength concept. The only difficulty in the stress-strength concept is that the strength needs to be expressed in the same parameter used to quantify the stress (site severity). The flashover probability (strength) of an insulator should thus be expressed in surface conductivity during artificial pollution tests.

5.5 DISCUSSION OF FLASHOVER EVENTS EXPERIENCED AT KIPTS DURING WEEK 15

This section is used to demonstrate typical IPMR measurements during the testing period. The IPMR measurements were compared to relative humidity and rainfall measurements, the critical voltage parameter calculated as well as the simultaneous leakage current measurements performed at KIPTS. The relative humidity and rainfall measurements were included as these parameters influence the conductivity measurements with natural wetting.

KIPTS experienced 11 pollution related flashovers during Week 15, which fell between 27/10/2002 and 04/11/2002. During this time a total of 44 insulators were tested at the station. The seasonal classification is late spring, having moderate temperatures and a likelihood of rain.

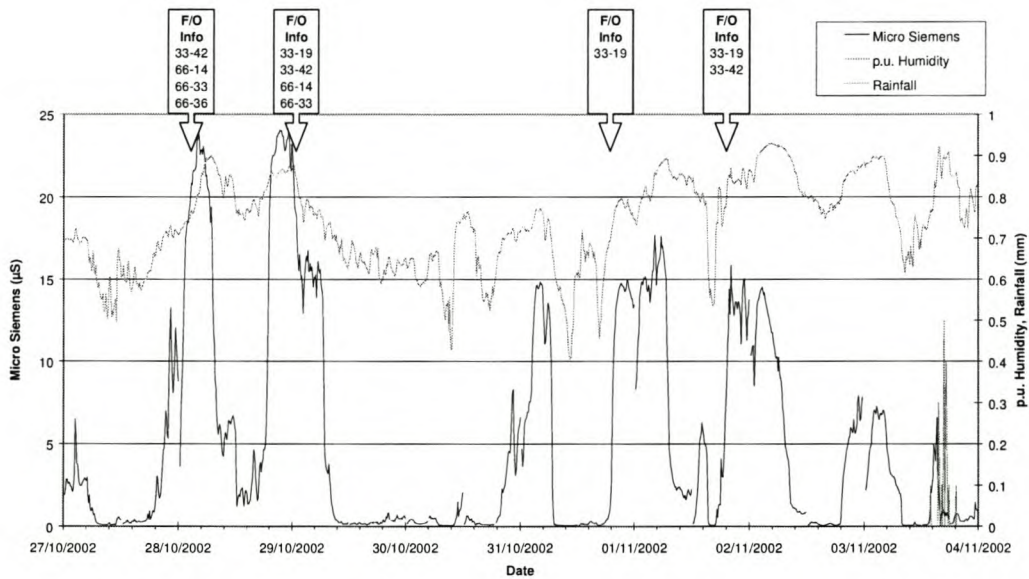
A brief description of the insulators that flashed over during Week 15 is given in Table 5-6.

CHAPTER 5

Table 5-6: Information on insulators which flashed during Week 15.

Insulator	Material	Type	mm/kV
33-19	Porcelain	Pin Type	26
33-42	Porcelain	Station Post	Unknown
66-14	Porcelain	Station Post	25
66-33	Porcelain	Station Post	27
66-36	Porcelain	Station Post	27

A period of rain was recorded on the 03/11/2002 where 2.5 mm was measured in 10 hours. The maximum 10-minute precipitation measurement during this period was 0.5 mm. When comparing the humidity and rainfall data plotted in Figure 5-9, it can be seen that all eleven flashover events coincided with periods of high humidity. This high humidity is also the main influence of the high conductivities measured during the same time. A clear trend can be seen between the daytime and nighttime conductivities, as well as a relationship between humidity and conductivity. Insulator flashovers occurred on the 31/10/2002 and 01/11/2002 due to a sudden increase in relative humidity.

**Figure 5-9:** Week 15 IPMR conductivity and weather parameters.

CHAPTER 5

Table 5-7 gives the relevant conductivity and weather information for this period.

Table 5-7: Statistics of measured conductivity and weather values.

	Micro Siemens (μS)	Temperature ($^{\circ}\text{C}$)	Dewpoint Temp. ($^{\circ}\text{C}$)	Humidity (%RH)	UV ($\mu\text{W}/\text{cm}^2$)	Wind Speed (m/s)	Rainfall (mm)
Minimum	0.06	7.93	4.73	40.58	0.00	0.00	0.00
Average	5.69	14.64	10.22	75.31	59.12	3.53	0.00
Maximum	24.05	24.36	15.94	93.08	246.24	10.66	0.50

The critical flashover voltage was calculated by using the form factor and creepage distance for two standard glass discs, as no form factors were available for the insulators that flashed over. As the critical flashover voltage parameter was derived empirically (using equation 4.2), a definite relationship can be seen that the critical flashover voltage will become smaller as conductivity increases. When the critical flashover voltage nears the applied voltage line (solid red line), insulator reliability would be at a minimum. The derived critical flashover voltage for two standard glass discs, shown in Figure 5-10, was at a minimum at all the occurrences of insulator flashovers.

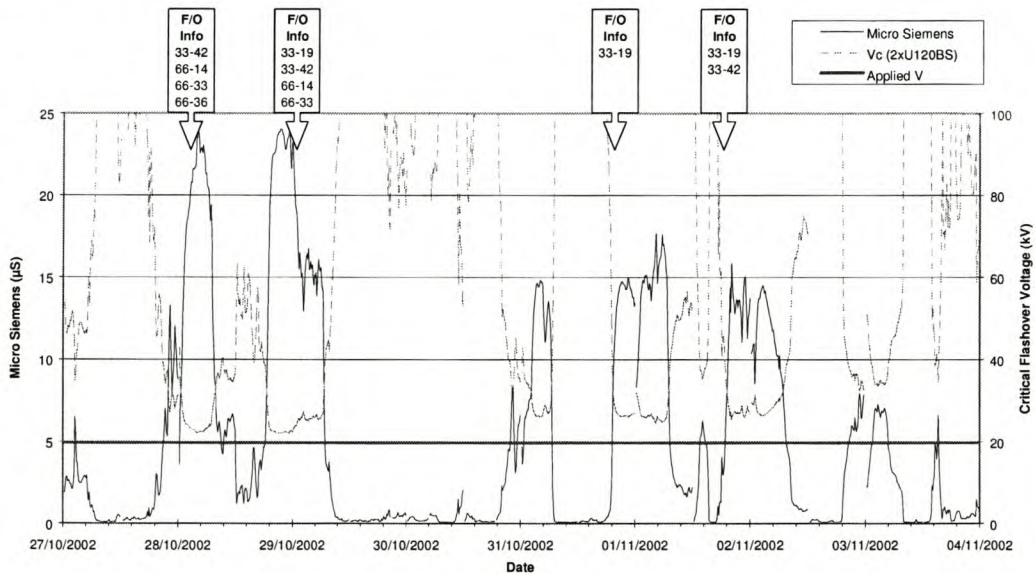


Figure 5-10: Week 15 IPMR conductivity and calculated critical flashover voltage.

CHAPTER 5

A rule of thumb to indicate possible risk of flashover can be stated as: humidity higher than 70%, surface conductivity measurements larger than $5 \mu\text{S}$ and any peak leakage current measured larger than 100 mA. This rule was based on observations that a value of $5 \mu\text{S}$ is usually measured when humidity is higher than 70%. The surface conductivity value usually starts to increase approximately a few hours after a change in humidity developed. As the humidity exceeds $\pm 70\%$, the pollution layer is dissolved into a solution, thereby increasing the leakage currents.

This rule of thumb thereby showed that the flashover process followed a definite order, starting with the increase in humidity, followed by an increase in surface conductivity and then the increase of peak leakage currents, which can lead to dry-band arcing and ultimately flashover. The $5 \mu\text{S}$ surface conductivity value was determined as the 62nd percentile in Figure 5-4. The use of a peak leakage current threshold of 100mA is to include a leakage current parameter so that the process, starting from an increase in humidity, possibly ending in flashover, can be anticipated. If there was no leakage current measurement, the rule of thumb could create a false alarm. (If the leakage current threshold was set too high, there will be no time between the alarm and the flashover.) Figure 5-11 below plots this rule of thumb with the coinciding humidity, surface conductivity and leakage currents.

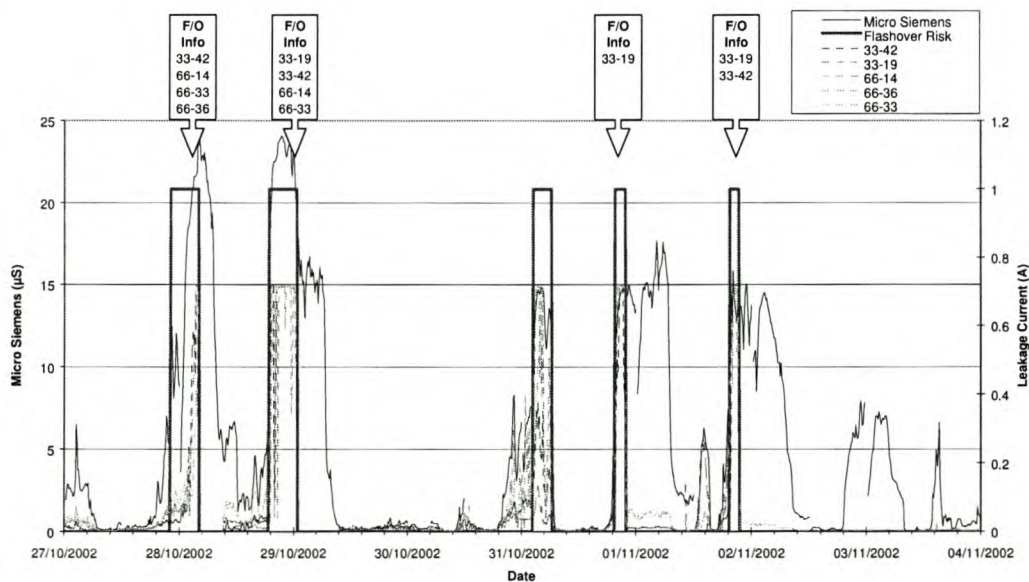


Figure 5-11: Week 15 IPMR conductivity, leakage currents and flashover risk.

CHAPTER 5

During the Week 15 period 5 instances were observed when the requirements of the rule were met. By comparing flashovers with these instances, 4 of the instances did experience flashovers. The instance that did not actually experience flashover, however, did have excessive leakage currents in the same order than those days that did experience flashover. The leakage currents were reduced after the humidity decreased below a 70% value. The flashovers on the 1st and 2nd November 2002 were caused by a rapid increase in humidity. This steep increase is also visible in the coinciding conductivity measurement.

The application of the IPMR as a device capable of predicting such instances is possible since the IPMR is equipped for the measuring of surface conductivity and peak leakage current. Knowledge of the climatic factors in the vicinity of the test area, a thorough understanding of the pollution types at the test area and a suitable test insulator for use with the leakage current measurement system should improve the risk of flashover predictions.

5.6 SUMMARY

It was shown in this chapter that the IPMR was installed at KIPTS, a pollution test station along the Cape west coast of South Africa. The test station is subjected to a variety of pollution sources, including marine, industrial and agricultural. A review on the operational performance of the device showed that the device mainly experienced problems with the artificial wetting tests. Two statistical methods were discussed to quantify the pollution severity value using the measured IPMR conductivity data. The calculated severity value can be applied in the assessment of flashover probability. A discussion was made on the measured conductivity values with natural wetting. The effect of wetting parameters was included as it mainly influences the conductivity values with natural wetting. A rule of thumb was developed after observations were made regarding the wetting mechanism, surface conductivity and peak leakage current at KIPTS.

6 RESULTS AND RECOMMENDATIONS

The objectives of this research programme were divided into two main groups, the testing of the device in a laboratory and the field evaluation at a natural pollution test site.

The scope of the work was:

- The development of a repeatable artificial wetting test method
- The calibration of the device
- The use of the device during artificial pollution tests
- Field evaluation of the device to assess insulator performance
- Quantification of site severity using IPMR conductivity measurements

The following objectives were successfully reached at the end of the research programme:

- A repeatable artificial wetting test method was developed after several modifications were made to the steam system, test chamber and the test routine. These modifications were made after various temperature and humidity measurements were made during artificial wetting tests. Conductivity results were used to determine how these modifications influenced the artificial wetting tests. The repeatable test method proved to be a non-destructive pollution measurement test.
- A standard resistor was constructed to verify the accuracy of the measuring system. The standard resistor can be used to verify the measurements of a newly built IPMR as well as a tool to ascertain whether the measurements of a field-installed IPMR are still correct.

CHAPTER 6

- The IPMR was successfully calibrated with insulators that were artificially polluted according to the solid layer method. Linear and polynomial relationships were determined after curve-fitting techniques were performed on the results. The measures of model accuracy, correlation coefficient and R^2 , both showed good results. The IPMR calibration showed that the IPMR is capable as a device relating the maximum conductivity during artificial wetting to the ESDD, a severity classification parameter.
- The IPMR was tested in a salt fog chamber to determine if the device is capable to evaluate the severity of an instantaneous pollution event. Conductivity measurements were compared to salt fog salinity values and peak leakage currents. The critical flashover values was calculated for the test insulators and compared to fuse operations. The test results showed that the IPMR is capable to relate critical insulator performance.
- The measured IPMR data was successfully applied to quantify the KIPTS site severity according to the conductivity measurement with natural wetting. The benefit using this method of site severity calculation is that it expresses the state of the pollution layer since the measurement is dependant on the degree of pollution as well as the wetting of this pollution layer. The site severity can also be determined for the conductivity measurement with artificial wetting, but it must be remembered that the conductivity measurement with artificial wetting describes the “worst case” conductivity to be expected during critical wetting.
- The IPMR was successfully installed at a natural pollution test site. The artificial wetting measurements unfortunately proved problematic and were not included in the thesis. (Possible remedies are given in the recommendation section in this chapter). The conductivity measurements with natural wetting showed good correlation to flashovers experienced at KIPTS.
- A rule of thumb was developed to indicate a possible risk of flashover. The development of this method was based on observations made on the relationship between humidity and surface conductivity. The IPMR can be used to assess

CHAPTER 6

pollution severity and possible risk of flashover at other test sites after a thorough investigation is made of the wetting processes at the particular site. Further work is needed to better the risk of flashover decision-making process.

The following recommendations can be made at the end of the research programme:

- The reliability of the IPMR with regard to the artificial wetting process will be improved if the steam generator control is included in the control unit of the IPMR. The failure of certain components e.g. the pressure switch or the heating element can be relayed via a diagnostic alarm to service personnel.
- The site severity can be more easily quantified when the equation used to determine the ESDD value for the artificial wetting test is modified so that the conductivity value with critical wetting is returned. The benefit in using this method is that the “worst case” conductivity is determined once-daily with the artificial wetting method and then all the conductivity values with natural wetting can be directly compared with this value. Decision-making can then be applied nearly real-time in this field of pollution monitoring.
- The correct time of day of the conductivity test with artificial wetting should be investigated for the specific area. At KIPTS it was found that the daily peaks in conductivity measurement with natural wetting started at $\pm 20\text{h}00$ and ended at $\pm 08\text{h}00$. The conductivity measurement with natural wetting is affected by the conductivity test with artificial wetting. The main factors that were found to affect the measurements were that no conductivity measurements are made when the artificial wetting test is running and that the insulator is returned with a warmer surface temperature after the test due to the dryer cycles. The conductivity measurement with natural wetting takes at least an hour to return to the same value as before the test. Valuable pollution event information can be lost when the device is set up to perform tests during these times.

REFERENCES

REFERENCES

1. Cigré Working Group 33.04, "The Measurement Of Site Pollution Severity and its Application to Insulator Dimensioning for AC Systems", Electra No. 64, May 1979, p. 101 – 116.
2. Du Toit C. K., "n Eksperimentele Ondersoek na die Verband Tussen die Hoogste Lekstroom en Soutgehalte in 'n Soutmistoets op "n Langsaafisolator", M.Ing Thesis, University of Stellenbosch, South Africa, November 1985.
3. Du Toit L. P., "Insulator Pollution: An Analysis of Flashover Mechanisms and a Comparative Study of Site Pollution Severity Assessment Methods", M.Ing Thesis, University of Stellenbosch, South Africa, March 1986.
4. Holtzhausen J. P., Du Toit L. P., "Insulator Pollution: Interrelationship of highest leakage current, specific creepage distance and salinity in a salt fog test", Transactions SAIEE, August 1987, p. 1 – 6.
5. Holtzhausen J. P., Smith J. M., Potgieter O. C. T., "Insulator Pollution: Monitoring of Leakage Currents During Artificial And Site Test Conditions", SAUPEC '90, Stellenbosch, South Africa, January 1990.
6. Holtzhausen J. P., "Leakage Current Monitoring On Synthetic Insulators At A Severe Coastal Site", Transactions SAIEE, September 1994, p. 131 – 138.
7. Potgieter O.C.T., "Development and Evaluation of an Insulator Pollution Monitoring Apparatus", M.Ing Thesis, University of Stellenbosch, South Africa, October 1991.
8. Bertazzi A., Perego G., Sampaoli G., Vachiratarapadorn Y., Eamsa-as V., "A Device For The Automatic Measurement Of Surface Conductivity Of Insulators", Paper 47.41, 6th ISH, New Orleans, USA, Aug./Sept. 1989.

REFERENCES

9. Davel P., "Development of a New Insulator Pollution Monitor, Including an Analysis of the Effects of Environmental Variables on the Results", M.Eng Thesis, University of Stellenbosch, South Africa, December 1994.
10. Van Wyk L., "Insulator Pollution Monitoring: Evaluation of Various Methods of Severity Measurements At A Coastal Site", M.Eng Thesis, University of Stellenbosch, South Africa, December 1996.
11. IEC Publication 60507, "Artificial Pollution Tests on HV Insulators to be Used On AC Systems", Second Edition, 1991.
12. Van Wyk L., Holtzhausen J. P., Vosloo W. L., "Surface Conductivity As An Indication Of The Surface Condition Of Non-Ceramic Insulators", IEEE Africon '96, Stellenbosch, South Africa, September 1996.
13. Vosloo W. L., "A Comparison of the Performance of High-Voltage Insulator Materials in a Severely Polluted Area", PhD (Eng.Sci) Thesis, University of Stellenbosch, South Africa, March 2002.
14. Pietersen D., Holtzhausen J. P., Vosloo W. L., "An Investigation Into The Methodology To Develop An Insulator Pollution Severity Application Map For South Africa", 7th IEEE Africon Conference, Gaborone, Botswana, September 2004, p. 697 - 703.
15. IEC Publication 60815, "Guide For The Selection Of Insulators in Respect of Polluted Conditions", 2002.
16. Cigré Task Force 33.13.03, "Round Robin Pollution Monitor Study", August 2000.
17. Macey R. E., "The Performance of High Voltage, Outdoor Insulation in Contaminated Environments", Transactions SAIEE, April 1981, p. 80 – 92.

REFERENCES

18. Vosloo W. L., Macey R. E., De Turreil C., "The Practical Guide to Outdoor High Voltage Insulators", Eskom Power Series, Crown Publishers, Johannesburg, 2004.
19. Cigré Working Group 33.04, "A Critical Comparison of Artificial Pollution Test Methods for HV Insulators", *Electra* No. 64, May 1979, p. 117 – 136.
20. Riquel G., Spangenberg E., Mirabel P., Siason J. Y., "Wetting Process of Pollution Layer on HV Glass Insulators", Ninth International Symposium on High Voltage Engineering (9th ISH), Graz, Austria, August 1995.
21. Auxel H., Weiss W., "Measuring Equipment For Determining The Risk Of Local Pollution Layers On H.V. Insulators", *Siemens Review*, Vol. 42, No. 1, January 1975, p. 20 – 25.
22. Lambeth P. J., Auxel H., Verma M. P., "Methods of Measuring The Severity of Natural Pollution As It Affects HV Insulator Performance", *Electra* No. 20, 1972, p. 37 – 52.
23. Sforzini M., Cortina R., Marrone G., "A Statistical Approach for Insulator Design in Polluted Areas", *IEEE Trans. on PAS*, Vol. PAS-102, No. 9, September 1983.
24. Petrusch W., Lange G., Schmitt W., Kluge W., Schumann P., "Experiences On The Continuous Monitoring Of The Leakage Current On Polluted Insulators In Service In The Federal Republic Of Germany", Cigré International Conference on Large High Voltage Electric Systems, Stockholm, Sweden, 1981.
25. Verma M. P., Niklasch H., Lipken H., Schreiber H., Luxa G. F., Heise W., "The Criterion for Pollution Flashover and its Application to Insulation Dimensioning and Control", Cigré Session 1978, Paper 33.09, August 1978.

REFERENCES

26. Schwardt W. H., Holtzhausen J. P., Vosloo W. L., "Determination Of A Calibration Curve For An Insulator Pollution Monitoring Relay", SAUPEC 2002, Vanderbijlpark, South Africa, January 2002.
27. CTLab (PTY) Ltd, "OLCA Product Description", Product Specification Document, Stellenbosch, South Africa, 2000.
28. Vosloo W. L., Burger H. S., Holtzhausen J.P., "On-line Leakage Current And Environmental Monitoring System", Cigré 4th Southern Africa Regional Conference, Cape Town, South Africa, October 2001, Paper 68.01.
29. Rizk, F. A. M., "Mathematical models for pollution flashover", *Electra*, Vol. 78, pp 71-103, 1978.
30. Holtzhausen, J. P., "A Critical Evaluation of AC Pollution Flashover Models for HV Insulators Having Hydrophilic Surfaces", PhD Thesis, University of Stellenbosch, South Africa, 1997.
31. Lambeth P. J., "Effect of Pollution on High Voltage Outdoor Insulators", Proc. IEE, Vol. 118, No. 9, 1971.
32. Verma, M. P., "Highest Leakage Current Impulse As Criterion For The Performance Of Polluted Insulators", CIGRE 33-73 (WG 04) (6) IWD.
33. Holtzhausen J. P., Vosloo W. L. "Insulator Pollution Test Station: Design And Operation", SAUPEC '94, Cape Town, South Africa, January 1994.
34. Vosloo W. L., Holtzhausen J. P. "Koeberg Insulator Pollution Test Station (KIPTS)", Ninth International Symposium on High Voltage Engineering (9th ISH), Graz, Austria, September 1995.
35. Vosloo W. L., Swinny R., Holtzhausen J.P., "Koeberg Insulator Pollution Test Station (KIPTS) –An In-house Insulator Product Ageing Test Standard", Cigré

REFERENCES

- 4th Southern Africa Regional Conference, Cape Town, South Africa, October 2001, Paper 69.01.
36. IEC Publication 601109, "Composite insulators for AC overhead lines with a nominal voltage greater than 1000 V - Definitions, test methods and acceptance criteria", 1992.
37. Naito K., Mizuno Y., Naganawa W., "A Study on Probabilistic Assessment of Contamination Flashover of High Voltage Insulator", IEEE Transactions on Power Delivery, Vol. 10, No. 3, July 1995.
38. Hileman, A. R., "Insulation co-ordination for Power Systems", Marcel Dekker, New York, 1999.
39. Engelbrecht C. S., Hartings R., Lundquist J., "Statistical dimensioning of insulators with respect to polluted conditions", Proc. IEE – Gener. Transm. Distrib., Vol. 151, No. 3, May 2004.

BIBLIOGRAPHY

BIBLIOGRAPHY

- i. Holtzhausen J. P., Smith J. M., Potgieter O. C. T., "Insulator Pollution: Monitoring Of Leakage Currents During Artificial And Site Conditions", SAUPEC '90, Stellenbosch, South Africa, January 1990.
- ii. Holtzhausen J. P., Potgieter O. C. T., "Continuous On Site Monitoring Of Insulator Surface Conductance And Leakage Currents", SAUPEC '91, Johannesburg, South Africa, January 1991.
- iii. Holtzhausen J. P., Potgieter O. C. T., Smith J. M., "The On Site Leakage Current Performance Of Insulators Of Various Designs And Materials As A Function Of Weather Data", SAUPEC '91, Johannesburg, South Africa, January 1991.
- iv. Holtzhausen J. P., Potgieter O. C. T., "Continuous On Site Monitoring Of Insulator Surface Conductance And Leakage Currents", Fifth International Symposium on High Voltage Engineering, Dresden, Germany, August 1991.
- v. Holtzhausen J. P., Potgieter O. C. T., Smith J. M., "The On Site Leakage Current Performance Of Insulators Of Various Designs And Materials As A Function Of Weather Data", Fifth International Symposium on High Voltage Engineering, Dresden, Germany, August 1991.
- vi. Holtzhausen J. P., Potgieter O. C. T., "Site Severity And Warning Systems: On Site Surface Conductance And Leakage Current Monitoring", Seminar: The Performance of High Voltage AC Insulators in Polluted Environments, SAIEE / NEC, 11 February 1992.
- vii. Holtzhausen J. P., "Leakage Current Monitoring Of Polluted Insulators On AC Power Systems At Elandsbaai And Kuils River", Seminar: The Performance of

BIBLIOGRAPHY

- High Voltage AC Insulators in Polluted Environments, SAIEE / NEC, 11 February 1992.
- viii. Holtzhausen J. P., "Leakage Current Monitoring Of Polluted Insulators On AC Power Systems At Elandsbaai And Kuils River", SAUPEC '92, Durban, South Africa, July 1992.
- ix. Holtzhausen J. P., Davel P., "Design And Calibration Of An Insulator Pollution Monitoring Apparatus", SAUPEC '94, Cape Town, South Africa, January 1994.
- x. Davel P., Holtzhausen J. P., Vosloo W. L., "Design And Calibration Of An Insulator Pollution Monitoring Apparatus", UPEC, Galway, Ireland, September 1994.
- xi. Holtzhausen J. P., "Leakage Current Monitoring On Synthetic Insulators At A Severe Coastal Site", Transactions SAIEE, September 1994.
- xii. Davel P., Holtzhausen J. P., "Low Voltage Measurement Of The Pollution On High Voltage Insulators", SAUPEC '95, Pretoria, South Africa, January 1995.
- xiii. Van Wyk L., Holtzhausen J. P., Vosloo W. L., "Laboratory Calibration And Preliminary Field Results Of An Insulator Pollution Monitoring Apparatus (IPMA)", SAUPEC '96, Johannesburg, South Africa, January 1996.
- xiv. Van Wyk L., Holtzhausen J. P., Vosloo W. L., "Relationship Between Surface Conductance, Leakage Current And Humidity On Ceramic Insulators", UPEC, Crete, Greece, September 1996.
- xv. Van Wyk L., Holtzhausen J. P., Vosloo W. L., "Surface Conductivity As An Indication Of The Surface Condition Of Non-Ceramic Insulators", IEEE Africon '96, Stellenbosch, South Africa, September 1996.
- xvi. Van Wyk L., Holtzhausen J. P., Vosloo W. L., "Surface Conductance As An Indication Of Leakage Current, Obtained For A Marine Test Site", Tenth

BIBLIOGRAPHY

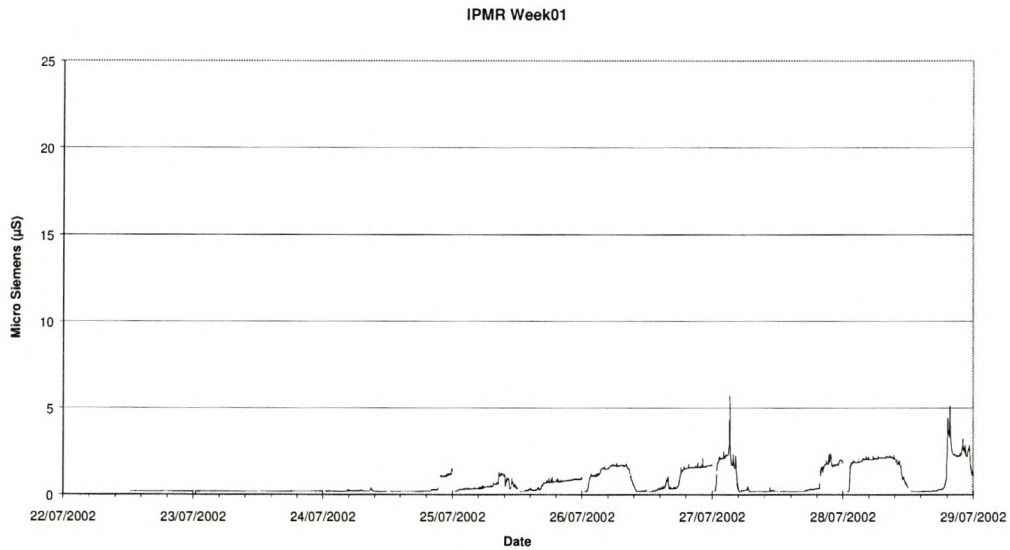
- International Symposium on High Voltage Engineering, Montreal, Canada, September 1997.
- xvii. Schwardt W. H., Holtzhausen J. P., Vosloo W. L., "Determination Of A Calibration Procedure For An Insulator Pollution Monitoring Relay", SAUPEC 2001, Cape Town, South Africa, January 2001.
- xviii. Schwardt W. H., Holtzhausen J. P., Vosloo W. L., "Determination Of A Calibration Curve For An Insulator Pollution Monitoring Relay", SAUPEC 2002, Vanderbijlpark, South Africa, January 2002.
- xix. Pietersen D, Vosloo W. L., Holtzhausen J. P., "An Investigation Into The Measurement Techniques To Compile An Insulator Pollution Application Map For South Africa", IEEE Africon, George, South Africa, October 2002.
- xx. Holtzhausen J. P., Vosloo W. L., "Insulator Pollution And Wetting Processes At A Severe Coastal Site", Thirteenth International Symposium on High Voltage Engineering, Delft, Netherlands, August 2003.
- xxi. Pietersen D., Holtzhausen J. P., Vosloo W. L., "An Investigation Into The Methodology To Develop An Insulator Pollution Severity Application Map For South Africa", 7th IEEE Africon Conference, Gaborone, Botswana, September 2004, p. 697 - 703.
- xxii. Schwardt W. H., Holtzhausen J. P., Vosloo W. L., "A Comparison Between Measured Leakage Current And Surface Conductivity During Salt Fog Tests", 7th IEEE Africon Conference, Gaborone, Botswana, September 2004, p. 597 - 600.
- xxiii. Schwardt W. H., Holtzhausen J. P., Vosloo W. L., "Risk Of Flashover Prediction Based On Site Severity Measurements", SAUPEC 2005, Johannesburg, South Africa, January 2005.

APPENDIX

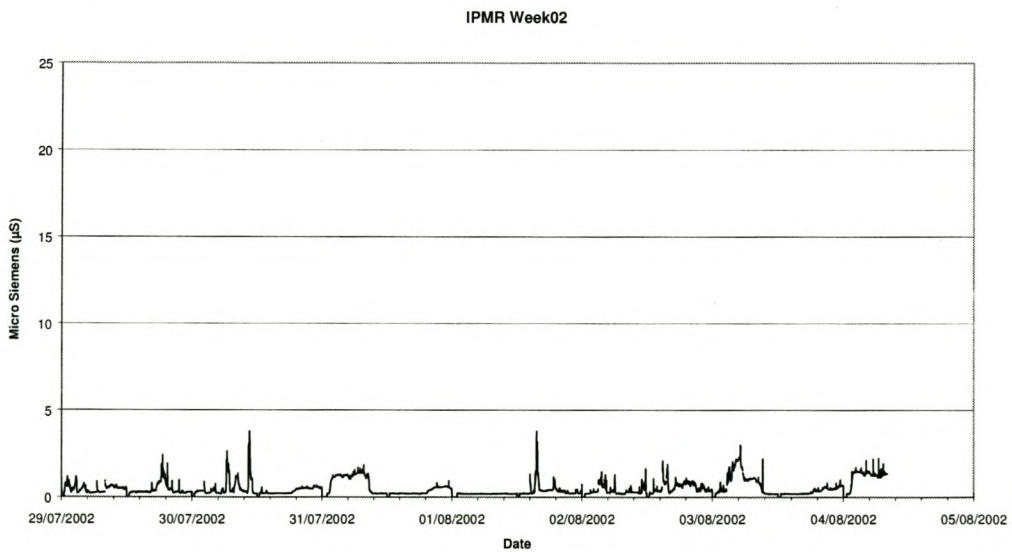
APPENDIX

(NOTE: Only conductivity measurements are shown for weeks with collected data.)

IPMR Conductivity Measurements during Week 01

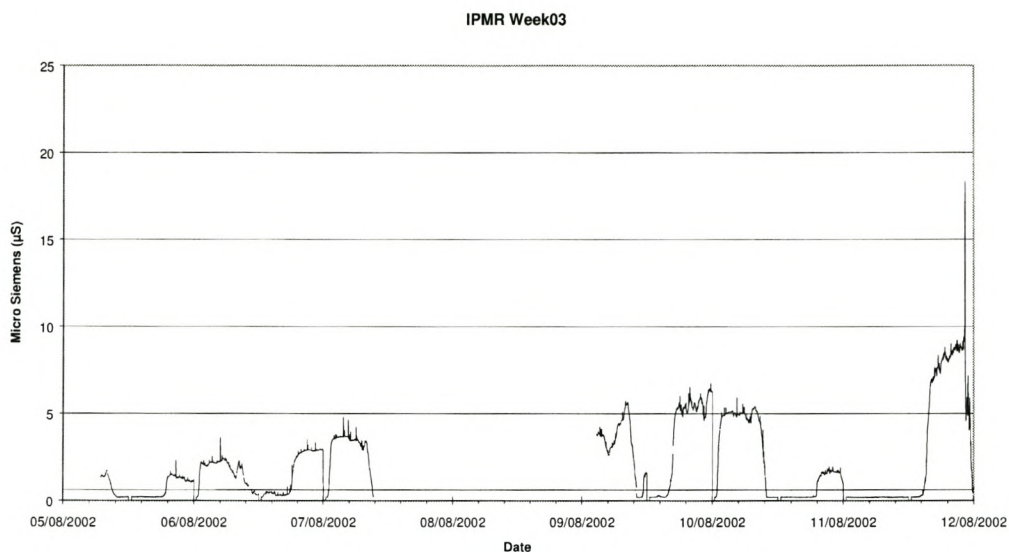


IPMR Conductivity Measurements during Week 02

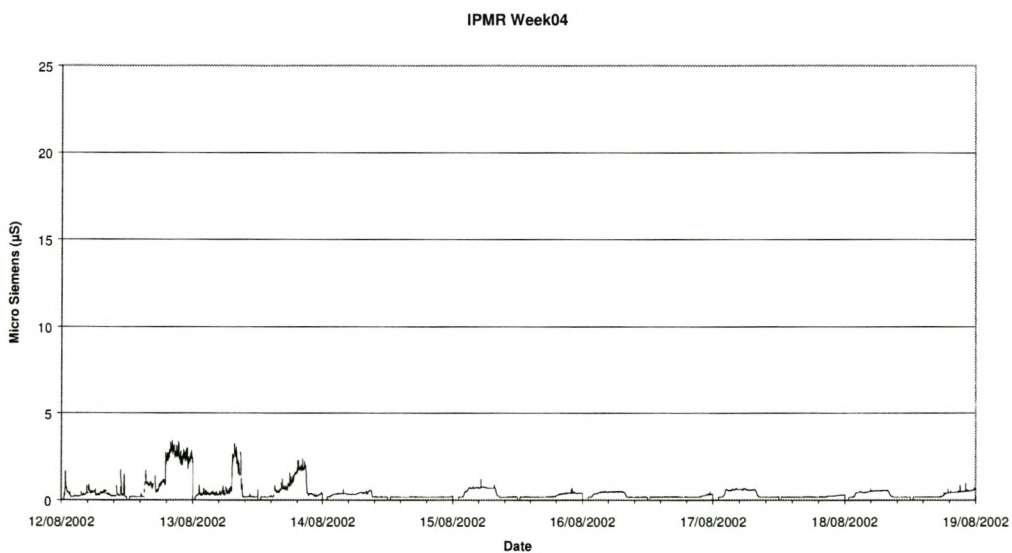


APPENDIX

IPMR Conductivity Measurements during Week 03

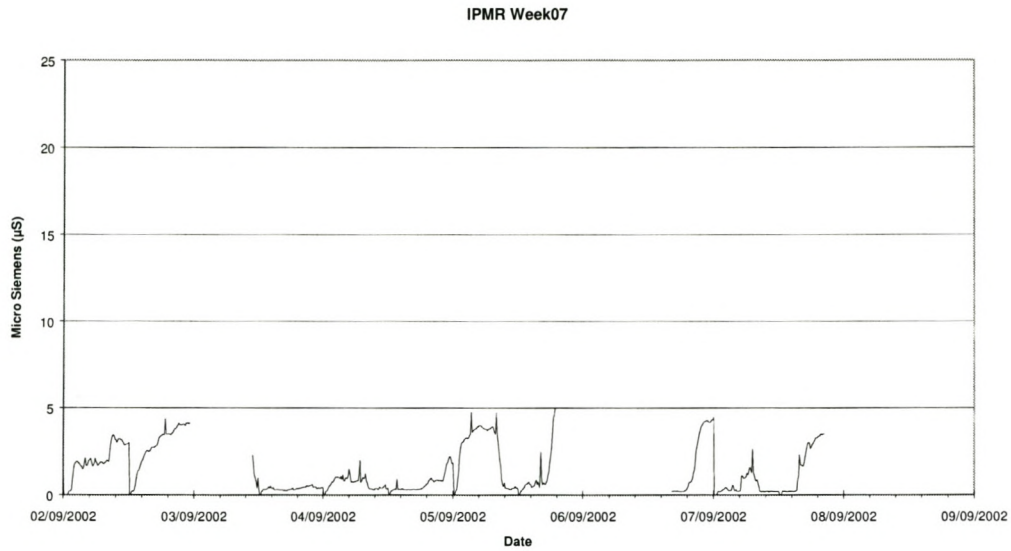


IPMR Conductivity Measurements during Week 04

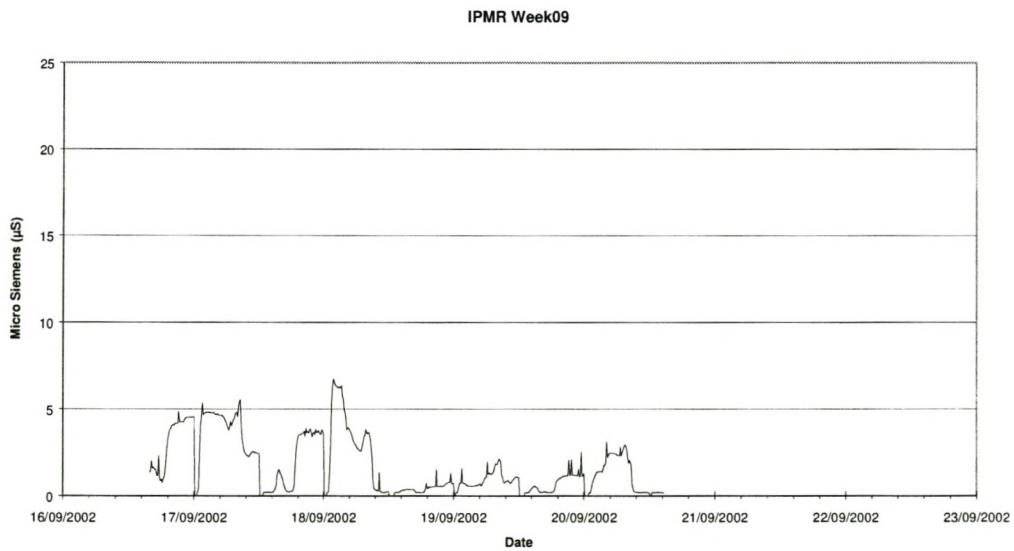


APPENDIX

IPMR Conductivity Measurements during Week 07

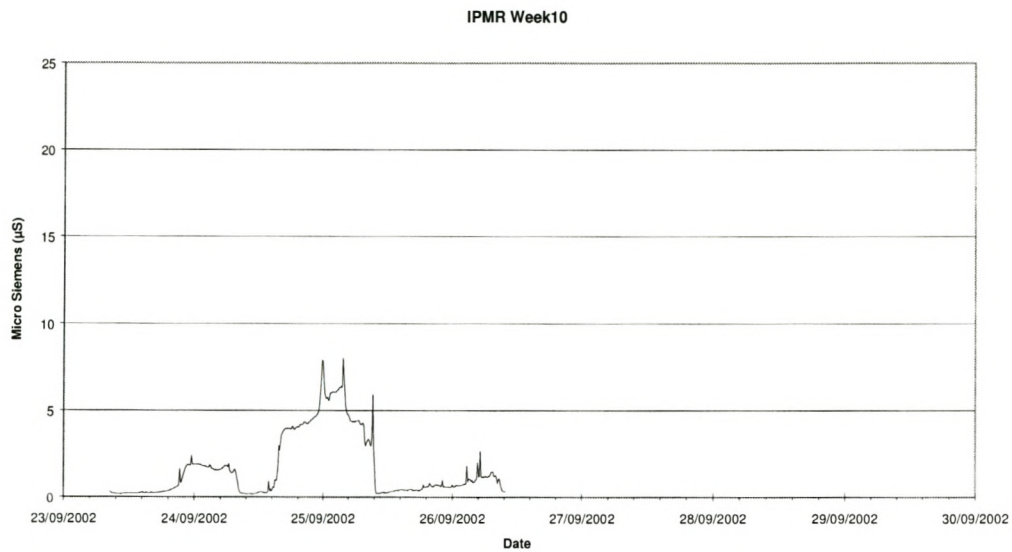


IPMR Conductivity Measurements during Week 09

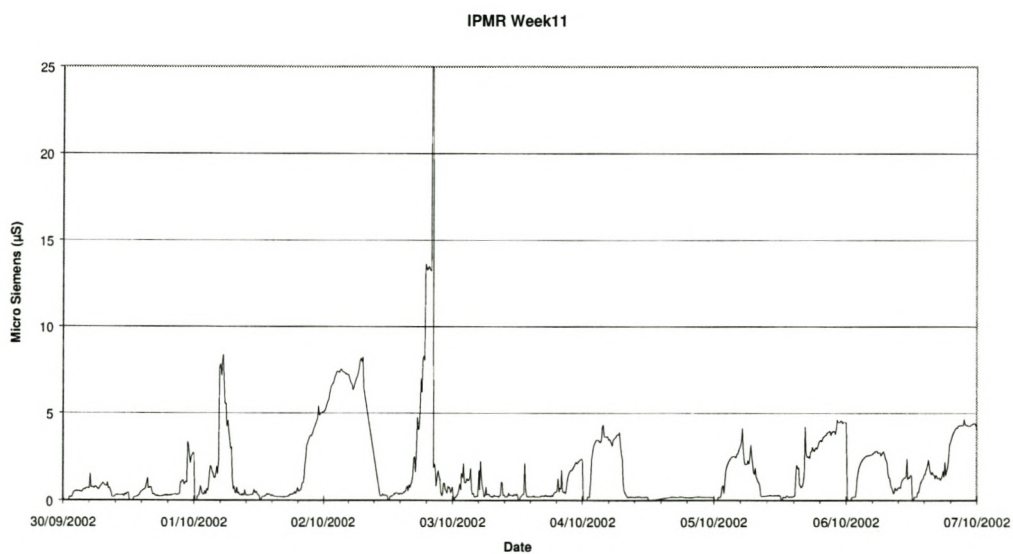


APPENDIX

IPMR Conductivity Measurements during Week 10

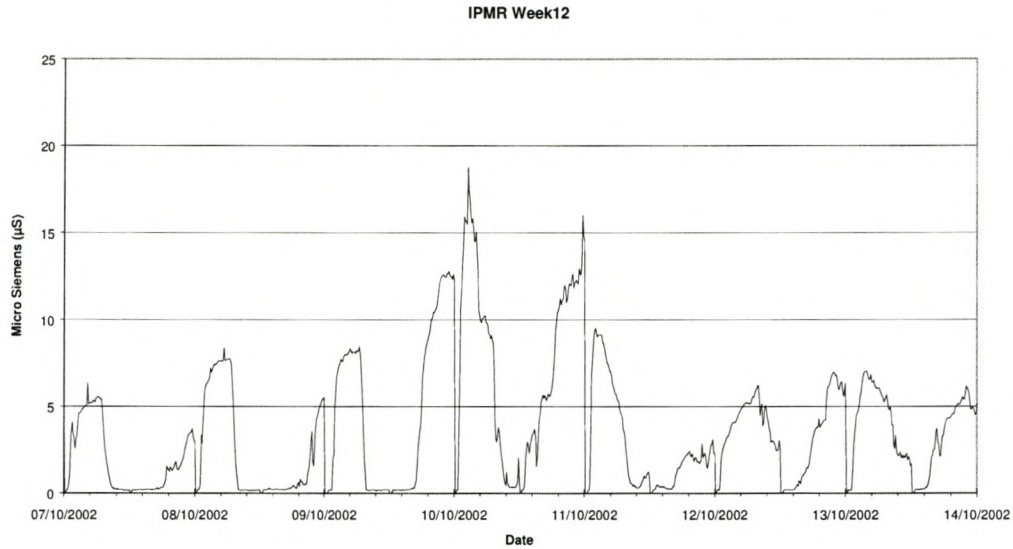


IPMR Conductivity Measurements during Week 11

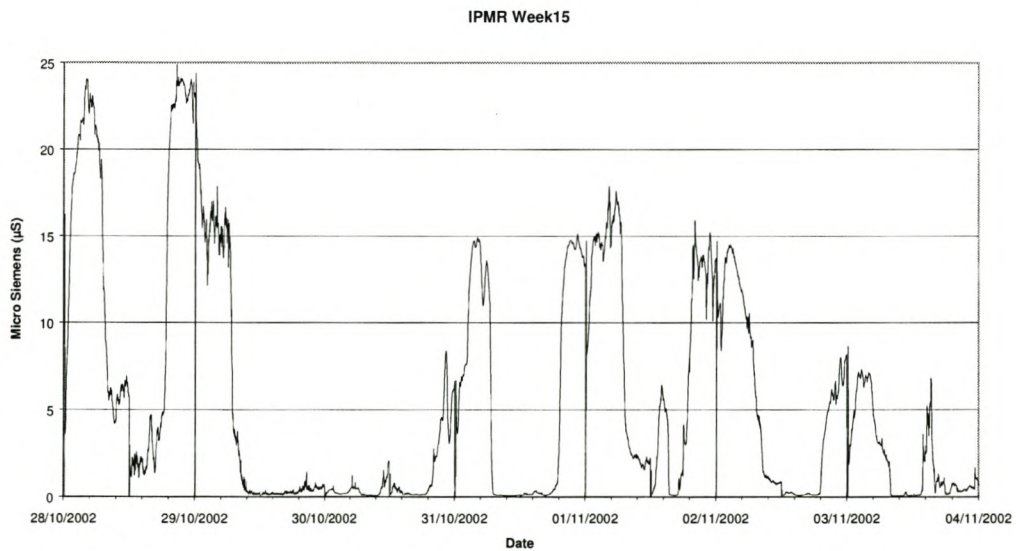


APPENDIX

IPMR Conductivity Measurements during Week 12

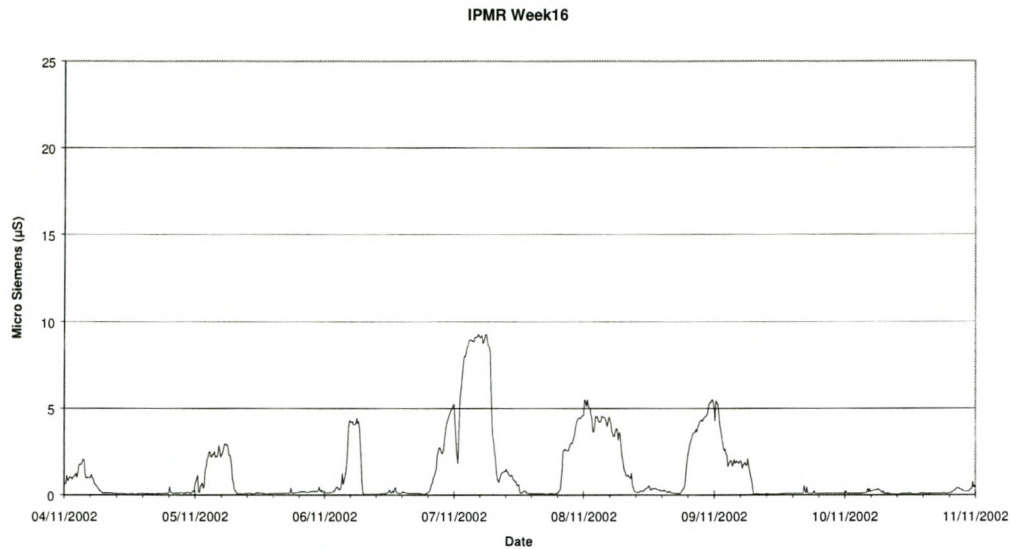


IPMR Conductivity Measurements during Week 15

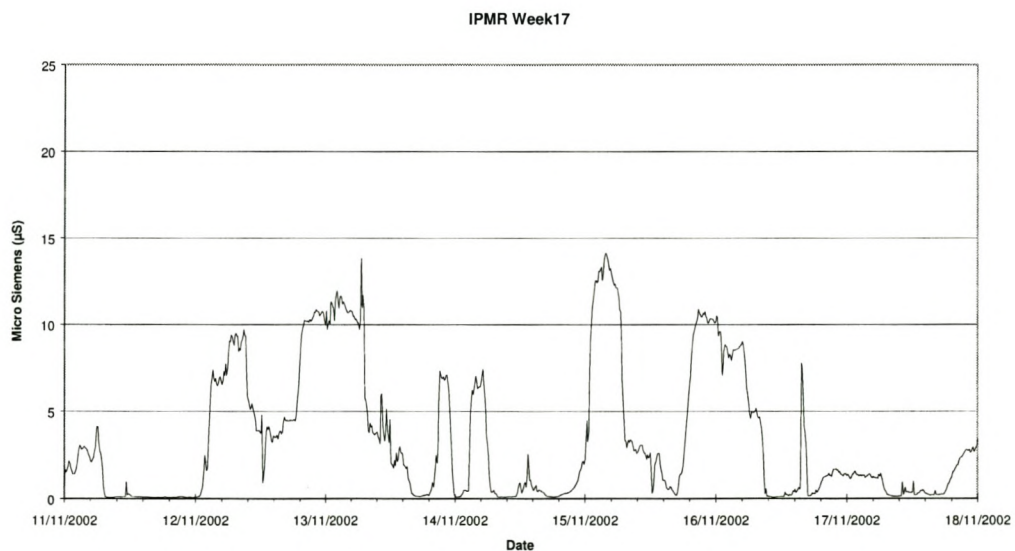


APPENDIX

IPMR Conductivity Measurements during Week 16

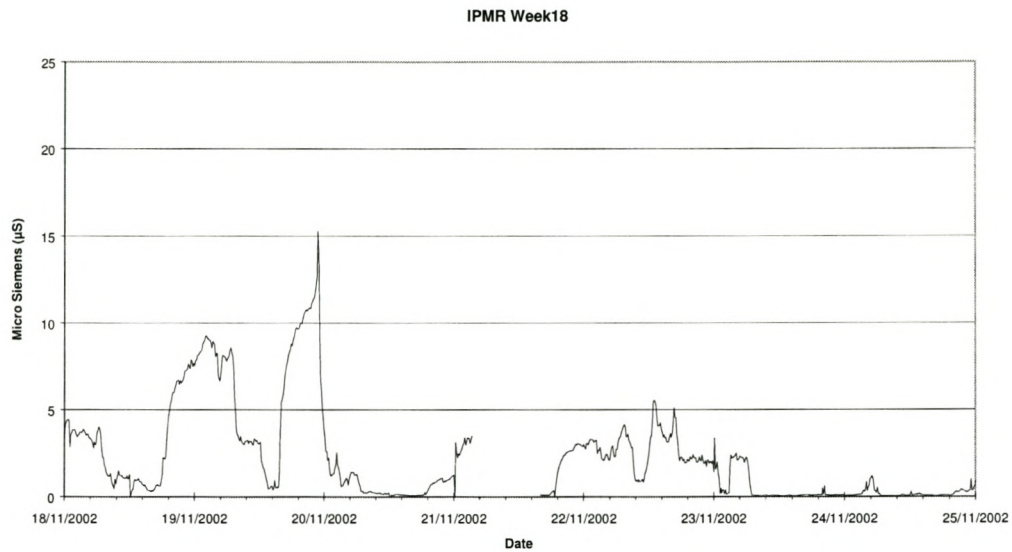


IPMR Conductivity Measurements during Week 17

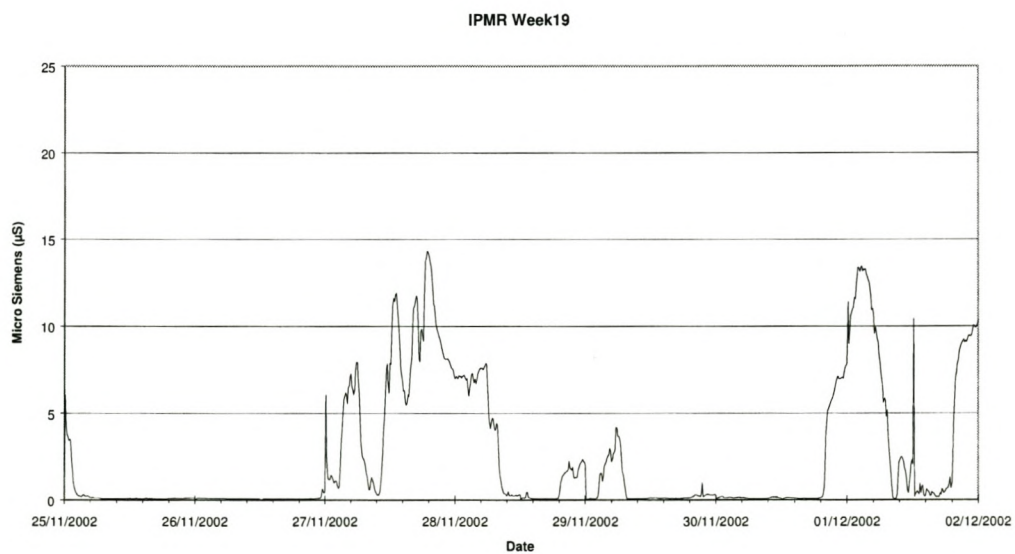


APPENDIX

IPMR Conductivity Measurements during Week 18

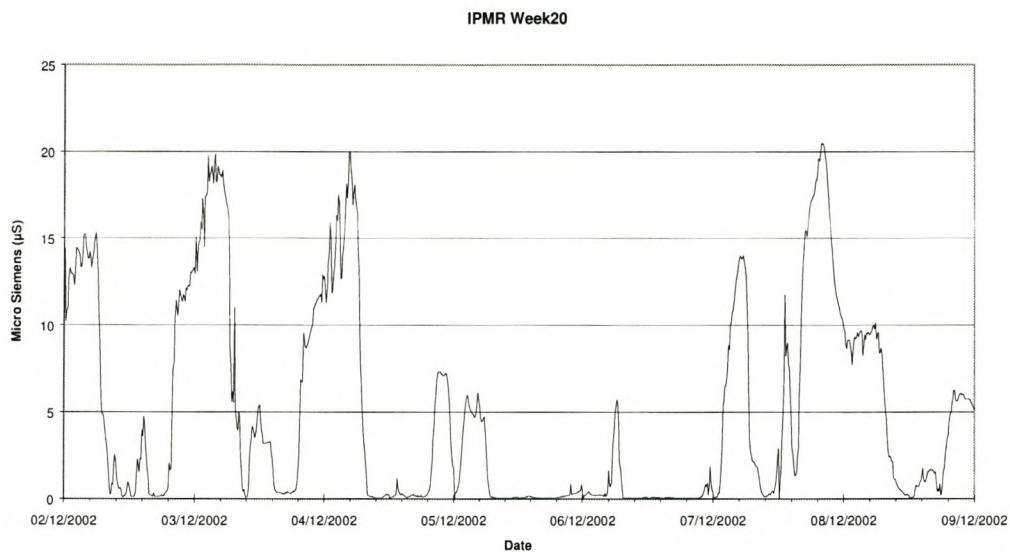


IPMR Conductivity Measurements during Week 19

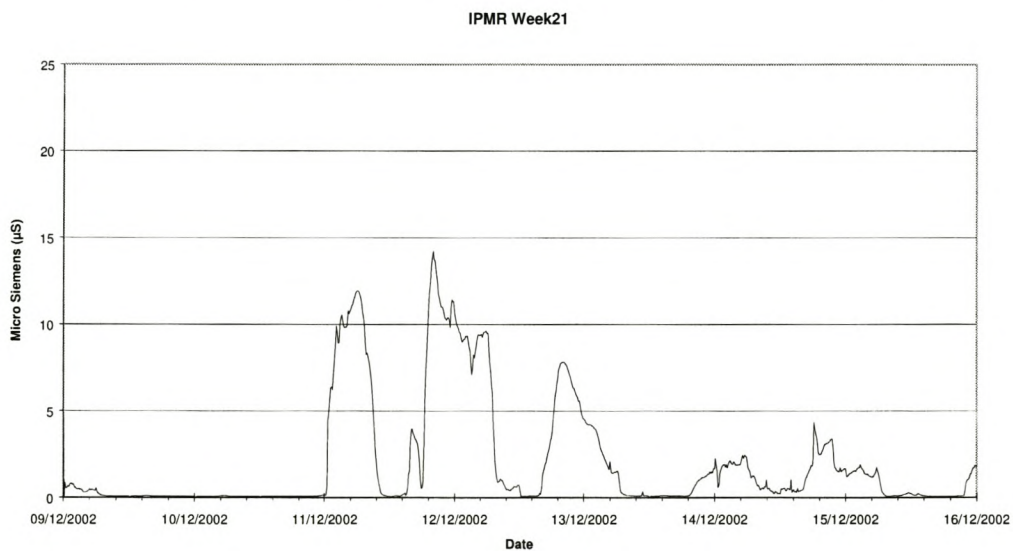


APPENDIX

IPMR Conductivity Measurements during Week 20

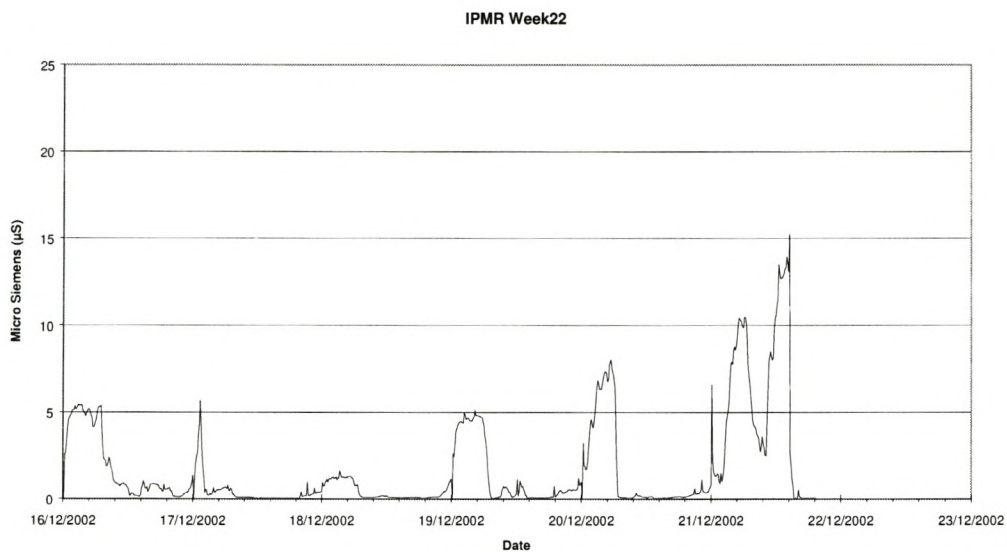


IPMR Conductivity Measurements during Week 21

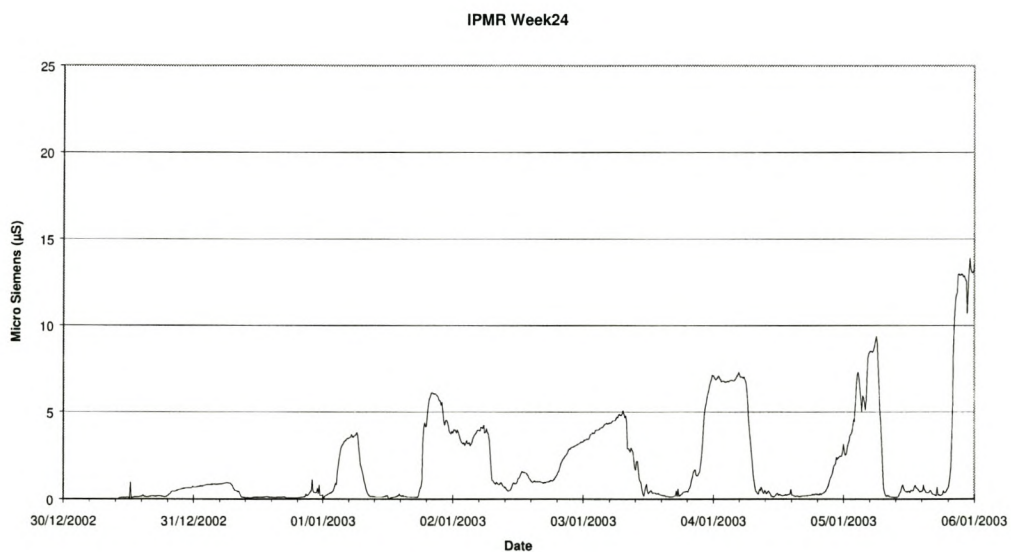


APPENDIX

IPMR Conductivity Measurements during Week 22

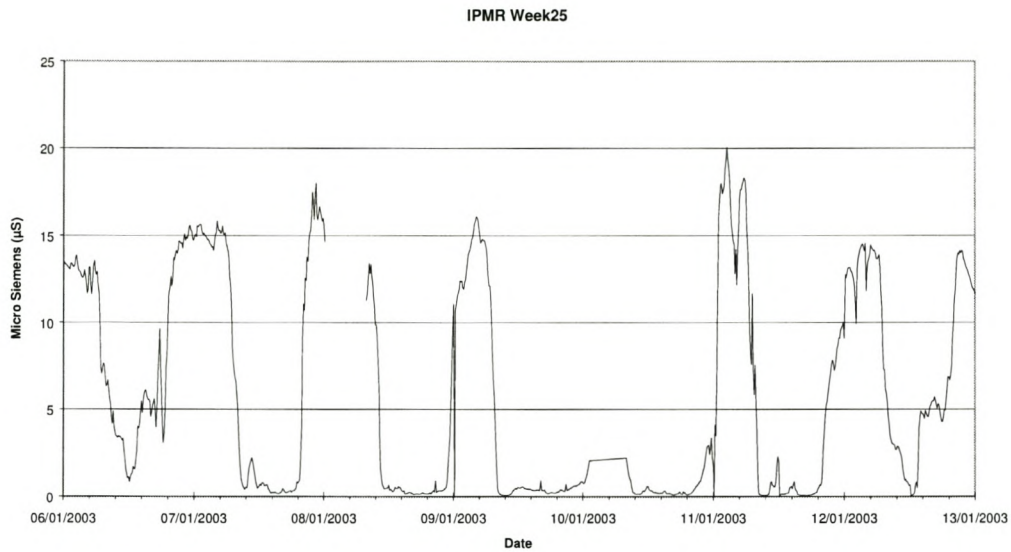


IPMR Conductivity Measurements during Week 24

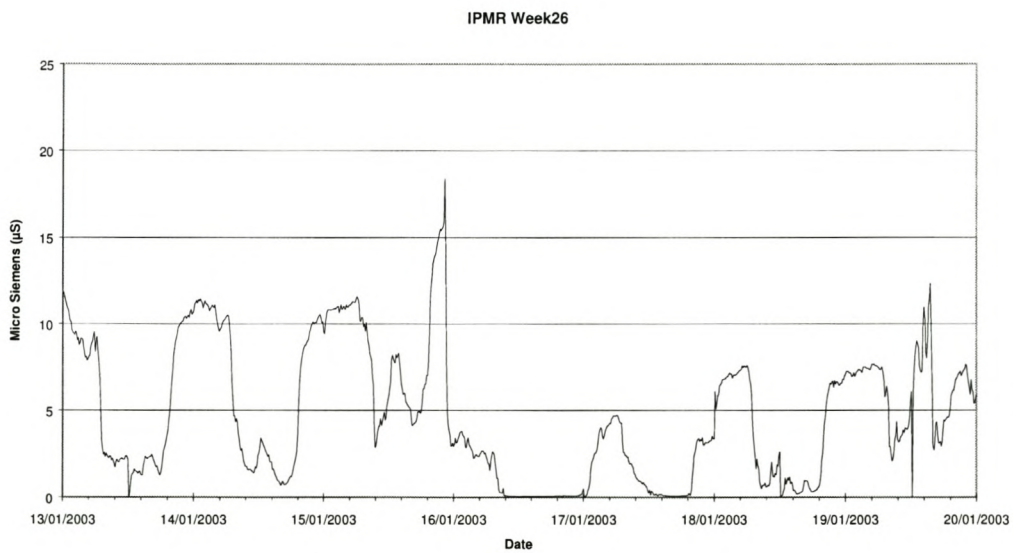


APPENDIX

IPMR Conductivity Measurements during Week 25

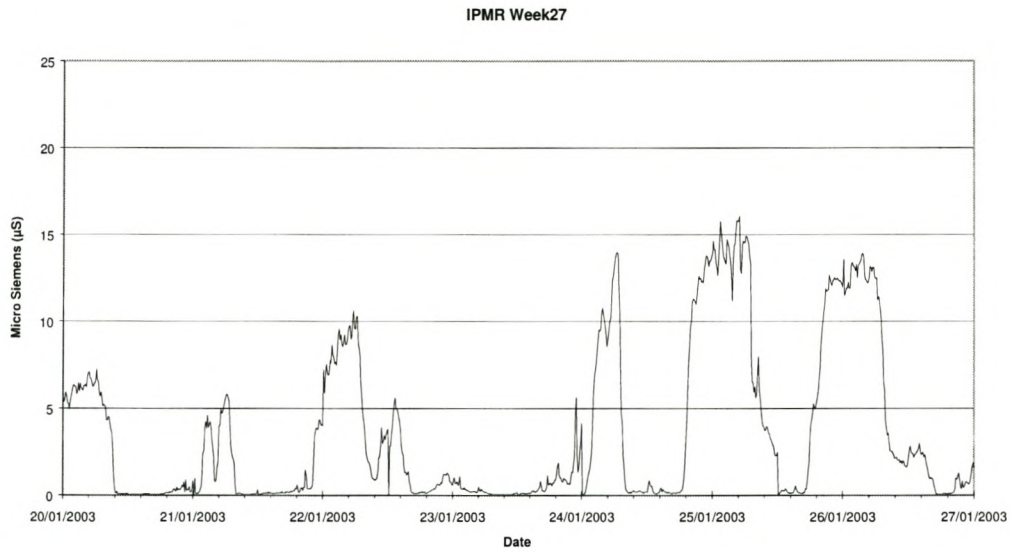


IPMR Conductivity Measurements during Week 26

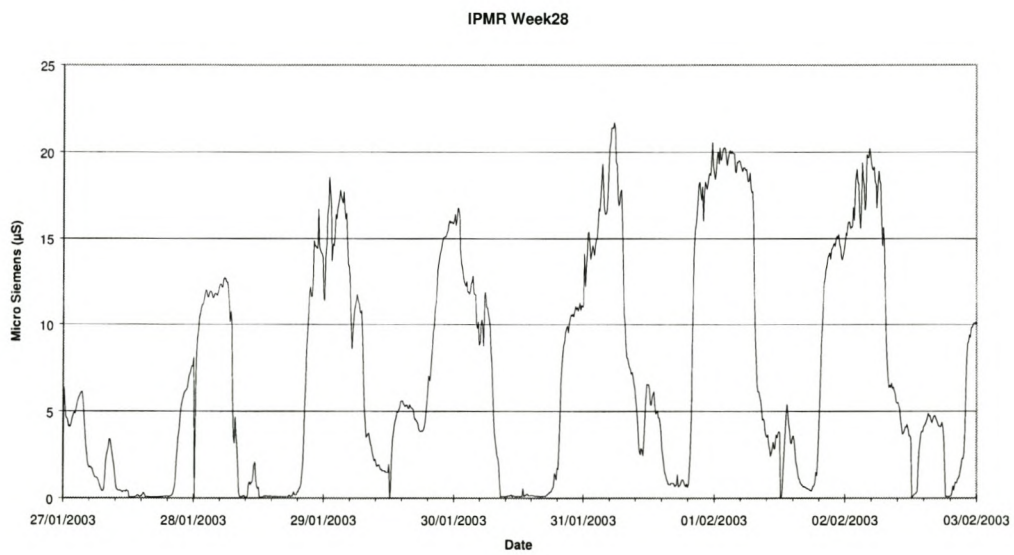


APPENDIX

IPMR Conductivity Measurements during Week 27

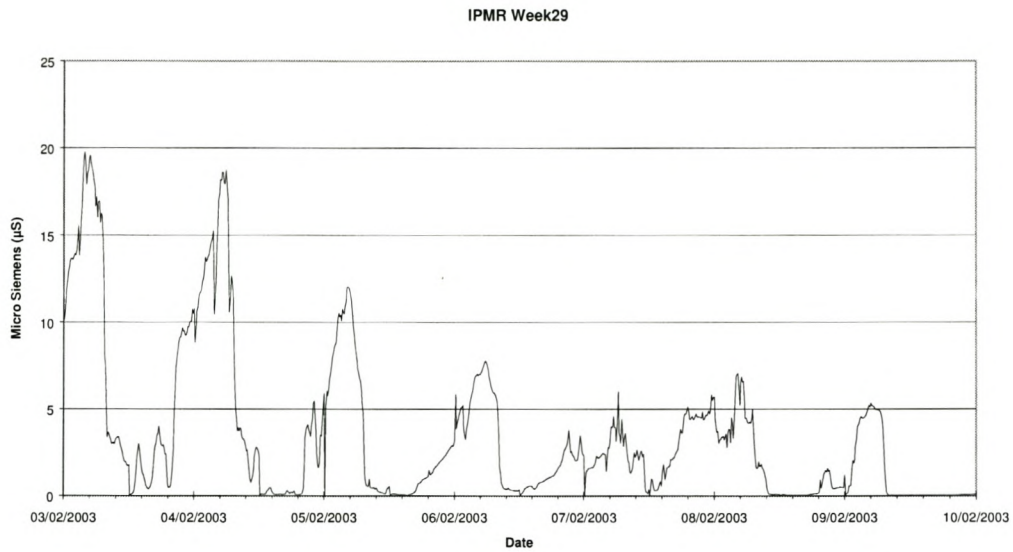


IPMR Conductivity Measurements during Week 28

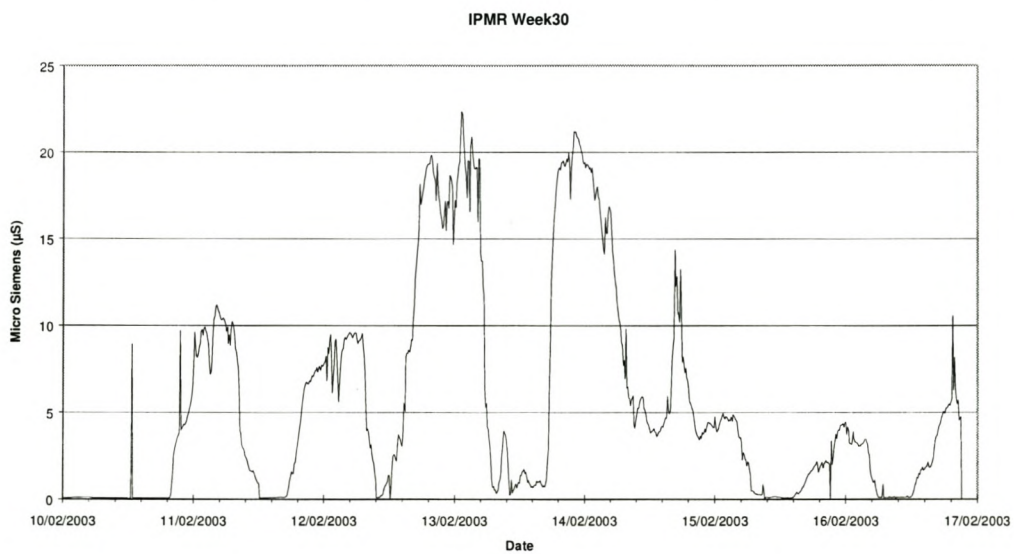


APPENDIX

IPMR Conductivity Measurements during Week 29

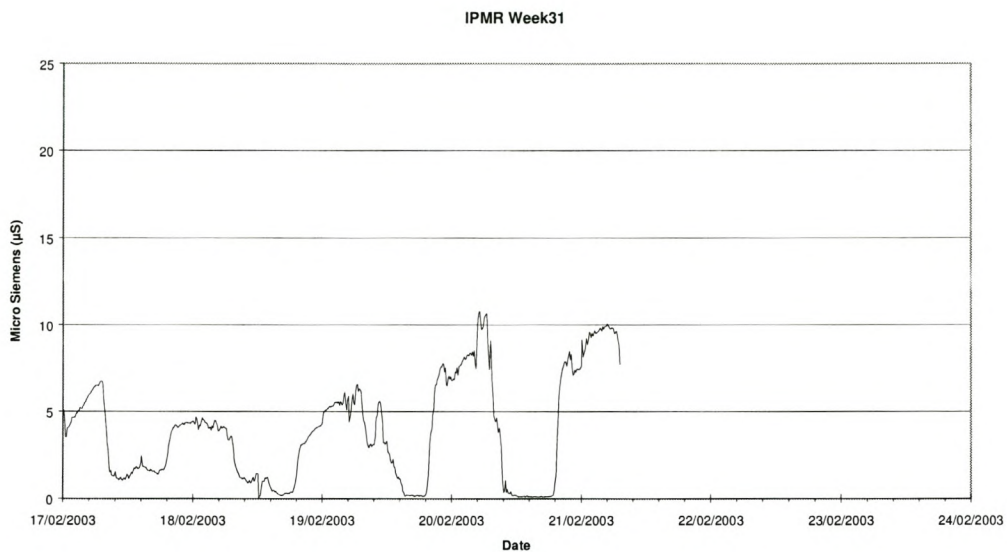


IPMR Conductivity Measurements during Week 30

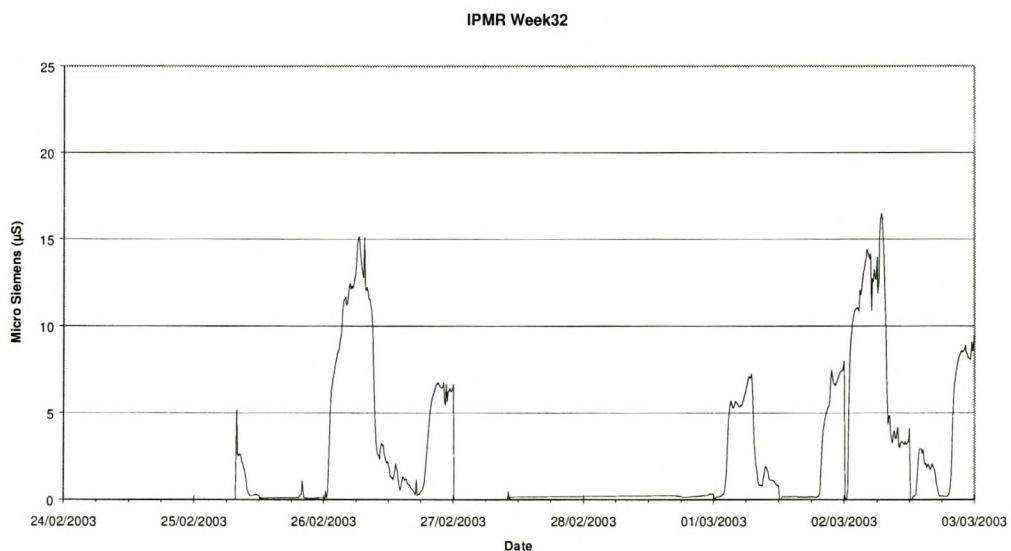


APPENDIX

IPMR Conductivity Measurements during Week 31

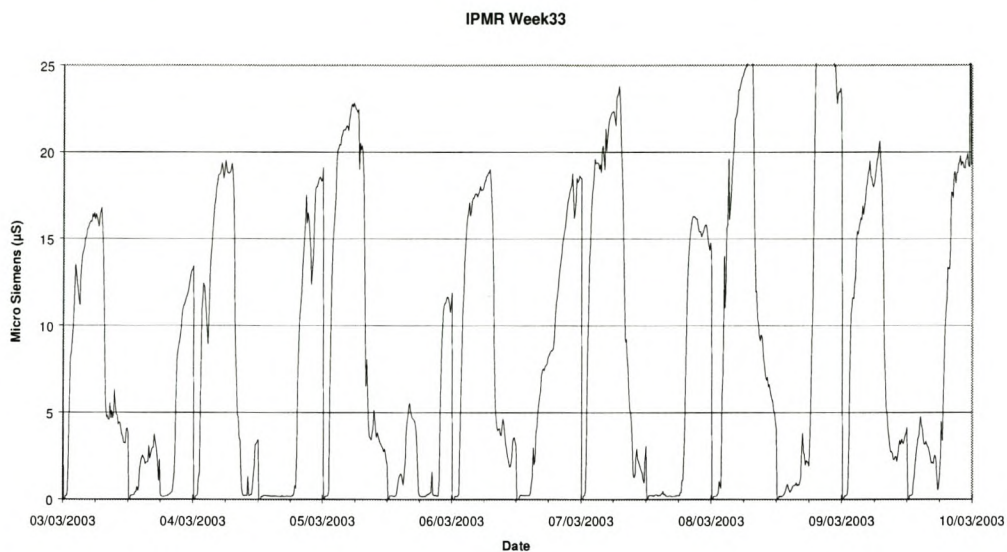


IPMR Conductivity Measurements during Week 32

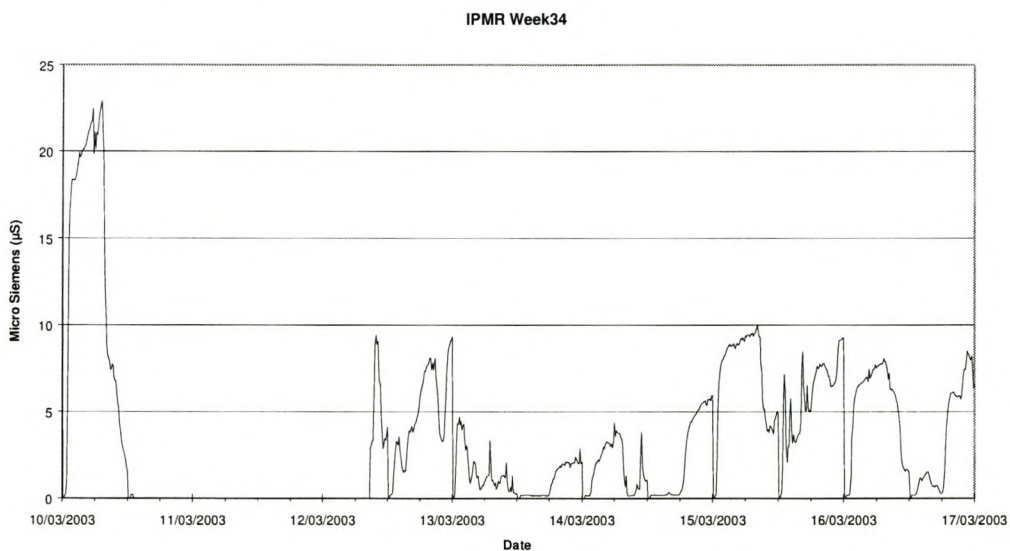


APPENDIX

IPMR Conductivity Measurements during Week 33

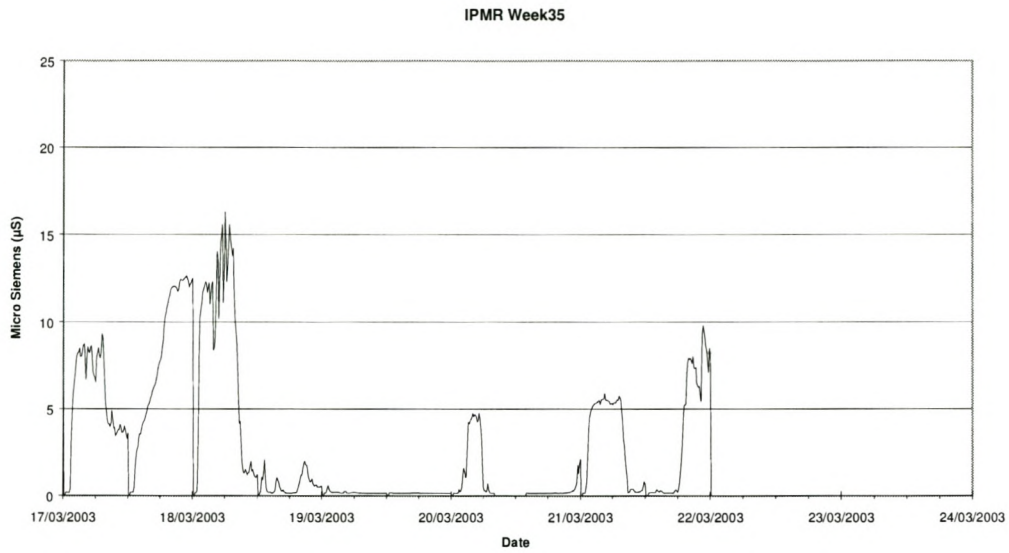


IPMR Conductivity Measurements during Week 34

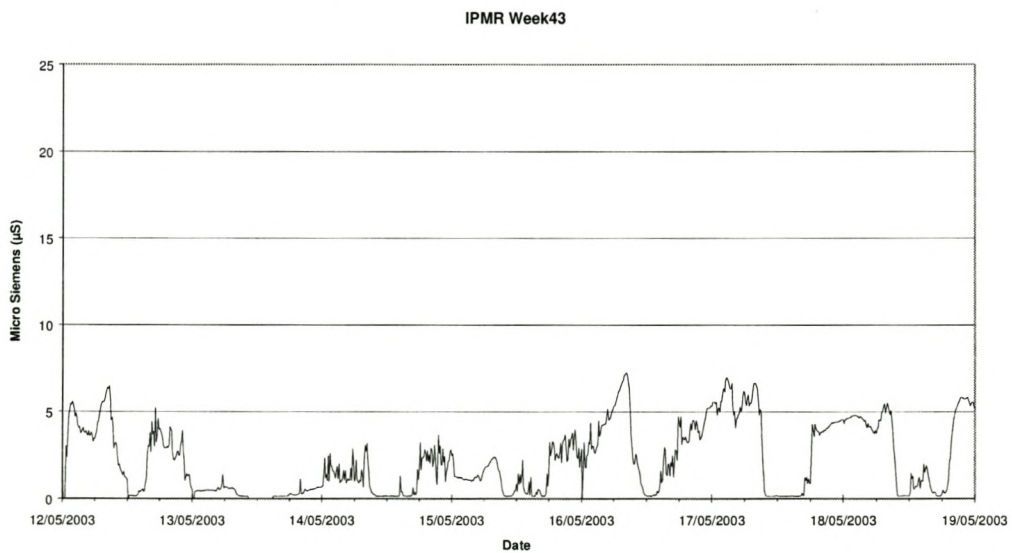


APPENDIX

IPMR Conductivity Measurements during Week 35

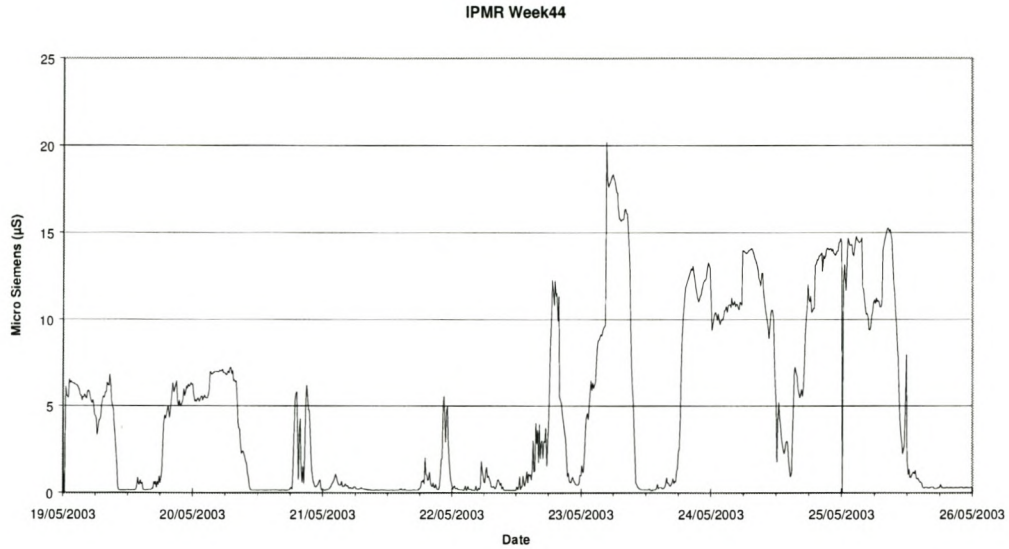


IPMR Conductivity Measurements during Week 43

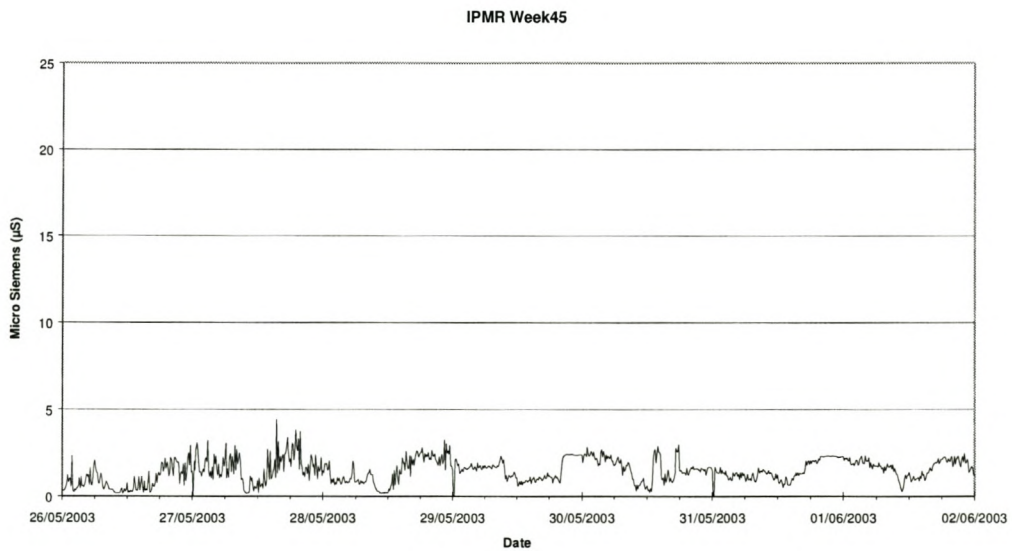


APPENDIX

IPMR Conductivity Measurements during Week 44

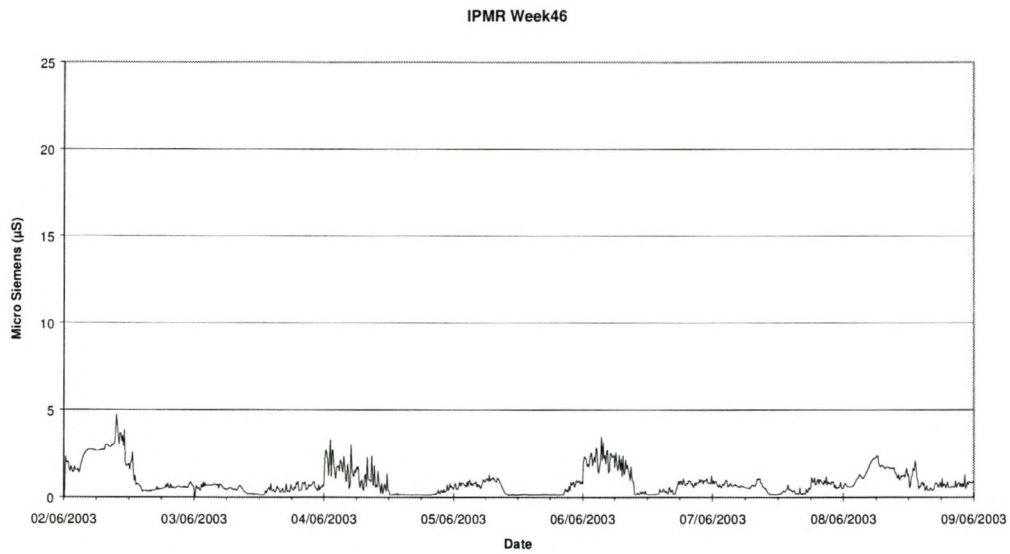


IPMR Conductivity Measurements during Week 45

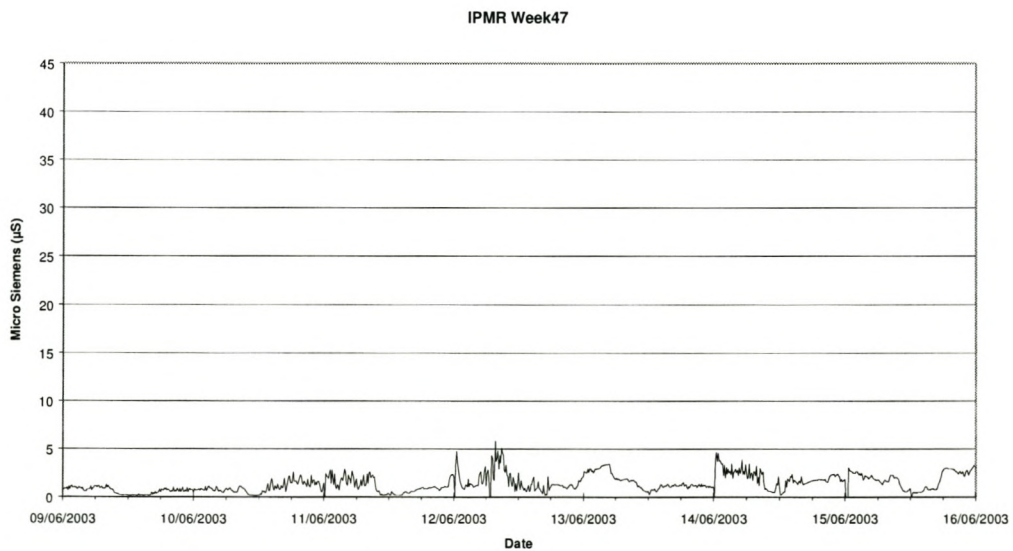


APPENDIX

IPMR Conductivity Measurements during Week 46

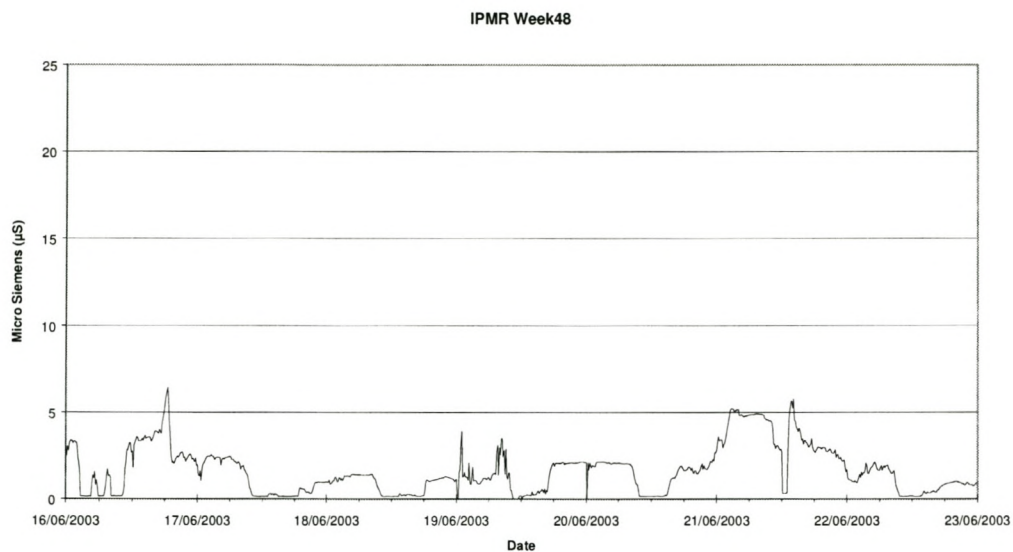


IPMR Conductivity Measurements during Week 47



APPENDIX

IPMR Conductivity Measurements during Week 48



IPMR Conductivity Measurements during Week 49

